



# Building Blocks for Small Aircraft APNT

**D3.1**

**NAVISAS**

**Grant:**

**699387**

**Call:**

**H2020-SESAR-2015-1**

**Topic:**

**Sesar-08-2015 Communication, Navigation and Surveillance (CNS)**

**Consortium coordinator:**

**TEKEVER ASDS**

**Edition date:**

**15 June 2017**

**Edition:**

**00.02.00**

Founding Members



## Authoring & Approval

### Authors of the document

Name/Beneficiary	Position/Title	Date
TEKEVER ASDS	Coordinator	04/01/2017
CSEM	Partner, WP3 Leader	04/01/2017
SHARK.AERO	Partner	04/01/2017
THALES AVIONICS	Partner	04/01/2017

### Reviewers internal to the project

Name/Beneficiary	Position/Title	Date
Ricardo Mendes / TEKEVER ASDS	COO	05/01/2017
André Oliveira / TEKEVER ASDS	Business Development Manager	06/01/2017

### Approved for submission to the SJU By — Representatives of beneficiaries involved in the project

Name/Beneficiary	Position/Title	Date
André Oliveira / TEKEVER ASDS	Business Development Manager	06/01/2017

### Rejected By - Representatives of beneficiaries involved in the project

Name/Beneficiary	Position/Title	Date
------------------	----------------	------

### Document History

Edition	Date	Status	Author	Justification
00.00.01	06/11/2016	First content input	TEKEVER ASDS	
00.00.02	26/11/2016	Integration of content	CSEM	
00.00.03	07/12/2016	Integration of content	SHARK.AERO	
00.00.04	12/12/2016	Integration of content	TEKEVER ASDS	
00.00.05	04/01/2017	Integration of content	THALES AVIONICS	
00.00.06	05/01/2017	Final harmonization	André Oliveira	
00.01.00	06/01/2017	Issued	André Oliveira	



---

00.02.00	15/06/2017	Second issue	André Oliveira	Addressing remarks of SESAR JU
----------	------------	--------------	----------------	--------------------------------

---



# NAVISAS

## NAVIGATION OF AIRBORNE VEHICLE WITH INTEGRATED SPACE AND ATOMIC SIGNALS

This project has received funding from the Single European Sky ATM (Air Traffic Management) Research Joint Undertaking under grant agreement No 699387.



### Abstract

---

This document comprises the work performed under WP3 - State-of-the-art and analysis of building blocks for small aircraft APNT (Months: 3-10) of NAVISAS. It provides an overview of the state of the art of navigation techniques (including those applicable to small aircraft) and an analysis of the state of the art for atomic clocks and atomic gyros. Furthermore, it reports on the experiments carried out to verify that the NAVISAS atomic gyro and atomic clock are in line with the current state of the art. At this stage of the project, the consortium has been able to achieve TRL2.5. Finally, the document proposes an operational concept for the use of NAVISAS by small aircraft.



## Executive Summary

---

The objectives of the deliverable D3.1 are to report upon the work carried out under WP3 “State-of-the-art and analysis of building blocks for small aircraft APNT” [Months: 3-10] which has the following objectives:

- To clearly define the state-of-the-art in navigation techniques, clocks and atomic gyros at the time of project execution and in the light of latest SESAR developments.
- To clarify the state-of-the-art on atomic gyros and clocks through experiments.
- To create a pool of building blocks that are in line with WP2 requirements and will serve as the solution workspace subset that will be used in WP4 for the concept design.

Concerning the first set of activities, the consortium analysed several navigation techniques including the following:

- Global Navigation Satellite System (GNSS)
- Space Based Augmentation System (SBAS)
- Ground Based Augmentation System (GBAS)
- Combination of GNSS with Inertial Navigation Systems (INS)
- Combination of INS with radar
- Combination of INS with imagery
- Beacon based navigation
  - Non Directional Beacons (NDB)
  - VHF Omnidirectional Radio range (VOR)
  - Distance Measuring Equipment (DME)
- Signals of Opportunity (SoOP) based on
  - Received Signal Strength (RSS)
  - Angle of Arrival (AOA)
  - Time Difference of Arrival (TDOA)
  - Pseudorange measurement

Not all of the techniques mentioned above apply to small aircraft. They have included in the analysis nonetheless for completeness. For all techniques, the consortium described the principle of operation, assessed the maturity of the technique (e.g. while beacon based navigation is state of play, SBAS is

state of the art and SoOP is still in infant research phases), identified the equipage and infrastructure needs and described the performances achievable.

Relevant research activities in these domains have also been identified and referenced.

The consortium concluded the majority of small aircraft (GA, VLA, UL and UAVs as defined by the project) rely on GNSS and the combination of GNSS with INS for navigation. Manned small aircraft tend to rely on GNSS receivers and make use of beacon based navigation mostly for instructional purposes. The vast majority of unmanned aircraft rely purely on GNSS or on the combination of GNSS with INS or other sensors (such as radio altimeters or imagery) to navigate and perform automatic approaches and landings. The combination of GNSS with imagery is being exploited mostly by very small UAVs flying indoors (outdoor flight tends to use the more versatile GNSS). Some small A/C also make use of SBAS but to a much smaller extent.

GBAS is almost solely used by commercial aircraft while SoOP techniques are not mature enough at the moment for regular use in aerial navigation.

Concerning the state of the art analysis of atomic clocks (MAC) and atomic gyros (Spin Nuclear Magnetic Resonance or SNMR), the consortium explained the principles of operation for each technology and performed patent surveys on both technologies. Commercial products on the market were identified and assessed. In order to make a MAC competitive, the performance in terms of frequency stability is essential but the form factor and the costs are of key importance as well. The physics package is a critical element needed to fulfill these challenges and so far no solution exists that is high performing and competitive in cost. The main aspects of the physics package are its form factor, power consumption and production cost.

The patent survey on MAC has demonstrated a peak in patent applications in this area around 2010 (coincident with major DARPA work funding). The main players in the domain are Honeywell, Microsemi and Northrop Grumman. Although Seiko/Epson is the top ranking patent applicant, they have neither a corresponding product nor a scientific demonstrator of a MAC. The high number of patents is in part due to a high number of patent families with only minor differences in the contained claims.

The consortium then explained the approaches used by different groups to realize MAC prototypes. Prototype packages developed by the following groups have been considered and presented:

- Westinghouse and Northrop Grumman
- National Institute for Standards and Technology (NIST)
- Microsemi / Symmetricom / Draper Laboratory / Sandia National Labs
- Teledyne Scientific/ Rockwell Collins / Agilent Technologies
- Honeywell
- Sarnoff / Princeton / Frequency Electronics
- MAC-TFC consortium and ISIMAC consortium
- Spectratime Orolia
- CSEM

With respect to the atomic gyros state of the art, the consortium analysed and explained the main technical aspects behind the operation and design of these devices. These include:



- Polarization, achieved through optical pumping (three different techniques are currently used);
- Precession – applying an oscillating field to induce coherence;
- Detection of the precessing nuclear magnetization, achieved through optical detection based on different techniques
  - o Dehmelt technique
  - o Faraday rotation
  - o Induction coils
  - o External magnetometers

Benchmarking of NMR gyros based on available public information was carried out (the results are summarized below). Afterwards, the consortium identified the main differences in terms of design between the NAVISAS gyro and Northrop Grumman's. Finally, the possible shared blocks between the SNMR gyro and the MAC for NAVISAS were identified:

- Same technology to fabricate MEMS cell
- Pump/probe laser
- Cell heating
- Use of the clock cell to stabilize pump laser for gyro
- Sharing of RF modulation of laser for (i) CPT (coherent population trapping) interrogation of clock and (ii) dual –frequency pumping of gyro
- Sharing of parts of magnetic shielding

In order to prepare and support the ER/IR gate at the end of the project, a TRL roadmap was developed and TRL milestones were introduced in the project Gantt chart in the Project Management Plan (PMP). During this reporting period, the consortium has managed to achieve TRL2+ through the successful of the first three steps of the TRL roadmap, as represented in the table below. The consortium carried out tests to verify the TRL of the NAVISAS gyro concept. The experimental setup and actual tests carried out as well as their results are presented. Some results of laboratory tests performed to measure key parameters of interest for the technologies of interest were obtained and the partners believe these can validate some of the assumptions of the previous maturity level concerning aspects like performance.

The final activity of WP3 was task 3.4 dedicated to the creation of a pool of building blocks in line with WP2 requirements that can serve as the subset of the solution workspace for WP4 and the beginning of the definition of the overall system at conceptual level. After internal discussion, the consortium concluded that at the current stage of development of the project (which has fulfilled its foreseen objectives) and given that a block diagram explaining the different blocks of NAVISAS was already proposed in WP2 (refer to Figure 41 elsewhere in this document) it would not make sense to carry out these activities as the team would be repeating work from WP2 and unable to progress more on the detailing of the blocks. Alternatively, it was agreed that NAVISAS was missing an operational concept for small A/C. Therefore, the consortium agreed to pursue the development of one or more operational concepts that explain how the consortium envisages the usage of NAVISAS by the small

A/C universe. The idea behind this is for the operational concepts to provide a bigger picture on what value NAVISAS can bring to small aircraft and help understand what is achievable and under what conditions. After this analysis is completed it will be possible to progress on the building blocks detailing work that was initially planned for WP3.4.

The discussions between partners have yielded the following potential operational concepts based on the assumption that baseline navigation in small aircraft (GA, VLA, UL and UAVs) is performed by using a combination of INS and GNSS:

- NAVISAS MAC can be used to detect GNSS spoofing - This case is applicable in all flight phases, all flight rules (IFR and VFR) and relevant for both manned and unmanned small aircraft;
- An INS comprising a set of 3 NAVISAS Gyros combined with accelerometers and a Kalman filter can be used to provide navigation in cases where GNSS signals are lost
  - o Under VFR conditions, NAVISAS can be used to provide conditions similar to IFR but with less constraints;
  - o Under IFR conditions and when flying en-route, a small aircraft can rely on the NAVISAS based INS to “buy time” and coast until GNSS signals are reacquired. If after a pre-determined period GNSS is still not available the A/C will have to revert to an emergency procedure;
  - o UAVs may use the NAVISAS gyros to carry out emergency procedures;
  - o The NAVISAS based INS may be used to reacquire GNSS signals faster;
  - o It may be possible to use the NAVISAS based INS to still get GNSS signals under jamming conditions;

The NAVISAS system comprising the GNSS plus MAC plus set of 3 gyros and accelerometers can be used to carry out auto-land operations for both unmanned and manned small aircraft as long as an additional sensor is considered to increase the vertical accuracy (e.g. radio altimeters or LIDAR).

Finally, a set of operational concepts for how NAVISAS technologies could be used in RPAS and GA / VLA is presented. The relationship between NAVISAS technological blocks and the SESAR ATM masterplan is established and a possible roadmap for developing an A-PNT based on NAVISAS technology is presented.

# Table of Contents

---

Abstract.....	4
<i>Executive Summary</i> .....	5
<i>Table of Contents</i> .....	9
<i>List of Tables</i> .....	11
<i>List of Figures</i> .....	12
<i>List of Acronyms</i> .....	15
<b>1 Introduction</b> .....	17
Scope and Structure of the document.....	17
<b>2 State of the Art in navigation</b> .....	19
2.1 Beacon based techniques .....	19
2.2 Global Navigation Satellite Systems (GNSS) .....	22
2.3 Space Based Augmentation System (SBAS).....	25
2.4 Ground Based Augmentation System (GBAS).....	28
2.5 Inertial Navigation Systems (INS).....	30
2.6 GNSS plus INS.....	32
2.7 INS plus Radar .....	34
2.8 INS plus imagery.....	36
2.9 Signals of Opportunity (SoOP) .....	37
2.10 Navigation in GA, VLA and Ultra-Lights.....	40
2.11 Navigation in UAVs and Drones .....	43
2.12 Compatibility with SESAR concepts .....	44
<b>3 State of the Art review on clocks and atomic gyroscopes</b> .....	49
3.1 Miniature atomic clocks .....	49

3.2	Miniature atomic gyroscopes .....	60
<b>4</b>	<b><i>Experiments to clarify SoA of technology on integration of clocks and atomic gyroscopes .....</i></b>	<b>77</b>
4.1	Relation with TRL management plan .....	77
4.2	Test 1: MEMS cells fabrication and characterization .....	78
4.3	Test 2: Experimental setup .....	81
4.4	Test 3: Residual fields measurements .....	85
<b>5</b>	<b><i>Operational Gains of a NAVISAS based A-PNT .....</i></b>	<b>88</b>
5.1	NAVISAS Operational Concepts .....	88
5.2	Method applied to define NAVISAS visions and operational concepts .....	91
5.3	NAVISAS proposed technologies.....	91
5.4	Foreseen operations.....	92
5.5	What can NAVISAS contribute .....	94
5.6	NAVISAS relation to the SESAR ATM Master Plan .....	96
<b>6</b>	<b><i>Conclusion .....</i></b>	<b>103</b>



# List of Tables

---

Table 1 – Acronyms and abbreviations. ....16

Table 2: Tasks of WP3. ....17

Table 3: comparison between satellite navigation and inertial navigation .....33

Table 4– Summary of alternate A-PNT technologies .....48

Table 5: Comparison of relevant oscillators and clocks. The last column also presents the C-MAC PP target specifications. ....52

Table 6: Performance requirements for different classes of gyroscopes .....62

Table 7 - Summary table of NMRG performances .....75

Table 8 – List of tests to support NAVISAS TRL progression.....78

Table 9 – Output power characterization of the cell heating unit .....84

Table 10 – Residual fields .....87

# List of Figures

---

Figure 1 - VOR/DME beacon.....	21
Figure 2 - Comparison between the constellations of several GNSS .....	23
Figure 3 - Typical General Aviation grade receiver (Garmin aera 796) .....	24
Figure 4 - Typical UAV receiver (u-blox LEA-M8T).....	25
Figure 5 - Global coverage of several SBAS .....	27
Figure 6 - Architecture of GBAS.....	29
Figure 7 - Two examples of inertial platforms. Left: a breakout board of the Invensense MPU-6050. Right: The Honeywell HGU1930 .....	32
Figure 8 - The Trimble AP20, a GNSS + Inertial platform which can be used for airborne applications	34
Figure 9: Latest Garmin G1000 NXi cockpit.....	41
Figure 10: Garmin G1000 architecture diagram.....	43
Figure 1. Bloc diagram of a MAC (i.e. a passive atomic clock) .....	51
Figure 2: Left: Number of patent applications for year related to MACs. Right: Top 19 patent assignees focusing on MAC PPs (# patents families related to MAC PPs per assignee) .....	53
Figure 3: Westinghouse / Northrop Grumman PP .....	54
Figure 4: NIST PP .....	54
Figure 5: Microsemi / Symmetricon / Draper Lab / Sandia National Labs PP .....	55
Figure 6: Teledyne / Rockwell Collins /Agilent PP .....	56
Figure 7: Honeywell PP.....	57
Figure 8: Sarnoff / Princeton /frequency Electronics PP .....	58
Figure 9: MAC-TFC PP .....	58
Figure 10: Spectratime PP .....	59
Figure 11: CSEM PP .....	60





Figure 12: Gyroscopes used for navigation and their performances .....	63
Figure 13 – Left: ARW as a function of signal-noise ratio and relaxation time, Ref [39]. Right: bias instability due to stray magnetic fields for different noble gas nuclei, Ref [39]. .....	65
Figure 14 - Principle of operation of an NMR gyroscope, Ref [39].....	66
Figure 15 - Scheme of the Litton gyroscope. From Ref [54].....	70
Figure 16 - Gyro internal structure, physics package of the latest version .....	72
Figure 17 - Schematic of the NIST gyroscope. From Ref [58]. .....	74
Figure 18 - Schematic diagram of the working principle of the differential magnetometer .....	74
Figure 19 – NAVISAS TRL roadmap.....	78
Figure 20 - Description of the MEMS cells. Left: wafer showing cells with different diameters. Middle-Right: Computer simulations of a mounted cell.....	79
Figure 21 – MEMS cells fabrication process.....	80
Figure 22 – Simulated absorption spectrum .....	81
Figure 23 – Absorption measurement .....	81
Figure 24 - Schematics and picture of the setup with closed shielding .....	82
Figure 25 - a) Test spherical cell with 3D printed ABS + resin cell and ferrules mount. To improve heating efficiency, black aluminium foil tape (Thorlabs AT205-1) is glued on the cell. b) MEMS cell mounted on machined Teflon holder, rotating ferrule holders are 3D printed with a resin. c) 18 W, 980 nm diode laser mounted on a cooling tower. d) Test spherical cell mounted inside the Hemholtz coils and probe-beam mirrors support that is sliding inside the shielding. ....	83
Figure 26 – Left: Spherical test cell, Right: 4 mm Ø MEMS cell.....	84
Figure 27 – Test spherical cell absorption spectra .....	85
Figure 28 – Magnetic fields axis definition with nT/mA scales .....	85
Figure 29 – Left: Signal measured on PD1 for different pump powers (probe beam removed). $B_z$ is swept at 1 Hz. $B_x=0$ , 50 kHz RF on coil Y. Right: position of the Rb87 and Rb85 dips as a function of the $B_z$ field. ....	86
Figure 30 - Left: Signal measured on PD1 for different pump powers (probe beam removed). $B_x$ is swept at 1 Hz around zero. $B_z=B_y=0$ . Right: position of the maxima as a function of the $B_x$ field. ....	87
Figure 41: Preliminary NAVISAS functional block diagram (taken from NAVISAS D2.1). ....	88



## List of Acronyms

---

Acronym / Abbreviation	Meaning
AM	Amplitude Modulation
ANSP	Air Navigation Service Provider
AoA	Angle of Arrival
APNT	Alternative Positioning, Navigation and Timing
ATM	Air Traffic Management
CNS	Communication, Navigation and Surveillance
CS	Certification Specifications
DF	Direction Finder
DGNSS	Differential GNSS
DME	Distance Measuring Equipment
EASA	European Aviation Safety Agency
EGNOS	European Geo-stationary Navigation Overlay System
ELT	Emergency Locator Transmitter
EPIRB	Emergency Position Indicating Radiobeacon
EVS	Enhanced Vision System
FAA	Federal Aviation Authority
FMS	Flight Management System
FOG	Fibre Optic Gyro
GA	General Aviation
GAGAN	GPS Aided GEO Augmented Navigation
GBAS	Ground Based Augmentation System
GLS	GBAS Landing System
GNSS	Global Navigation Satellite System
HEO	Highly Elliptical Orbit
IAOPA	International council of Aircraft Owner and Pilot Associations
ICAO	International Civil Aviation Organization
IFALPA	International Federation of Air Line Pilots' Associations
IFR	Instrument Flight Rules
IFR	Instrument Flight Rules
ILS	Instrument Landing System
IMG	Industry Management Group

IMU	Inertial Measurement Unit
INS	Inertial Navigation System
ION	Institute of Navigation
LIDAR	Light Distance and Ranging
LORAN	Long Range Navigation
MAC	Miniature Atomic Clock
MAG	Miniature Atomic Gyroscope
MEMS	MicroElectroMechanical Systems
MEO	Medium Earth Orbit
NDB	Non Directional Beacon
PBN	Performance Based Navigation
PP	Physics Package
RAIM	Receiver Autonomous Integrity Monitoring
RLG	Ring Laser Gyro
RNAV	Area Navigation
RNP	Required Navigation Performance
RPAS	Remotely Piloted Aircraft System
RSS	Received Signal Strength
SBAS	Space Based Augmentation System
SNMR	Spin Nuclear Magnetic Resonance
SoOP	Signals of Opportunity
TBD	To Be Determined
TDoA	Time Difference of Arrival
TRL	Technology Readiness Level
UAS	Unmanned Aerial System
UAV	Unmanned Aerial Vehicle
UL	Ultra Light
VDB	VHF Data Broadcast
VFR	Visual Flight Rules
VFR	Visual Flight Rules
VLA	Very Light Aircraft
VOR	VHF Omnidirectional Range
VSG	Vibrating Structure Gyro
WAAS	Wide Area Augmentation System
WAM	Wide Area Multilateration
WP	Work Package

Table 1 – Acronyms and abbreviations.

# 1 Introduction

---

WP3 aimed to establish the state of the art in terms of navigation techniques specifically for small A/C as defined by the project and commercial aviation in general and in the field of atomic clocks and atomic gyros. It was also its objective to define and carry out a number of experiments designed to clarify the state of the art on the integration of atomic clocks and atomic gyros and to progress the TRL of both technologies. Finally, it aimed to analyse and propose descriptions of the building blocks of NAVISAS to be used for the development of a APNT system for small aircraft. The WP was divided into four tasks as represented below in Table 2.

WP3 Task	Title	Leaders
T3.1	State-of-the-art in navigation	TEK, SHARK
T3.2	State-of-the-art review on clocks and atomic gyros	CSEM
T3.3	Experiments to clarify state-of-the-art of technology on integration of clocks and atomic gyroscopes	CSEM, TEK
T3.4	Analysis of building blocks for small aircraft APNT	TEK, TAV

Table 2: Tasks of WP3.

The document reports on the work carried out under the tasks above and provides descriptions and summaries of the analyses carried out.

## Scope and Structure of the document

The scope of this document is to clearly define the state of the art for the domains that are directly related to NAVISAS and its technologies, i.e. aircraft navigation techniques and miniaturized atomic clocks and miniaturized atomic gyroscopes. The steps taken by the consortium to verify the technology readiness level of the proposed miniaturized atomic gyro are also described and the results obtained by the laboratory experiments are given. Finally, after identifying a gap concerning the possible usage

of NAVISAS by small aircraft, the consortium presents the possible operational gains for an APNT system based on NAVISAS for small aircraft.

The document is structured as follows:

Chapter 2 Provides the state of the art on navigation techniques and current SESAR work on APNT and possible applicability to small aircraft.

Chapter 3 Presents the state of the art analyses for both the miniaturized atomic clocks and the miniaturized atomic gyros.

Chapter 4 Explains the steps taken to assess the current TRL of the NAVISAS atomic gyro and presents the experimental setup used by the consortium to implement the tests that enable the conclusion that TRL2.5 has been achieved.

Chapter 5 Provides a rationale for not advancing further on the development of the building blocks of NAVISAS and proposes a set of operational gains for a NAVISAS based APNT system.

Chapter 6 Comprises the conclusions derived from the various activities carried out.

## 2 State of the Art in navigation

---

Concerning the first set of activities of WP3, the consortium analysed several navigation techniques including the following:

- Global Navigation Satellite System (GNSS)
- Space Based Augmentation System (SBAS)
- Ground Based Augmentation System (GBAS)
- Combination of GNSS with Inertial Navigation Systems (INS)
- Combination of INS with radar
- Combination of INS with imagery
- Beacon based navigation
  - Non Directional Beacons (NDB)
  - VHF Omnidirectional Radio range (VOR)
  - Distance Measuring Equipment (DME)
- Signals of Opportunity (SoOP) based on
  - Received Signal Strength (RSS)
  - Angle of Arrival (AOA)
  - Time Difference of Arrival (TDOA)
  - Pseudorange measurement

Not all of the techniques mentioned above apply to small aircraft. They have been included in the analysis nonetheless for completeness. For all techniques, the consortium describes the principle of operation, assesses the maturity of the technique (e.g. while beacon based navigation is state of play, SBAS is state of the art and SoOP is still in infant research phases), identifies the equipage and infrastructure needs and describes the performances achievable.

Relevant research activities in these domains have also been identified and referenced.

Afterwards, an overview of what techniques are currently in use by small aircraft is presented. The consortium also addresses current SESAR R&D activities concerning APNT and assess their possible applicability to small aircraft (GA, VLA, UL and UAVs).

### 2.1 Beacon based techniques

## 2.1.1 Principle of operation

The use of radio beacons for navigation has been the primary form of navigating in aviation for years. Ground stations, the location of which is given in charts, broadcast specific signals that help locate the aircraft in relation to the station. This relative position can be known in terms of heading, distance, or both.

### 2.1.1.1 Non Directional Beacons (NDB)

NDB's are an inexpensive way to implement radio beacons for navigation. An omnidirectional antenna broadcasts a signal, the frequency of which is known and between 200 MHz and 1.6 GHz. Aboard the aircraft, a system with a directional, rotating antenna can tell in which the direction the signal is the strongest. Using that information, combined with the current heading of the aircraft, the pilot or navigator is able to reduce the possible position of the aircraft to two opposed cones, centred on the beacon, taking into account inaccuracies of the system. Using two of these measurements, the location of the aircraft can be deduced.

### 2.1.1.2 VHF Omnidirectional Range (VOR)

The VOR is used to know the relative position of the aircraft. Unlike NDB's, the aircraft equipment requires no moving parts. The station broadcasts one omnidirectional signal at all times (a 30 Hz signal modulated), and one rotating signal that rotates at 30 revolutions per second. The phase difference between the two signals is then the angle between magnetic north at the station and the aircraft. An indicator in the instrument panel shows this angle, which is known as a radial.

### 2.1.1.3 Distance Measuring Equipment (DME)

The DME is a pulse-based system that allows an aircraft to know its distance to a station. The aircraft interrogates a station with a set of pulses. The ground beacon then retransmits the pulses to the aircraft in a different frequency, after a set delay of 50 microseconds. From the time delay, the distance to the station can be calculated. With this information, the aircraft position can be reduced to a toroid region centred on the station. DME's are frequently coupled with VOR's to produce an estimate of the exact aircraft position. Each beacon is required to handle at least 50 aircraft simultaneously, however 100 is a more typical number.





Figure 1 - VOR/DME beacon

#### 2.1.1.4 Instrument Landing System (ILS)

The ILS is a beacon based navigation system that is meant to assist with approaches and landings, especially in conditions of poor visibility. For each ILS installation, three types of signals are provided:

- Localizer – At the end of the runway, opposite of the approaching direction, two AM signals (at 90 and 150 Hz), slightly offset from the runway centre line, are broadcast. Aboard the aircraft, the amplitudes of the two signals are compared. If they are the same, the aircraft is horizontally aligned with the runway centreline. These signals provide lateral guidance;
- Glide Slope – Beside the runway, another pair of AM signals work in the same way as the Localizer, but with the equal-amplitude region on an optimal glide path, thus providing vertical guidance;
- Marker beacons – Placed at known distances from the runway, these alert pilots of their progress along the glide path.

#### 2.1.2 Maturity

These systems are fully developed and deployed. For commercial aircraft, the use of these technologies is being phased out in favour of GNSS navigation. They are still used, for some application, such as marking the location where an approach or landing using ILS is to be initiated.

They're still used for instructional purposes in general aviation, but the GNSS receivers in this type of aircraft typically offer databases of the ground beacons, so they can be used for flight planning, not necessarily using the beacons' signals to determine the position.

For UAVs, this type of equipment doesn't pose a significant advantage, so it's disregarded in favour of GNSS + Inertial navigation.

### 2.1.3 Equipage and infrastructure

This type of navigation is dependent on the ground stations on the ground. Furthermore, required on-board equipment includes antennas and receivers/transmitters to communicate with the beacons, and means to display the location or make it useful, such as display panels or interfacing with Flight Management Systems.

### 2.1.4 Performance

Minimum accuracy for NDB's, as dictated by ICAO, is of  $\pm 5^\circ$ . At 100 NM, this results in an accuracy of 8.72 NM.

For VOR, the predictable accuracy is of  $\pm 1.4^\circ$ . At 150 NM away from the beacon, this means that the accuracy is of  $\pm 3.66$  NM. However, studies show that 99.94% of the time, the error does not exceed  $\pm 0.35^\circ$ . At the same distance of 150 NM, the accuracy is  $\pm 0.92$  NM.

The accuracy of DME is  $\pm 185$  m. It's important to state that this distance is in straight line from the station to the aircraft, and takes into account the altitude difference.

## 2.2 Global Navigation Satellite Systems (GNSS)

### 2.2.1 Principle of operation

Navigation through GNSS is based on signals transmitted by the satellites. These transmit parameters that are used to locate the satellite vehicle precisely on orbit, as well as periodical timing information. By measuring the travel time of the signals pertaining to several satellites (which can be distinguished since they have unique signatures), the receiver's position, velocity and time (PVT) can be determined with accuracy. This travel time is computed by differencing the arrival and departure time of the signals, which are contaminated with clock errors from both the receiver and satellite. For this reason, this distance is known as a pseudorange.

While this positioning can be done autonomously, it can also be complemented with data from nearby base stations, the location of which is known with a very high degree of accuracy. This type of positioning is known as Differential GNSS, or DGNSS, and relies on the fact that for nearby receivers, the signal path is roughly the same, and so are the atmospheric delays that occur on the troposphere

and ionosphere, which can be cancelled by differencing pseudoranges. Furthermore, the satellite and receiver clock errors can be cancelled by successively differencing measurements, which allow relative positioning to be done with a higher degree of accuracy than that of autonomous positioning.

## 2.2.2 Maturity

A multitude of GNSS are deployed and ready for use. The United States' Global Positioning System (GPS) and Russian GLONASS are the systems that display the highest level of maturity, having full constellations operational. Both GPS and GLONASS exclusively use constellations in Medium Earth Orbits (MEO), with GPS using 6 distinct orbital planes with an inclination of 55 degrees, and GLONASS using 3 orbital planes with a 64.8 degree inclination.

The People's Republic of China is currently deploying the Beidou System, with an expected global coverage by 2020. It is expected to contain geostationary, inclined geosynchronous and medium-earth orbit satellites. At this point, coverage is not global, and started in the vicinity of China, expanding with each satellite launch. The full constellation is expected to have 35 satellites.

The European Union has also launched an effort to deploy a GNSS. Called Galileo, and developed by the European Space Agency in conjunction with the European GNSS Agency. The system started operating in December 2016, initially with 18 satellites in orbit. The full constellation is expected to have 27 active satellites and 3 spares, and to be operational by 2020.

There are also regional satellite navigation systems, developed to be used autonomously or in conjunction with data from other global systems. India has the Navigation Indian Constellation (NAVIC, formerly Indian Regional Navigational Satellite System or IRNSS), with seven satellite vehicles which orbit above the Indian subcontinent, while Japan's Quasi-Zenith Satellite System consists of three satellites in Highly Elliptical Orbits (HEO) and one geostationary satellite.

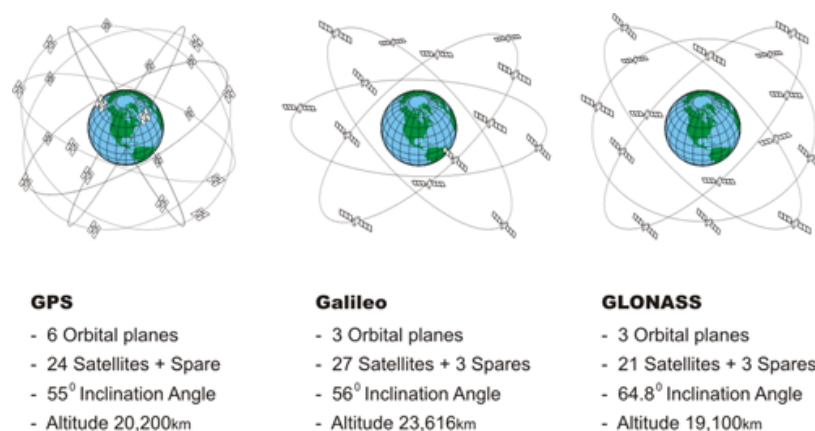


Figure 2 - Comparison between the constellations of several GNSS

### 2.2.3 Equipage and infrastructure

Global Navigation Satellite Systems are typically divided into three segments:

- The **Space Segment** consists of the satellite constellation, which, as mentioned before, regularly broadcast signals pertaining to the satellite vehicle's position and time.
- The **Control or Ground Segment** consists of the station or network of stations that monitors the health and orbits of the satellites, issuing corrections, predicting the orbits and making sure the broadcast information is accurate and up to date.
- The **User Segment** is made up of all the receivers that use the signals to determine their position, velocity and time. Since there is no communication from the receivers to the satellites, the capacity of this kind of systems is limitless.

Autonomous GNSS is used in hobby grade UAVs for mission planning and path following, but its performance in terms of integrity is not suitable for civil aviation, in particular for critical flight phases such as approach and landing. Thus, augmentation systems have been developed to increase performance. These can be satellite or ground based.

Hobby grade UAVs usually receive location from GPS receivers using the NMEA standard, offered by makers such as SiRF and u-blox. For General Aviation use, Garmin is the most popular maker, and offers a range of GPS units which feature databases of conventional waypoints, such as VOR and DME beacons, and newer RNAV waypoints.



Figure 3 - Typical General Aviation grade receiver (Garmin aera 796)



Figure 4 - Typical UAV receiver (u-blox LEA-M8T)

## 2.2.4 Performance

The main advantage of GNSS positioning is the ability to accurately determine the position and velocity of a vehicle in a continuous way, regardless of weather conditions and amount of traffic. Commercially available receivers are usually able to compute position information with an accuracy of 10 meters or better.

Despite the GPS having a good track record for availability, autonomous GNSS are not totally dependable and are not to be used as the sole means for navigation. A large concern with GNSS is that of integrity, or the ability of the system to tell whether it should be used for navigation. To comply with RNP, the receiver is required to feature Receiver Autonomous Integrity Monitoring (RAIM), which provides integrity to the system by detecting failures in satellite signals and disregarding them from the position computation. Some installations have been certified for B-RNAV or RNAV 5 (accurate within +/- 5 NM 95% of time) under IFR.

## 2.3 Space Based Augmentation System (SBAS)

### 2.3.1 Principle of operation

Satellite Based Augmentation Systems (SBAS) are a type of system that complements GNSS solutions by improving accuracy, reliability or availability. Ground monitoring stations perform ranging measurements to GNSS satellites and upload correction data to satellites. The satellites then broadcast correction parameters pertaining to the GNSS vehicles (such as finer clock corrections or more accurate ephemerides) or the propagation medium (like the ionosphere and troposphere). These corrections

can't account for the receiver-related errors (such as multipath and the local characteristic of tropospheric effects). Coverage of these systems is usually reserved to a continent or region. Apart from that, SBAS vehicles can be used as a generic GNSS vehicle, its pseudorange aiding the position computation. Errors detected by SBAS are transmitted and can be used by the end user within as little as six seconds of a malfunction.

### 2.3.2 Maturity

There are a number of SBAS, their maturity ranging from deployed and ready to be used, to decommissioned in favour of newer, better systems that cover the same area:

- The Wide Area Augmentation System (WAAS) is developed by the United States' Federal Aviation Agency (FAA). It consists of a network of 38 ground stations in the continental United States, Alaska, Hawaii, Canada and Mexico, three geostationary satellites, and its intended area of coverage is North America. It only supports GPS.
- The European Geostationary Navigation Overlay Service (EGNOS) is developed by the European Space Agency, the European Commission, and EUROCONTROL. The ground network consists of 34 Receiver Integrity Monitoring Stations (RIMS), which receive the GNSS signals, 4 Master Control Centers (MCC – one active, one hot backup, and two cold backups), which process the data, and 6 Navigation Land Earth Stations (NLES – two for each satellite for redundancy reasons), which upload the data to the satellites. The constellation consists of three geostationary satellites, and its intended area of coverage is Europe. It provides corrections for GPS, GLONASS and Galileo.
- Japan's MTSAT Satellite Augmentation System (MSAS) is owned and operated by the Japanese Meteorological Agency and Japanese Ministry of Land, Infrastructure, and Transport. It supplements the GPS in a similar way to the former two systems. Four ground stations receive the satellite signals, which are forwarded to two Master Control Stations (one for each satellite in orbit), which process them and calculate the corrections and send them to the satellites.
- India's GPS Aided Geo Augmented Navigation System (GAGAN) provides SBAS service on the Indian subcontinent. It features three geostationary satellites, maintained by two base stations that process the data from 15 reference stations.
- The Russian Federation is currently developing the System for Differential Corrections and Monitoring (SDCM), to complement the GPS and GLONASS systems in Russia. Three satellites have been launched, which broadcast corrections based on data collected by 19 stations in Russia and 5 stations abroad. One central processing facility in Moscow processes and uploads the data, along with one reserve facility.
- The Satellite Navigation Augmentation System (SNAS) is being developed by China, although very little public information is known at the moment.
- The StarFire system has been developed by the John Deere Corporation, to be used with their GPS receivers, for farming and field surveying applications.



- Canada had the GPS Correction (GPS-C) service, which was deactivated since it required a separate receiver, making it less cost effective than WAAS or StarFire.

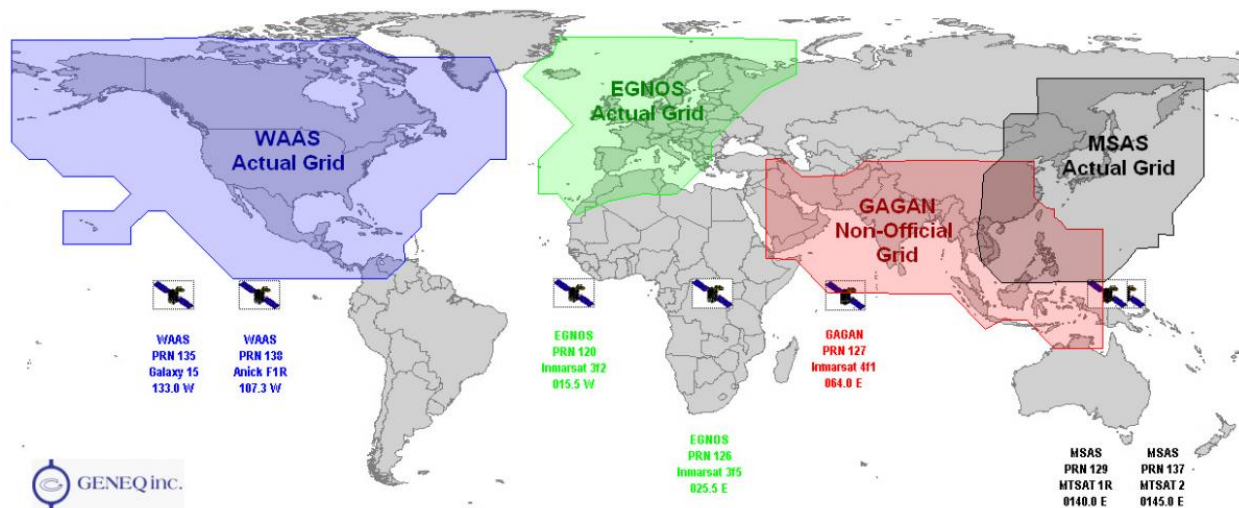


Figure 5 - Global coverage of several SBAS

### 2.3.3 Equipage and infrastructure

Satellite Augmentation of GNSS is reliant on the constellation and ground control network of each system, which is particular to each implementation. Furthermore, the GNSS receiver onboard the aircraft has to be compatible with SBAS messages. As explained before, the SBAS satellites can be used as a generic GNSS vehicle, computing the pseudorange from the signal travel time, but its greatest advantage are the correction messages that allow the receiver to cancel a part of the satellite and propagation medium-related errors.

### 2.3.4 Performance

Augmentation systems are, as stated before, not used independently, but instead improve already available GNSS. The main concern, for airborne applications, is that of integrity, or the ability to tell whether the system should be used for navigation purposes. A secondary objective is to increase precision. Achievable SBAS performance requirements include:

- En-route RNP 4 (Oceanic/Continental), for a horizontal accuracy of 4 NM (95%);
- En-route RNP 2 (Continental), for a horizontal accuracy of 2 NM (95%);

- En-route RNP 1 (Terminal), for a horizontal accuracy of 1 NM (95%);
- Non-Precision Approach, for a horizontal accuracy of 220 m (95%);
- APV-I, for a horizontal accuracy of 16 m, and vertical accuracy of 20 m (95%);
- APV-II, for a horizontal accuracy of 16 m, and vertical accuracy of 8 m (95%);
- Category I precision approach, for a horizontal accuracy of 16 m, and a vertical accuracy between 6 and 4 m.

## 2.4 Ground Based Augmentation System (GBAS)

### 2.4.1 Principle of operation

Many of the principles that SBAS is based on apply to GBAS. However, GBAS is intended to have a much smaller area of coverage, generally in the vicinity of an airport. This type of system was designed to aid in the approach and landing phases of flight, providing an alternative to the Instrument Landing System (ILS). The implementation of GBAS to provide approach and landing capability is called GLS. Several GNSS receivers in the area forward the satellite signals to a base station, which computes the corrections and broadcasts them. The messages standard includes, in addition to the GNSS differential corrections and integrity information, GBAS related data, and information about the Final Approach Segment, with support for more messages.

The main advantage of GBAS/GLS over ILS is in the fact that for one airfield, only one GBAS equipment is required, regardless of the number of runways. For ILS, one localizer/glide slope pair is needed for each runway and heading. It also frees up the electromagnetic spectrum, since one GBAS station is capable of broadcasting information for up to 48 approach procedures.



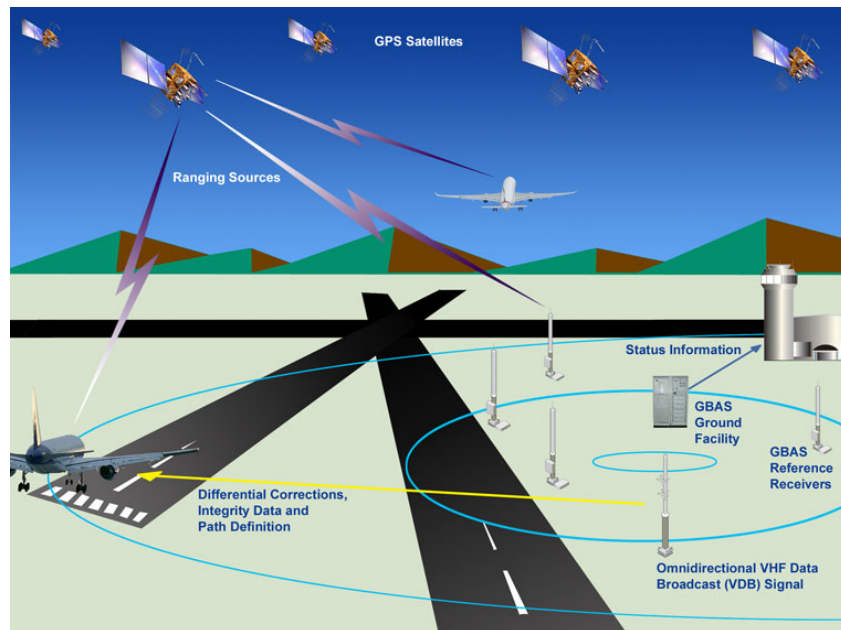


Figure 6 - Architecture of GBAS

## 2.4.2 Maturity

Several airports worldwide have approved systems in place for Category I precision approaches. As of February 2015, two locations in the United States (Newark and Houston) and twenty in the rest of the world (including four in Europe and fifteen in Russia) supported the GBAS Landing System (GLS), with plans to implement the system in more locations.

Several avionics manufacturers provide aircraft equipment that is approved by the regulating bodies to be used for GBAS approaches, and are being installed in new commercial aircraft by Boeing and Airbus. For small aircraft, it is a technology with interest in the General Aviation category, since it offers an alternative to the ILS.

## 2.4.3 Equipage and infrastructure

Since it augments one or several GNSS, the basic equipment for these systems is required on and off-board the aircraft. These include the satellites and ground stations which monitor them and control them, and the basic GNSS equipage aboard (receiver(s) and antennae).

Furthermore, each airfield requires several GNSS receivers and antennae, a unit that retrieves the data from the receivers and processes it, and a radio transmitter to broadcast the GBAS signal. These transmissions happen over VHF Data Broadcast (VDB).

## 2.4.4 Performance

GBAS is currently rated for Category I approaches. The requirements include

- Horizontal accuracy of 16 m (95%);
- Vertical accuracy between 6 and 4 m (95%);
- A Time-to-alert of 6 seconds, in case of malfunction;
- Availability of 99% or better.

## 2.5 Inertial Navigation Systems (INS)

### 2.5.1 Principle of operation

Inertial Navigation Systems allow the determination of vehicle position and attitude, by directly measuring the accelerations and angular velocities the aircraft is subjected to.

This has three main advantages:

- The sensors have very quick response, so very high data rates and bandwidths can be achieved;
- No external equipment is required, so the system is self contained and not vulnerable to jamming. It's also not dependant on ground stations or satellite vehicles;
- It provides very accurate measurements of position, ground speed, azimuth, and vertical.

There are, however, several disadvantages:

- The position accuracy degrades over time;
- High end applications are expensive, especially if we factor that multiple sensors of the same type are often necessary for redundancy reasons;
- The system needs to be initially aligned. It is commonly done when the aircraft is parked, since airfield charts offer coordinates for its apron spaces or gates;
- The accuracy of the solution is dependent on the manoeuvres performed by the vehicle.

Inertial navigation systems are almost always the conjunction of two types of sensors:

- Accelerometers – measure acceleration along a particular axis. Acceleration is then integrated over time once to deduct velocity, and integrated one more time to compute displacement from original position. The basic concept is that of sensing the force applied on a loosely suspended mass. Since the equipment is rigidly attached to the aircraft body, this correlates to the acceleration the aircraft is experiencing.
- Gyroscopes – provide a measurement of the attitude of the aircraft. Early implementations were spinning masses or wheels, which tend to hold their position, and as such provide the



angular displacement from a nominal position. More sophisticated models use microelectromechanical systems (MEMS), or take advantage of the Sagnac effect (fiber optic gyroscope – FOG, and ring laser gyroscope – RLG), or the Coriolis effect (Vibrating Structure Gyroscope – VSG)

Since these devices measure accelerations and angular velocities in one axis, three of each, perpendicular to each other, are needed to completely define the aircraft orientation and position.

## 2.5.2 Maturity

The devices that allow inertial navigation to be performed are available on the market, its cost varying from a few Euros for a six axis Gyroscope + Accelerometer device (such as the MPU-6050 from InvenSense, frequently used in hobby grade UAVs) to hundreds of thousands of Euros for navigation grade inertial navigation systems (such as the Honeywell HG9900, used in commercial aircraft which usually employ multiple units to average the measurements and for redundancy purposes). Even higher end solutions, such as those for marine applications, can cost in the neighbourhood of 1 million Euros. Apart from the more accurate measurement, higher end devices support higher sample rates, and display less degradation over time.

## 2.5.3 Equipage and infrastructure

Inertial navigation requires no external equipment. Commercial products combine accelerometers and gyroscopes for all three axes, and these communicate directly with the flight computer, be it a microcontroller for hobby grade UAVs, or a Flight Management System. These systems are also in charge of the initial calibration of the Inertial Navigation System.

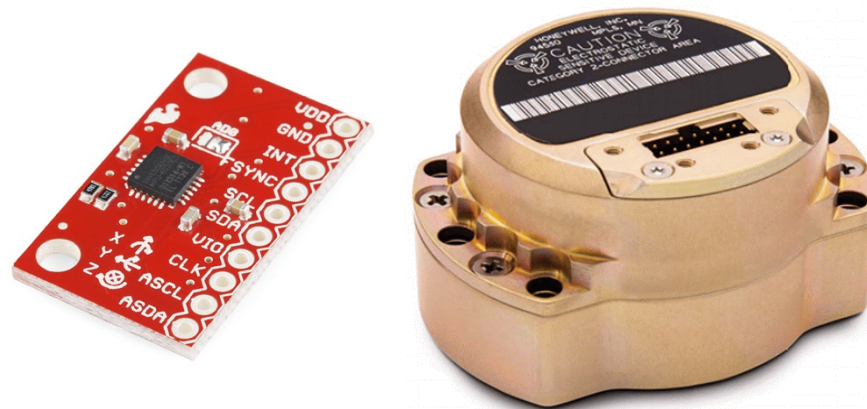


Figure 7 - Two examples of inertial platforms. Left: a breakout board of the Invensense MPU-6050. Right: The Honeywell HGU1930

## 2.5.4 Performance

Since we are only able to directly measure accelerations and angular velocities, any acceleration error will get amplified quadratically over time. For this reason, inertial measurements are never used exclusively, since implementations can diverge up several thousand kilometres within one hour for cheaper platforms. Navigation grade platforms will typically diverge a few kilometres within one hour, and this can be mitigated by using several independent sensors and using algorithms such as Kalman Filtering. The independence that INS displays of other external navigations aids made it optimal for use in oceanic operations, since the navigational requirements in terms of accuracy were of 20 nautical miles across track, and 25 nautical miles along track.

## 2.6 GNSS plus INS

### 2.6.1 Principle of operation

Combining GNSS and Inertial Navigation brings a number of advantages. First of all the GNSS position solution does not drift, so it can be used to tell whether the inertial platform is drifting too much. Conversely, inertial platforms reach much higher sampling rates than GNSS, so they can provide position between GNSS updates, or the signal is lost. The measurements from the several systems are used by a Kalman Filter or Extended Kalman Filter to provide position and attitude updates. The following table summarizes the main characteristics of each technique.

Satellite navigation	Inertial navigation
<ul style="list-style-type: none"> <li>– Absolute position data</li> <li>– Limited resolution</li> <li>– Slow</li> </ul>	<ul style="list-style-type: none"> <li>– Drift in integrated terms</li> <li>– High resolution (rel.)</li> <li>– Fast (kHz)</li> </ul>



– Worse at orientation	– Best at orientation
– Easily disturbed	– Disturbance-free (no external ref.)
– Best at X&Y	– Best at Z

**Table 3: comparison between satellite navigation and inertial navigation**

## 2.6.2 Maturity

GNSS+INS navigation is currently available for commercial applications in every category of aircraft. For commercial aircraft, it is the main way of navigating oceanic airspace and continental remote areas. For small aircraft, UAVs use the combination of sensors for control and path following purposes; General Aviation users utilize the inertial platform for control of the aircraft, while GNSS augments the conventional navigation experience by implementing databases of conventional beacons (e.g. VOR, NDB) and newer RNAV waypoints, without the need to resort to flight charts.

## 2.6.3 Equipage and infrastructure

The inertial part of the system is, as stated before, self-contained and independent of external navigation aids. It requires one (or several, for redundancy) Inertial Navigation Systems that deduct the position and attitude directly from the accelerations and angular velocities of the aircraft.

The GNSS part requires specialized receivers aboard the aircraft, and is dependent on the satellite vehicles and network of ground stations that monitor them.

Using the two systems in tandem requires a third piece of equipment aboard the aircraft, which receives the data from the GNSS receivers and the inertial platforms and uses algorithms such as Kalman Filtering to output the position, velocity and attitude of the aircraft. This is known as flight management system (FMS) and can also interface with radio navigation systems.



Figure 8 - The Trimble AP20, a GNSS + Inertial platform which can be used for airborne applications

## 2.6.4 Performance

Navigation using GNSS combined with inertial platforms is used in en-route operations, being employed for the following types of Performance-Based Navigation (PBN):

- En-route RNP 10 (Oceanic/Remote Continental), for a horizontal accuracy of 10 NM (95%);
- En-route RNP 4 (Oceanic/Remote Continental), for a horizontal accuracy of 4 NM (95%);
- En-route RNP 2 (Continental), for a horizontal accuracy of 2 NM (95%);
- En-route RNP 1 (Terminal), for a horizontal accuracy of 1 NM (95%);
- Non-Precision Approach, for a horizontal accuracy of 220 m (95%);

## 2.7 INS plus Radar

### 2.7.1 Principle of operation

One other way that INS measurements might be augmented is by combining them with Radar Observations. Specifically, by using several microwave signals pointing in different directions (at least three noncoplanar beams are required to determine velocity, typically four beams are used), and by measuring Doppler shifts, one can infer the aircraft velocity, which can be integrated to find displacement from a known initial location. This plays to the two systems' strong points, as it takes advantage of the small long-term velocity error of the Doppler radar, and the small short-term velocity error of the inertial platforms, which are known to diverge over long periods of time.

This conjunction has the following advantages:

- Velocity is measured relative to the Earth's surface. Air data systems measure velocity with respect to the air mass (which is relevant for aerodynamic purposes), and most terrestrial radio navigation systems measure velocity by differencing successive position measurements;
- It is a self-contained system, meaning it requires no external equipment or infrastructure. This also means that it requires no international agreements;
- Airborne transmitters have low power requirements, which makes them low weight, size, and cost.
- The radar beams are narrow and pointed at steep angles towards the ground, which makes the aircraft hard to detect;
- It works in every type of weather conditions, save for extreme conditions of rain;
- It can operate over land and water (except for completely still water bodies);
- It provides very accurate average velocity information;
- Using Doppler radar is very suitable for measuring three-dimensional velocity at low speeds, which is required when helicopter and multi-rotor aircraft are hovering.

It does, however, have some disadvantages:

- Vertical reference information (such as that of an altimeter) is needed to convert velocity information into positional coordinates;
- Like standalone inertial navigation, its accuracy degrades over time;
- Instantaneous or short-term velocity output is not as accurate as averaged or smoothed velocity;
- While operating over water, accuracy is degraded due to backscattering characteristics and water motion.

## 2.7.2 Maturity

As with most technologies, airborne Doppler radar velocity measurement had its inception in the military. It was first used for airborne moving target indication, as well as velocity determination by combining it with airspeed indicators. In the 1960's, this migrated to commercial aviation, where it began being used primarily for operations in oceanic areas, by joining it with inertial platforms.

By the 90's, the biggest use of Doppler radar was in military helicopters, for navigation as well as operations such as hovering. They were also deployed in UAVs and drones.

Despite being a fully developed technology, the use of Doppler radar didn't become widespread since it suffers from one shortcoming that also affects inertial navigation, i.e., its solution degrades over time. Due to this, these systems are often coupled with GNSS. GNSS solves the initialisation problems, while Doppler radar provides continuity when GNSS signal is lost, be it due to terrain, aggressive manoeuvres, or jamming.

### 2.7.3 Equipage and infrastructure

Since this is a self-contained system, no external equipment is required. The only on-board equipment needed is the inertial platform, the radar transmitter/receiver equipment, and the flight computer that couples the two measurements.

### 2.7.4 Performance

Standalone Doppler radar has a typical velocity accuracy of  $0.06 \text{ m/s} \pm 0.2\%$ , while high performance implementations are usually a factor of two better. For positioning performance, coupling with an inertial platform can yield an accuracy of about 0.15% of distance travelled. It is important to mention that Doppler radars have a service ceiling, which is typically of at least 3000m above terrain.

As stated before, performance is poorer over water, since the scattering coefficient varies with the angle of incidence, which causes velocity to be underestimated. These errors can be as large as 5% and even larger over very still bodies of water. Older systems provided the user with two switchable modes, one for use over land, and one over water, which could reduce residual errors to as little as 0.3%, while newer systems typically use a different beam shape.

## 2.8 INS plus imagery

### 2.8.1 Principle of operation

Because of the quick drift of standalone inertial solutions, several techniques have been developed to get around these limitations. For indoor applications, vision data from one or more cameras can be used to complement the inertial system's measurements. These techniques use image processing algorithms, which take into account the width of field of view, as well as the frame rate and other parameters, to accurately estimate the change in orientation and position over time, independently from the inertial platform. This can then be fed into a Kalman Filter which combines the measurements to return a solution for position, velocity and orientation.

### 2.8.2 Maturity

This type of navigation has little applicability for outdoor aircraft, since several GNSS are available and their precision is appropriate for almost all phases of flight, but advancements are being made for indoor UAVs. This is, however, still a highly experimental field.

In his 2014 PhD thesis ([http://www.diss.fu-berlin.de/diss/servlets/MCRFileNodeServlet/FUDISS\\_derivate\\_00000017227/Stereo-Vision-Aided Inertial Navigation.pdf](http://www.diss.fu-berlin.de/diss/servlets/MCRFileNodeServlet/FUDISS_derivate_00000017227/Stereo-Vision-Aided%20Inertial%20Navigation.pdf)), Grießbach develops a navigation system based on inertial





measurements and stereo vision (dual cameras to simulate the human eyesight). The conclusion was that the measurements complemented each other quite well, its accuracy being as good as 2%, or a deviation of 74 centimetres in a 310 metre run.

### 2.8.3 Equipage and infrastructure

There is no need for off-board equipment for this type of navigation, all processing is done based on physical variables directly observable by the sensors.

However, it requires one or more Inertial Measuring Units (IMUs), one or more cameras, and a CPU that is capable of running the image processing algorithms.

### 2.8.4 Performance

Given the relatively low level of maturity of these techniques it is risky to advance specific values for their performance. Nevertheless, R&D work such as the one mentioned above has shown deviations of 74 centimetres over a 310 metre run.

## 2.9 Signals of Opportunity (SoOP)

### 2.9.1 Principle of operation

The designation “Signals of Opportunity” (SoOP) refers to the use of signals that are not intended for navigational purposes. Signals of Opportunity have several advantages to the user:

- Quantity – There are many signals available. These include analogue and digital TV broadcast stations, AM and FM radio, and Bluetooth, Wi-Fi, and cellular networks;
- High power – GNSS transmitters such as GPS have power consumption restrictions, so their transmitted power is quite low. High power SoOP transmitter signals can penetrate walls, so they can be used for indoor navigation;
- No infrastructure required – The transmitter infrastructure is already in place, since the signals are already being transmitted for other purposes;
- Technology is making it more feasible – The main advancement in this regard is that of Software-Defined Radio (SDR), where receivers can quickly switch frequencies and analyze different types of signals, resorting to a computer that controls the receiver and processes these signals. Using several frequencies all over the spectrum also reduces the potential for jamming.

They are, however, not without drawbacks:

- Not optimized for navigation – The main disadvantage of this is timing. In order to use the travel time of the signal to determine the distance to the transmitter, the exact transmission time must be known. Most communication systems do not provide synchronization to within a few nanoseconds (like GPS does), and usually require an additional reference receiver.
- Varying availability – The transmitters are much more common in or nearby urban centers, and rarer in remote or rural areas. Moreover, different countries might have different frequency and protocol standards, which can make implementation more complex.
- Transmitter locations must be known – Like beacon based navigation, the locations of the transmitters are necessary information to locate the receiver. Moreover, there are occasions where several transmitters are located closely together, which introduces a factor of poor geometry, and makes it so that in practice, only one of those transmitters should be used.
- Challenges building the navigation equipment – despite the advancement in SDR technology, there are a lot of considerations to have in mind. A wideband antenna is needed so that no part of the spectrum is too disregarded; high bandwidth and high sample rates are needed, which in turn requires processing power. These signals can range in frequency from 100 KHz (AM radio) to 5 GHz (newer Wi-Fi signals).

There are several ways that SoOP can be used to determine a receiver's position and velocity:

- Received Signal Strength (RSS);
- Angle of Arrival (AoA);
- Time Difference of Arrival (TDoA);
- Pseudorange measurements

#### **2.9.1.1.1 Received Signal Strength (RSS)**

Since the received signal strength decreases with the distance to the transmitter, the distance to the transmitter can be inferred from the received power. This is dependent on knowing the transmitting and receiving powers, as well as having a model for the path loss. The biggest drawback of this model is that it's not adequate if there are many obstacles between the transmitting station and the receiver, which is the case for indoor applications.

#### **2.9.1.1.2 Angle of Arrival (AoA)**

This works in a similar way to Non-Directional Beacons. Since most long-range, broadcasting antennas transmit in an omnidirectional pattern, a rotating, directional antenna can be used to find the heading of the station. Combining two of these allows the location of the receiver to be found, and more measurements increase the accuracy of the solution.



### 2.9.1.1.3 Time Difference of Arrival (TDoA)

This relies on a reference station relies on measuring the difference in arrival time between two different receivers. Of course, it's reliant on the clocks of both stations not diverging too much from each other, but with signals from several sources, it's possible to determine the position of a moving receiver.

### 2.9.1.1.4 Pseudorange measurements

Similarly to the GNSS operation, if the transmission and reception times are known, the distance can be deduced by dividing the transit time by the propagation velocity. It's dependent on the transmitting station having some kind of signal that repeats reliably at a known time and rate. If this is the case, the receiver can use GNSS signal from only one satellite to ensure its own clock doesn't diverge too much, and measure the transmission times to find the distance.

## 2.9.2 Maturity

From the techniques explained above, the most attractive to use as an actual navigation aid is perhaps that of TDoA using AM radio. AM signals have relatively low frequencies, therefore long ranges, so a quantity of signals are available, from commercial radio stations that still broadcast, to amateur radio enthusiasts. In his PhD Thesis (<https://pdfs.semanticscholar.org/73c9/e528570e38637454875140a6d54f4668c8bc.pdf>), Hall develops a radiolocation system using the carrier phase of these signals. Making sure the antennae positions are accurate, one can expect similar accuracy to that of GPS in open areas. The main advantage, however, is that these signals are more powerful and have lower frequencies, so they are able to better to pass through buildings and can pose an advantage in heavily forested areas, where sky view is obstructed and GNSS struggles. One disadvantage of this solution is that AM stations are required by law to decrease their output power at night (since there can be skywave propagation which interferes with other stations), so there are not as many signals available to be used during night time.

Another implementation, from a 2005 paper titled "A New Positioning System Using Television Synchronization Signals", written by Matthew Rabinowitz, uses digital television broadcast signals for standalone position or to augment GNSS positioning. These signals have the advantage of sending a Synchronization Segment which repeats at a known rate, and as such they do not suffer of one of the greatest disadvantages of general-purpose signals. They also use much higher frequencies than AM radio, so they're not limited in power at night. And, since the frequencies aren't as high as that of GNSS, the signals are able to penetrate buildings, allowing navigation in challenging urban environments and even indoors.

## 2.9.3 Equipage and infrastructure

The off-board equipment is already deployed and active. In terms of onboard equipment, the antenna and receiver need to be as versatile as the range of signals in use. For a more varied spectrum, wider bandwidth and higher quality equipment is necessary. This also influences the computational power necessary, although this is no longer at a premium, with single board computers being affordable and capable of running SDR programs.

## 2.9.4 Performance

Hall's implementation, even if just a proof of concept, uses the carrier phase of AM signals, and is able of attaining precisions better than 15 meters, 95% of the time, for distances under 35 kilometres from the reference station. For distances under 10 kilometres, the error was smaller than 7 meters, 95% of the time. This work was developed little after GPS precision stopped being degraded purposefully for security reasons, and receivers were still relatively expensive. So, there was a void for low cost, semi-precise positioning. At this time, with the plethora of GNSS available, there is little danger of a worldwide shutdown of every GNSS, and receivers are inexpensive, so this void is almost non-existent.

For the Rabinowitz system, accuracy of the system was similar to standalone GNSS in outdoor scenarios, and between 4.4 and 19.6 metres of standard deviation in indoor environments, where GNSS is unable to locate a receiver. This system can complement GNSS since it performs well in urban environments, where transmitters are more common, while GNSS generally performs better in rural areas, where Digital Television transmitters are rarer.

However, one aspect where signals of opportunity can be very useful is to constrain the drift of inertial systems using the Doppler deviation from the nominal frequency.

## 2.10 Navigation in GA, VLA and Ultra-Lights

Many GA aircraft are fitted with a variety of navigation aids, such as Automatic direction finder (ADF), inertial navigation, compasses, radar navigation, VHF omnidirectional range (VOR) and GNSS. All of these navigation aids made huge improvements in aircraft navigation. Today's tendency is to make navigation easier, more reliable and cost effective. GNSS combined with continuously improved MEMS sensors and new advanced techniques might have big impact to navigation systems of small aircraft. The main technological evolutions underway with application to GA include most of the techniques mentioned in previous sub-sections:

- Augmentation of a global navigation satellite system (GNSS)
- Application of dual frequency GNSS receivers (GPS - L1/L5)
- Upcoming Galileo services
- Application of MEMS (i.e. Micro Electro Mechanical Systems) inertial sensors
- Combination of Inertia and GNSS techniques (long term precision for GNSS, dynamic and autonomy for inertia).

Although the most recently designed cockpits for general aviation encompass a number of novelties in term of safety or capability (satellite weather status, synthetic vision system, traffic alert, infrared camera, touch screen, wireless transfer of flight plans between a mobile device and the avionics ... ) the navigation sensors have not been following this trend.



Figure 9: Latest Garmin G1000 NXi cockpit

Reliance on GPS is now a standard in General Aviation for VFR and IFR for several years. All recent airborne GPS receivers include SBAS capability and are compliant to TSO C145c or TSO C146c. GPS position is largely used by the avionics and is feeding all on-board systems (2D map, Synthetic vision system, Traffic advisory, ADS-B,...). Basic RNP capability may also be available on some aircraft.

The new IFR-designed avionics are LPV capable (meaning that two GPS/SBAS receivers are embedded for safety issue). A number of older aircrafts are also retrofitted with LPV to increase their operational capability or keep it unchanged following the decommissioning of ILS beacons replaced with LPV approaches.

Although in the US or Europe general aviation is allowed to fly IFR equipped only with SBAS receiver (Title 14 → Chapter I → Subchapter F → Part 91 → Subpart C → §91.205) this will prevent the pilot from flying VOR or NDB published approaches where overlay is not allowed. With only GPS/SBAS on board the pilot would be limited to RNAV and RNP IFR routes. Moreover in case of GPS loss, VOR or NDB remain a safe backup navigation mean. That's why General Aviation avionics usually come with legacy VOR and NDB receivers in addition to the GPS. General Aviation is usually neither equipped with DME nor with inertial unit (which are a costly and power consuming device, and are not required by regulation).

New GNSS constellations are not used yet on board aircraft. The GLONASS mandate in force from January 1<sup>st</sup> only targets aircraft weighting more than 12,500 pounds and registered on an operational certificate issued by Russia's civil aviation authority. Galileo initial capability is still too recent to be operationally used on board aircraft.

### 2.10.1 Major players list

Founding Members



© - 2016 – NAVISAS Consortium. All rights reserved. 41

The following is non-extensive list of the main manufacturers of navigation equipment for small aircraft:

- AEL Sistemas (BR) (displays among other avionics systems for fixed, rotary wing and unmanned vehicles)
- Aircraft Radio Corporation (US) (avionics and flight control system for GA aircraft such as Cessna)
- Astronics Max-Viz (US) (suppliers of EVS and displays)
- Avidyne Corporation (US) (integrated avionics, displays and traffic advisory systems)
- Chelton Flight Systems (US) (synthetic vision systems and avionics)
- Dynon Avionics (US) (non-certified electronics including transponders, autopilots and displays)
- Furuno (JP) (GNSS receivers used in both manned and unmanned aircraft)
- Garmin (US) (GNSS receivers used in both manned and unmanned aircraft)
- Honeywell (US) (suppliers of sensors and inertials)
- JP Instruments (US) (flight instruments and engine management systems)
- L-tronics (US) (DF, ELT and EPIRB equipment)
- Rockwell Collins (US) (communication systems and avionics for all types of aircraft)
- S-TEC Corporation (US) (autopilots for small and mid-size aircraft)
- Thales Avionics (FR) (avionics for different categories of aircraft)
- TI Elektronik (CZ) (manufacturer of instruments and on-board systems)
- Universal Avionics (US) (FMS and instrument displays for private aircraft)

The vast majority of newly designed glass cockpit for certified aircraft use a Garmin integrated avionics suite from the G500 (Piper), G1000 (Cessna, Piper, Diamond, Cirrus, etc...), G1000NXi (King Air), G2000 (Cessna) or G3000 (Socata) series. The navigation means (GPS, VOR) are directly integrated into the avionics suite. Other avionics manufacturers target regional or business aircraft (Rockwell Collins, Honeywell), or only provide GPS or VOR receivers that can be included in an existing avionics. The following figure provides an example of a Garmin system architecture.

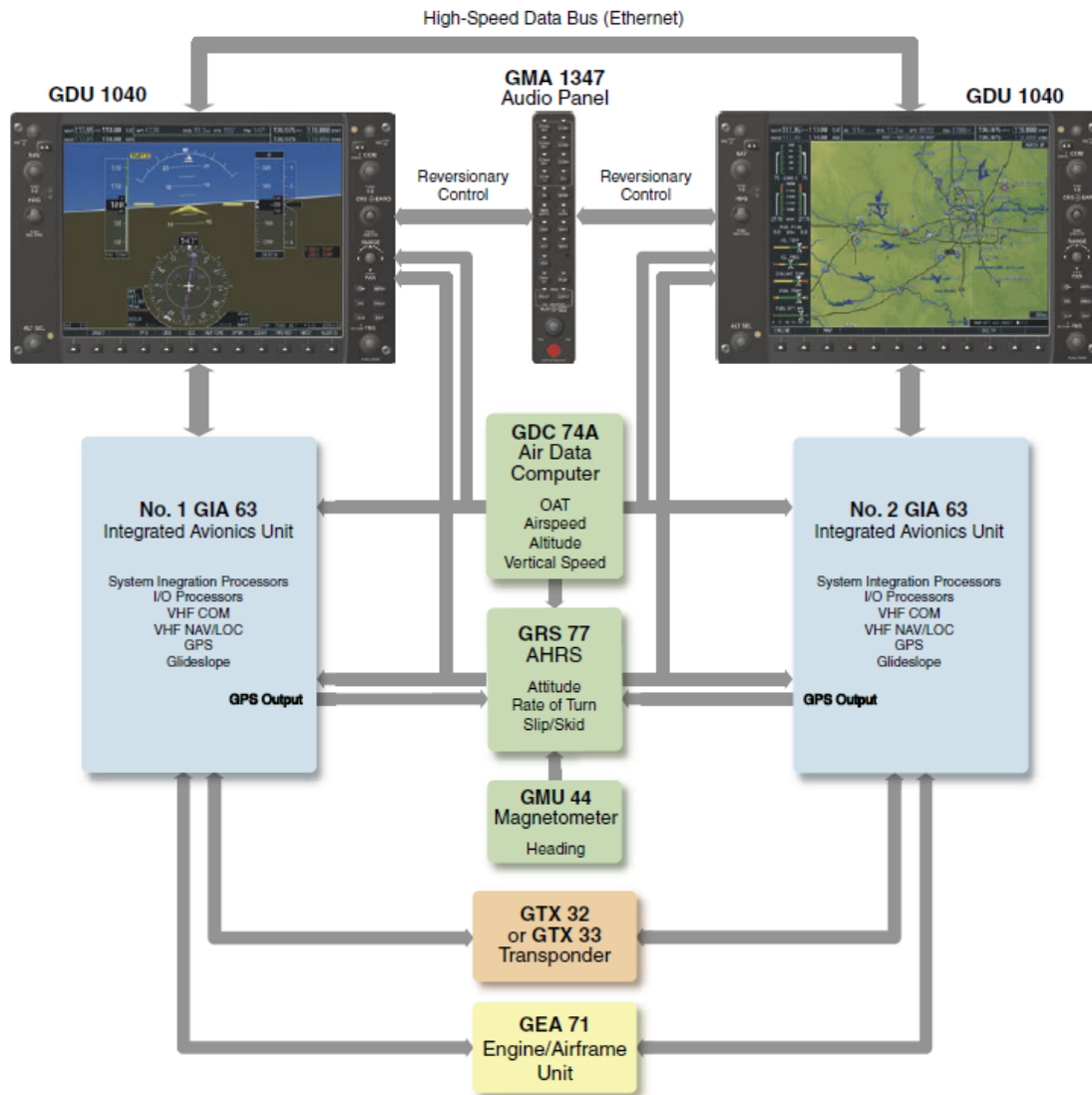


Figure 10: Garmin G1000 architecture diagram

## 2.11 Navigation in UAVs and Drones

Currently, navigation in UAVs or drones is fundamentally based on GNSS (namely GPS). GPS is often complemented with other techniques depending on the size of the drone. At this point it is important to differentiate between small drones (or according to EASA’s proposed regulation, CAT A0 – toys and mini-drones below 1Kg and CAT A1 – small drones below 4Kg) and larger drones above 20Kg. While the former may not even have GPS (the case of toys) and can rely on video for navigation, the larger



drones often combine GPS with some form of commercial grade inertial sensors (accelerometers), video (as mentioned previously) or radar. For example several manufacturers achieve autoland capabilities by combining GPS with radio-altimeters.

Given that drones have no cockpit per se, instruments are procured by drone manufacturers directly to sensor, transducer or GNSS receiver suppliers. The majority of sensor data is then represented digitally in GCS (Ground Control Stations). The majority of drone manufacturers tend to develop their own GCS so that displays are then provided directly by the platform manufacturer. From the list of players above, Garmin is probably the most active in supplying the drone market.

## 2.12 Compatibility with SESAR concepts

A SESAR A-PNT study has been started in the course of the SESAR project addressing the emerging need of aircraft resilience to GPS outage. The work is currently continued in the frame of the SESAR2020 project. A parallel activity is conducted by FAA in the frame of NextGen project. In 2016, the FAA released its PBN NAS (Performance Based Navigation Strategy 2016) describing its Performance Based Navigation roadmap including resiliency to GPS outage. The major steps are detailed below:

### *NEAR TERM (2016–2020):*

*By the end of the near term, the NAS will remain resilient with PBN services throughout Class A airspace provided by phasing in DME RNAV coverage down to 18,000 feet above mean sea level (MSL). The exception is areas in the Western Mountainous Region, where terrain severely limits line-of-sight coverage at altitudes below 24,000 feet MSL. DME coverage will exist without the need for an IRU, though operators without IRU may need to confirm critical DMEs are not out of service in the terminal area. Class A airspace will require DME/DME positioning for operators needing to access the airspace during a GNSS service disruption. Operators equipped with only a single FMS, and thus only a single DME/DME navigation source, will be allowed to use VOR (non-RNAV) or Tactical Air Navigation as an authorized second form of navigation to continue to dispatch during the disruption. [...]*

- *Increasing situational awareness of GNSS disruption events and the ability to quickly communicate information to the affected parties is an essential capability needed throughout the NAS to ensure effective and timely use of resilient infrastructure. In the near term, the FAA will define requirements for a Satellite Operations Coordination Concept (SOCC) position at the FAA's Air Traffic Control System Command Center to manage realtime information on the NAS navigation status.*

### *MID TERM (2021-2025)*

*By the end of the mid-term, the resilience of the NAS will be increased further with the following FAA commitments:*

- *DME/DME coverage, providing RNAV 1 navigation, will be extended down to NSG 1 and 2 airports to facilitate a conventional approach, as required (for example, 1,500 feet height above airport). This coverage will require the installation of additional DME facilities. Note that for departures, DME/DME may not provide needed coverage to support all PBN departures due*



*to the aircraft computer processing delay that exists after receiving DME ground transponder signals. To maintain acceptable departure operations during a GNSS disruption, local facilities will have to develop contingency plans. DME/DME equipment will be required for those operators needing to access the airspace during a GNSS service disruption; and*

- *The SOCC will begin operations in the mid-term, providing the real-time, system-level view of NAS navigation resiliency and coordinating mitigation to service disruptions.*

*The provision of DME/DME RNAV coverage in Class A airspace in the near term and at the selected airports during the midterm will constitute a resilient position and navigation service for the NAS. The FAA will continue to evaluate alternatives for position and navigation as technologies and capabilities advance.*

#### **FAR TERM (2026–2030)**

*In the far term, the FAA will focus on the completion of legacy infrastructure divestment, making PBN the standard method of navigation. Conventional navigation will exist to ensure the resiliency of non-DME/DME operations, low-visibility approaches and DoD requirements. The FAA will be able to complete programs to recapitalize and divest from additional ground-based infrastructure. Priorities for the 2026–2030 timeframe include:*

*[...]*

- *Continuing research into Alternative Position, Navigation and Timing (APNT) capabilities.*

#### **BEYOND 2030**

*As the near- and mid-term solutions are implemented, DME and VOR will serve into the far-term timeframe. During the far term and moving out into the 2030 timeframe and beyond, the FAA will continue to research the best methods for APNT [...]*

The European A-PNT concept is under definition but is likely to have a similar approach.

One part of the SESAR A-PNT study aimed at listing all the possible alternatives to GPS (future or already existing) while the second part has been focusing on DME enhancement at ground or at airborne level.

The following is a summary of the studied alternative technologies and their applicability to NAVISAS project.

A-PNT Technology	Concept	Applicability		
		General aviation	Ultra-light	UAV

<p>Enhanced DME-FMS</p>	<p>Existing on-board FMS and DME receiver already compute a DME/DME position but do not provide integrity. Updating the FMS software with an integrity computation capability (similar to the RAIM algorithm) could be sufficient to provide RNP 1 capability based on DME only. Further populating the current DME network will be needed to guarantee sufficient coverage.</p>	<p><b>Not applicable</b> <b>DME equipment is required</b></p>		
<p>Wide Area Multilateration (WAM)</p>	<p>WAM is able to find aircraft positions by time difference of arrival measurements between several ground stations. The system is composed by a number of receiver/interrogators located in precisely surveyed positions, receiving mode A/C and Mode-S (and in some systems ADS-B also) replies.</p>	<p>Yes</p>	<p>Yes if equipped with transponder</p>	<p>Yes if equipped with transponder</p>
<p>Mode-N</p>	<p>Mode N system is characterized by ground stations (synchronized in time) that transmit on a single frequency their coordinates. These periodic transmissions are referred to as Mode N squitter.</p> <p>The main difference between DME and Mode N using is related to the number of useful ground stations: while DME is limited to a maximum of five sources per DME interrogator, a Mode N transceiver can utilize all Mode N ground stations</p>	<p><b>Not applicable</b> <b>Mode N squitter equipment is required</b></p>		

	<p>within radio line of sight. So Mode N function of the transceiver is able to estimate the aircraft position from Mode N squitters of different ground stations using time differences of arrival .</p>	
LDACS	<p>LDACS (L-band Digital Aeronautical Communication System) is the future ground-based communications link (960-1164 MHz) and is already used by Aeronautical navigation services and Aeronautical military communications systems.</p> <p>To calculate correct airborne position, it is necessary to multilaterate the received signals from at least four ground transmitters.</p>	<p><b>Not applicable</b> <b>LDACS equipment is required</b></p>
Mosaic DME	<p>This solution consists of a single conventional DME transponder and multiple pseudolites installed in the same location. The DME transponder operates according to the current standards on the basis of a two-way ranging principle, while the pseudolites broadcast one-way continuous signals for carrier phase measurements.</p>	<p><b>Not applicable</b> <b>DME equipment is required</b></p>
eLORAN	<p>Loran (LONg RANGE Navigation) is a ground-based radio-navigation system that preceded</p>	<p><b>Not applicable</b> <b>LORAN equipment is required</b></p>

	<p>satellite navigation. Loran is based on the broadcast of extremely high power signals in the low frequency portion of the radio spectrum (operating between 90 kHz and 110 kHz).</p> <p>An updated LORAN version (called Enhanced LORAN) provides changes to the last LORAN system to improve accuracy, reliability, integrity, service availability and robustness against the interference.</p>	
--	--	--

Table 4– Summary of alternate A-PNT technologies

## 3 State of the Art review on clocks and atomic gyroscopes

---

Here, a State of the Art (SoA) analysis on both miniature atomic gyroscopes (MAG) and atomic clocks (MAC) is presented with key performances, limitations and advantages compared with existing solutions for APNT IMUs and GNSS, respectively.

### 3.1 Miniature atomic clocks

#### 3.1.1 Introduction

The capability to maintain accurate timing over extended period of time with compact and low power consumption devices is a key benefit for a number of applications.

In GNSS, frequency spectrum congestion generates interferences that represent a key challenge for service integrity and persistence. Thanks to its superior timing accuracy over extended period of time, miniature atomic clocks guarantee fast re-acquisition of the signal and long coherence integration, thereby improving service availability in adverse environment (provided the actual location is estimated from inertial navigation). While this is of obvious benefit for high-end GNSS user terminals, it is also of high interest for on-board GNSS receivers that are being increasingly used for geostationary satellite station keeping, especially in the highly occupied orbital slots.

A number of Earth observation instruments (radiometers, GNSS radio occultation...) operating in non-coherent mode could significantly improve their sensitivity and resolution by integrating the signal over longer period of time. Thanks to its compact form factor and low power consumption, a miniature atomic clock (MAC) could be directly integrated in the instrument and would not require power-hungry and bulky reference oscillator.

There is however no MAC technology available in Europe, the sole worldwide supplier being in the US (Microsemi Corporation). While over the last decade, some efforts have been dedicated worldwide and also in Europe to the development of MACs at the system level, there is currently a lack of activity dedicated to a high-performing physics package.

### 3.1.2 Working principles

A miniature atomic clock (MAC) is an oscillator providing a signal with exquisite frequency and hence timing stability. This frequency stability is derived from the intrinsically stable frequency of atoms (Rubidium or Cesium atoms for a MAC). A MAC is basically a quartz local oscillator that is frequency locked to an atomic reference transition (so-called passive atomic clock). The gaseous phase reference atoms are enclosed in a vapor cell. In order to access the hyperfine atomic reference transition which is at e.g. 6.8 GHz for the isotope 87 of Rubidium, a vertical-cavity semiconductor laser (VCSEL) has its injection current modulated at half the atomic hyperfine frequency in order to generate sidebands in which are resonant with the atomic hyperfine frequency, while the wavelength of the laser is stabilized to one optical atomic absorption line (typically at 795 nm). In these conditions there is a slight increase of the light transmission through the atomic vapor cell. This effect called Coherent Population Trapping (CPT) is at the heart of a MAC.

A typical MAC architecture is displayed in Figure 11. The physics package (PP) is central to the clock and contains the MEMS atomic vapor cell, the VCSEL, some micro-optics to prepare the light emitted by the laser that interacts with the atoms, heaters and temperature sensors for the MEMS cell and the VCSEL, coils to generate a straight magnetic field (B field) for the atoms, and a photodiode (PD) to detect the atomic signals. The PP is driven with electronics that has to provide DC injection current to the VCSEL, control loop for the VCSEL temperature, control loop to stabilize the VCSEL wavelength on an atomic optical transition (laser lock), an RF synthesizer to generate the appropriate microwave signal used to interrogate the atomic hyperfine frequency via the laser and phase locked loop (PLL) to phase lock the clock local oscillator (typically a 10-MHz quartz oscillator). Not shown in Figure 11 but necessary to control the full clock is a microcontroller. Also not represented is a magnetic shield in order to isolate the atoms from external magnetic fields.

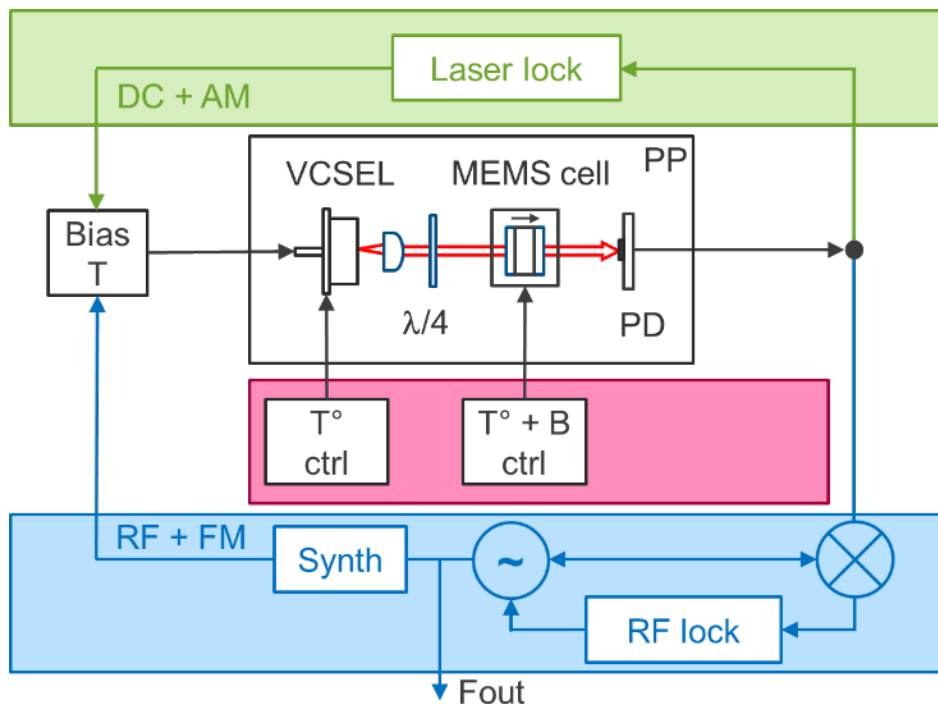


Figure 11. Bloc diagram of a MAC (i.e. a passive atomic clock)

### 3.1.3 Challenges

In order to make a MAC competitive, the performance in terms of frequency stability is essential but the form factor and the costs are of key importance as well. The PP is a critical element needed to fulfill these challenges and so far no solution exists that is high performing and competitive in cost.

The **form factor** of today's prototypes is cubic since the different known PPs are realized with a stack of the components. Recent R&D activities towards a flat design are undertaken, e.g. at CSEM.


The **power consumption** of the PP is essentially driven by the laser and cell thermal management with temperatures in the order of 80°C. Careful thermal management and hermetically sealed vacuum encapsulation are essential at laser-package and cell-package interfaces to ensure high thermal resistivity and thus also improve thermal stability.

The **production cost** of the PP is strongly dependent on the packaging technique (assembly process) and the technology selected for the package itself. Apart from the cost, yield and reliability of the components, the assembly process is complex and thus a big challenge for low-cost mass production.

### 3.1.4 Specifications

In Table 5, a comparison of relevant competing technologies parameters is presented (the last column, in red, summarizes the flat CSEM PP target specifications).

Miniature Atomic Clocks (MACs)



	TCXO (typic.)	OCXO (typic.)	Standard Rb (typic.)	Microsemi SA.45*	CSEM Swiss-MAC	C-MAC (target)
<b>Freq. stability @ 1 day</b>	1E-8 (1s)	1E-10 (10ms)	1E-12 (0.1ms)	1E-11 (1ms)	1E-11 (1ms)	1E-11 (1ms)
<b>Freq. stability @ 1 year</b>	1E-5	1E-6	2E-10	1E-9	1E-9	1E-9
<b>Volume [cm<sup>3</sup>] (PP volume / height [cm])</b>	0.025 ( - )	5 ( - )	220 (40 / 17)	16 (0.8 / 0.6 )	50 (6 / 1.1)	- (1.4 / 0.5)
<b>Power consumpt. [mW] (PP only)</b>	10 ( - )	400 ( - )	11'000 ( - )	125 (20)	500 (200)	- (50)
<b>Price [€]</b>	8	210	750	1'200	250	50

Table 5: Comparison of relevant oscillators and clocks. The last column also presents the C-MAC PP target specifications.

The two first columns are for temperature-controlled crystal oscillators (TCXO) and oven-controlled crystal oscillators (OCXO). Such oscillators are very wide spread due to their low cost and good performances. Another wide spread technology is the Standard Rb atomic clock, which offers excellent frequency stability and relatively low cost with a price below 1000€ per unit, while its size and power consumption are prohibitive for its use in portable applications. Then comes the Microsemi SA.45 which has performances offering a compromise between OCXO and Standard Rb. Nevertheless the price per unit is not yet competitive for a mass adoption of this technology which is now implemented in niche markets like oil and gas exploration. For illustration, the two CSEM prototypes (C-MAC is still at low TRL) are compared. Their position in the SoA will be specified below.

### 3.1.5 IP survey on MAC PPs

An IP survey has been carried out by CSEM, focusing on MAC PPs. The number of patent application per year (shown in Figure 12, left panel) shows the actuality of the field. After reaching a peak around the year 2010 (stimulated by major US funding by DARPA) the IP activity is still on an elevated level. A distribution of top 19 patent assignees in the context of MAC PPs is shown in Figure 12, right panel. The top assignee, Seiko/Epson, is strongly represented although there is neither a corresponding product nor a scientific demonstrator of a MAC. This is in part due to a high number of patent families



with only minor differences in the contained claims. Moreover, only few of those patent families correspond to granted patents.

Consecutive ranks are occupied by Honeywell, Microsemi, and Northrop Grumman, which are well known for their demonstration and actual implementation of working MACs. Notably, Microsemi/Symmetricom have already commercialized a MAC system.

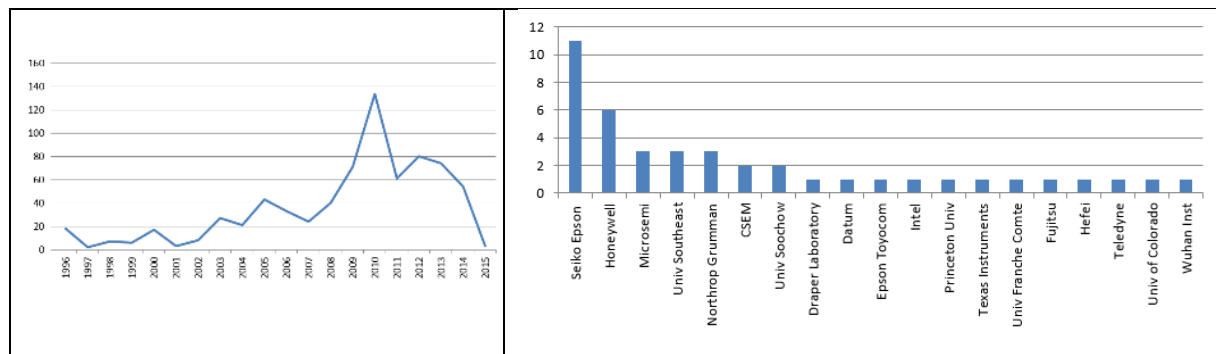


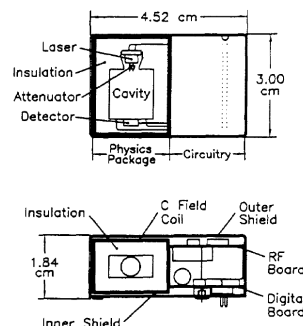
Figure 12: Left: Number of patent applications for year related to MACs. Right: Top 19 patent assignees focusing on MAC PPs (# patents families related to MAC PPs per assignee)

### 3.1.6 Survey of already realized MACs

This section summarizes previous and current efforts towards MACs and corresponding IP.

#### 3.1.6.1 Westinghouse/Northrop Grumman

The volume of the Westinghouse PP is 16 cm<sup>3</sup> and the power consumption is 300 mW. The PP includes a laser diode, a cesium- and buffer gas filled glass blown cell, and a dielectrically loaded 9.2 GHz microwave cavity. The total package including the electronics has a volume 25 cm<sup>3</sup>.

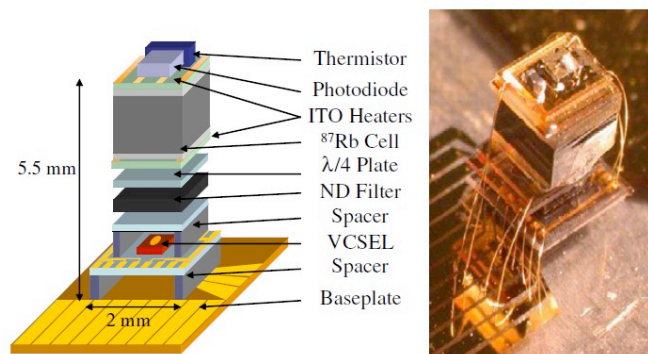


**Figure 13: Westinghouse / Northrop Grumman PP**

Technical details on this system can be found in literature<sup>1</sup> and several patents such as those selected below<sup>2,3</sup>.

### 3.1.6.2 National Institute for Standards and Technology (NIST)

The volume of the NIST PP is only 4 mm<sup>3</sup>. The PP includes a VCSEL (795 nm), a waveplate and a MEMS cell with <sup>87</sup>Rb and buffer gas. CPT interrogation is done at 3.4 GHz (no microwave cavity). In 2006 NIST completed a CSAC clock using the miniature PP. The full Clock volume is 15 cm<sup>3</sup> and the power consumption 300 mW at 25°C. The physics package alone consumes 110 mW.

**Figure 14: NIST PP**

Technical details on this system can be found in literature<sup>4,5</sup> and several patents such as those selected below<sup>6,7</sup>.

<sup>1</sup> Chantry et al., "Miniature laser-pumped caesium cell atomic clock oscillator", Frequency Control Symposium (1996)

<sup>2</sup> H. Abbink, E. Kanegsberg, K. Marino, C. Volk, "Micro-cell for NMR gyroscope", US pat. N° 2006/0132130

<sup>3</sup> D. B. Hall, "Small optics for miniature nuclear magnetic resonance gyroscope", US pat. N° 2009/006011

<sup>4</sup> S. Knappe et al., "A microfabricated atomic clock", Appl. Phys. Lett. 85, 1460 (2004)

<sup>5</sup> S. Knappe et al., "Chip-scale atomic devices at NIST", Proc. SPIE 6604, 14th International School on Quantum Electronics: Laser Physics and Applications, 660403, 2007

<sup>6</sup> J. Kitching et al., "Micromachined alkali-atom vapor cells and method of fabrication", US pat. N° 2005/0007118

<sup>7</sup> J. Kitching et al., "Compact atomic magnetometer and gyroscope based on a diverging laser beam", US pat. N° 2009/0039881

### 3.1.6.3 Microsemi / Symmetricom / Draper Laboratory / Sandia National Labs

The volume of the Microsemi PP is approx. 1 cm<sup>3</sup>. The PP includes a VCSEL (894nm), waveplate, MEMS cell with <sup>133</sup>Cs and buffer gas. CPT interrogation is done at 4.6 GHz (no microwave cavity). The MEMS cell (2x2x2 mm<sup>3</sup>) is suspended by polyimide (Kapton) tethers and the PP is evacuated. The cell is heated to 85°C with 10 mW at 25°C (This corresponds to a total thermal resistance of 6°C/mW including radiation losses). The SA.45s datasheet specifies an overall clock volume of 16 cm<sup>3</sup> and power consumption 125 mW. Temperature range from -40°C to +85°C depending on model. Allan Deviation: 2E-10 @1s, 7E-12 @1000s, aging < 3E-11/month. However, in the field service bulletin from 2014 the specifications for the SA.45s have been restricted until further notice. The PP is very effective in terms of power consumption (<15mW) but at the cost of assembly complexity and hence assembly costs. The overall height of the SA.45s cubic form factor PP is 6.4 mm (without encapsulation).

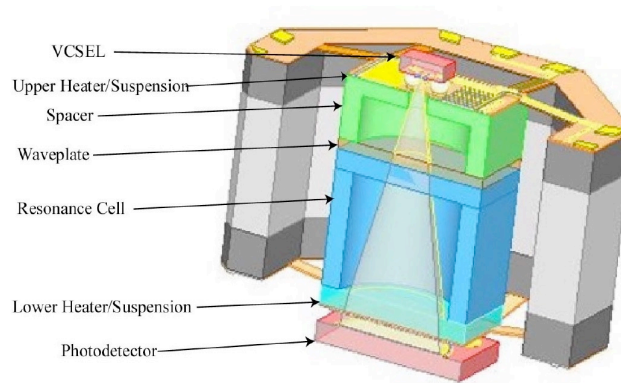


Figure 15: Microsemi / Symmetricom / Draper Lab / Sandia National Labs PP

Technical details on this system can be found in literature<sup>8,9</sup> and several patents such as those selected below<sup>10,11</sup>.

<sup>8</sup> SA.45s Chip-Scale Atomic Clock, 098-00055-000 User Guide, Microsemi 2016

<sup>9</sup> R, Lutwak et al., "The Miniature Atomic Clock – Pre-Production Results", Frequency Control Symposium, 2007 Joint with the 21st European Frequency and Time Forum. IEEE International

<sup>10</sup> R. O. Kim, "Chip-scale atomic gyroscope", US pat. N° 2014/0361768

<sup>11</sup> J. J. Bernstein, "Alkali-metal generator and absorber", US pat. N° 2011/0247942

### 3.1.6.4 Teledyne Scientific/ Rockwell Collins / Agilent Technologies

The volume of the Teledyne PP is  $0.7 \text{ cm}^3$ . The PP design uses a dual pass optical configuration in combination with a dual focus Fresnel lens to reduce the PP's size. The PP has a power consumption below 30 mW. Fractional frequency stability is reported to be  $<1\text{E-}11$  at 1hour.

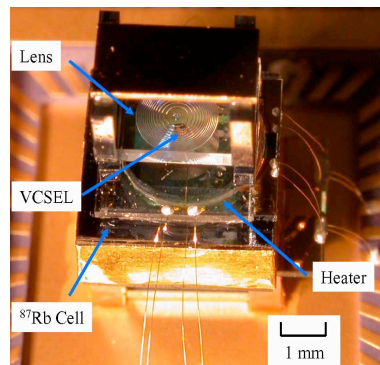


Figure 16: Teledyne / Rockwell Collins / Agilent PP

Technical details on this system can be found in the literature<sup>12,13</sup> and several patents such as those selected below<sup>14,15</sup>.

### 3.1.6.5 Honeywell

The clock volume is  $1.7 \text{ cm}^3$ , power consumption 57 mW @3.4 GHz output frequency. Allan deviation is  $2\text{E-}10$  at 1s, and  $4\text{E-}12$  at 1E4s. The PP design uses a VCSEL (795 nm), MEMS cell with  $^{87}\text{Rb}$  and buffer gas and CPT interrogation at 3.4 GHz (no microwave cavity). The optical path is parallel to the wafer plane which results in a compact (flat) form factor of the PP.

<sup>12</sup> J. F. DeNatale et al., "Compact, low-power chip-scale atomic clock", Position, Location and Navigation Symposium, 2008 IEEE/ION

<sup>13</sup> J. Fr. DeNatale et al., "Compact, Low-Power Atomic Time and Frequency Standards", Army Science Conference, 2008

<sup>14</sup> R. W. Berquist et al., "Ruggedized chip scale atomic clock", US pat. N° 8031010 B1

<sup>15</sup> R. L. Borwick, J. F. DeNatale, "Chip-scale optics module for optical interrogators", US pat. N° 8654332 B2

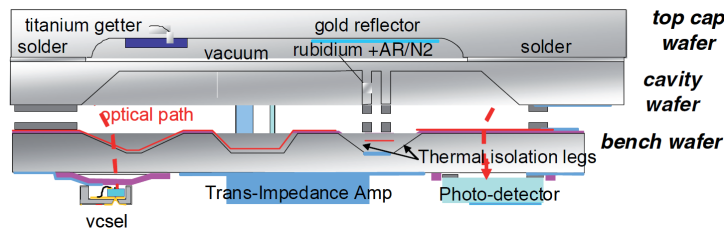
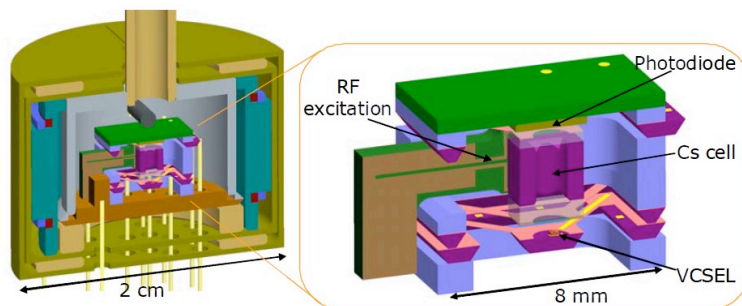


Figure 17: Honeywell PP

Technical details on this system can be found in the literature<sup>16</sup> and several patents such as those selected below<sup>17,18</sup>.

### 3.1.6.6 Sarnoff / Princeton / Frequency Electronics

The Sarnoff PP has a volume of 4 cm<sup>3</sup>. It includes a custom titanium package with getter and copper tube pinch-off for evacuation. The PP power consumption is 25 mW at 25°C ambient temperature. The PP design includes a VCSEL (894 nm), a MEMS cell with <sup>133</sup>Cs and buffer gas. A pair of 9.2 GHz microwave antennas are used for end-state RF-interrogation. The end-state interrogation scheme uses optical pumping to increase signal contrast (40%) and eliminate spin exchange line-broadening. However, the end-state clock transition is first order magnetically sensitive and an additional servo-loop is needed to stabilize the C-field. Reported Allan deviation is 6E-11 at 1sec which integrates down to 1E-11 and then rises again due to a temperature related drift.



<sup>16</sup> D. W. Youngner et al., "A Manufacturable Chip-Scale Atomic Clock", Solid-State Sensors, Actuators and Microsystems Conference, 2007. TRANSDUCERS 2007.

<sup>17</sup> R. Compton et al., "Folded optics for batch fabricated atomic sensor", European pat. N° 2685460

<sup>18</sup> J. A. Ridley et al., "Vapor cell atomic clock physics package", US pat. N° 9164491 B2

Figure 18: Sarnoff / Princeton /frequency Electronics PP

Technical details on this system can be found in the literature<sup>19</sup> and several patents such as those selected below<sup>20,21,22</sup>.

### 3.1.6.7 MAC-TFC consortium and ISIMAC consortium

The MAC-TFC project is based on CPT interrogation @4.6 GHz with an 894nm custom fabricated VCSEL. The 4.6 GHz is generated with a custom ASIC. The MEMS cell is filled with neon buffer gas and <sup>133</sup>Cs from a dispenser source. The alkali source is encapsulated inside the cell and activated after sealing off the cell. The cell support is fabricated with LTCC and the PP is vacuum encapsulated in a metallic housing. Reported frequency stability is 4E-11 @1s and <1E-11 @1day. The volume of the PP is 1.5 cm<sup>3</sup> without vacuum encapsulation. The power consumption is 200 mW for the full system and 50 mW for the PP only.

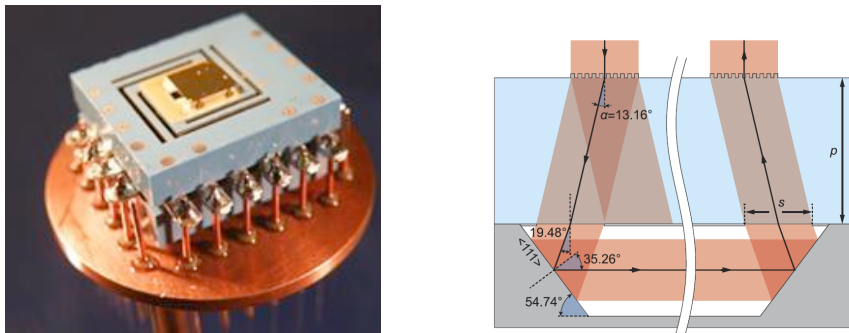


Figure 19: MAC-TFC PP

In a recent, follow-up cell design the laser passes through an elongated alkali gas cell. This allows for a longer interaction length and hence smaller laser beam diameters. This design also reflects efforts towards a flat form factor, by arranging VCSEL laser and photodetector in a planar configuration next to each other.

<sup>19</sup> A. M. Braun et al., "RF-interrogated end-state chip-scale atomic clocks", 39<sup>th</sup> Annual Precise Time and Time Interval Meeting, 2007

<sup>20</sup> A. M. Braun et al., "Batch-fabricated, fr-interrogated, end transition, chip-scale atomic clock", US pat. N° 2007/0247241

<sup>21</sup> Y-Y. Jau et al., "Method and system for operating an atomic clock using a self-modulated laser with electrical modulation", US pat. N° 2009/0080479

<sup>22</sup> T. Davis et al., "System and method for modulating pressure in an alkali-vapor cell", US pat. N° 2010/0026394

Technical details on this system can be found in the literature<sup>23,24</sup> and several patents such as those selected below<sup>25,26</sup>.

### 3.1.6.8 Spectratime Orolia

Results realized in the frame of the ESA Project “mUSO” (2007-2010). Compact physics package based on coherent population trapping (CPT) in rubidium 85. With this package Spectratime obtained a short term frequency stability  $\sigma_y(\tau) = 7 \cdot 10^{-11} \cdot \tau^{-1/2}$  ( $\tau < 100$  sec) and  $\sigma_y(\tau) \sim 1 \cdot 10^{-11}$  ( $100 \text{ sec} < \tau < 10^4 \text{ sec}$ ).

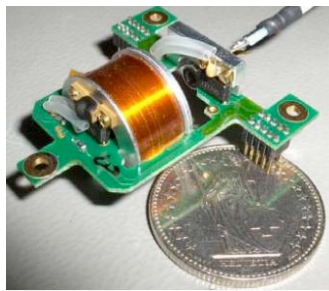


Figure 20: Spectratime PP

Technical details on this system can be found in the literature below<sup>27</sup>.

### 3.1.6.9 CSEM

The core volume of the CSEM PP (left) is roughly  $1 \text{ cm}^3$  but the ceramic package and magnetic shield increase the volume to  $22 \text{ cm}^3$ . The ceramic package is evacuated and sealed with a combination of seam welding and pinhole laser soldering. The PP design is based on CPT @3.4 GHz using a 795 nm VCSEL. The MEMS cell ( $4 \times 4 \times 1.6 \text{ mm}^3$ ) is filled with  $\text{RbN}_3$  which is decomposed under UV after cell sealing. Functionalized MEMS cell have been designed, fabricated and tested in collaboration with Spectratime. The PP’s power consumption is estimated to 200 mW. On the electronics side the 3.4 GHz microwave and control electronics has been integrated into an ASIC. The ASIC power consumption is

<sup>23</sup> R. Boudot et al., “Development of miniature atomic clocks based on coherent population trapping”, FRG Laser Symposium – Besançon, 2013

<sup>24</sup> R. Chutani et al., “Laser light routing in an elongated micromachined vapor cell with diffraction gratings for atomic clock applications”, Nature Scientific Reports, 5:14001, (2015)

<sup>25</sup> M. Le Prado et al., “Method of calibrating an atomic-functioning apparatus”, US pat. N° 2012/0062221

<sup>26</sup> N. Passilly et al., “Alkali-metal vapour cell, especially for an atomic clock, and manufacturing process”, WO 2014/057229

<sup>27</sup> C. Schori et al., “CPT atomic clock based on rubidium 85”, EFTF-2010 24th European Frequency and Time Forum



26 mW. Reported clock frequency stability is  $6\text{E-}11$  at 1s and  $3\text{E-}11$  at 1 day. Technical details on this system can be found in the literature<sup>28,29</sup> and several patents such as those selected below<sup>30,31</sup>.

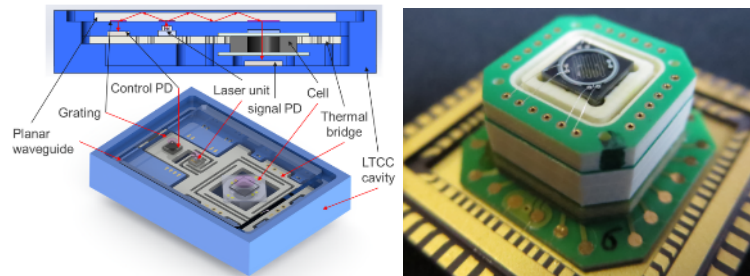


Figure 21: CSEM PP

CSEM is currently working on decreasing the overall size of its MAC, especially its height (5 mm or a total volume  $1.4\text{ cm}^3$ ). Such a flat packaging is made possible by planar arrangement of the individual components (cell, laser and detectors) next to each other's as opposed to stacking them. In this configuration, the optical connection is achieved via a planar multimode waveguide structure with gratings for input and output light coupling, as shown in the right figure above. Technical details on this system can be found in the literature<sup>32</sup> and a recent patent<sup>33</sup>.

### 3.1.6.10 Other approaches

Recent ideas for replacing atomic vapour cells by solid-state systems such as nitrogen-vacancy centers in diamond have been proposed theoretically<sup>34</sup>, however so far no physical implementation has been reported.

## 3.2 Miniature atomic gyroscopes

### 3.2.1 Introduction

<sup>28</sup> J. Haesler et al., "The Integrated Swiss Miniature Atomic Clock", European Frequency and Time Forum (2013)

<sup>29</sup> CSEM annual scientific report, 2013

<sup>30</sup> S. Lecomte et al., "Device for an atomic clock", US pat. N° 8816779 B2

<sup>31</sup> T. Overstolz, J. Haesler, "Micromachined vapor cell", EU pat. N° 2738627 A2

<sup>32</sup> CSEM annual scientific report, 2015

<sup>33</sup> B. Gallinet et al., "Atomic clock", WO 2016/008549 A1

<sup>34</sup> J. S. Hodges et al., "Timekeeping with electron spin states in diamond", Phys. Rev. A 87, 032118 (2013)



Gyroscopes are used in inertial navigation systems for measuring inertial motion of aircrafts, ships... Depending on their operating principle, they can be classified into different technologies including mechanical gyroscopes, low-cost microchip MEMS gyroscope devices found in consumer electronic devices (smartphones), fiber optic gyroscopes (FOGs), solid-state ring laser gyroscopes (RLGs) and extremely sensitive quantum gyroscopes. Vibration sensitivity of MEMS gyroscopes excludes them from inertial navigation devices. Currently, optical gyroscopes (RLGs and FOGs) dominate the market (80-85%) and are largely used in navigation systems and most generally as inertial grade gyroscopes<sup>35</sup>.

Important developments in the field of nuclear magnetic resonance gyroscopes were carried out in the 1970s and 1980s. Then, in the 1990s, very few researches were dedicated to this technology due to the improvements made in the concurrent technology of ring laser gyroscopes. In recent years, a renewed interest for atomic gyroscopes has appeared due to the synergies with developments realized on atomic clocks and atomic magnetometers<sup>1</sup>. Nowadays, atomic gyroscopes hold the promise of reaching even better performances, smaller dimensions and lower costs than current inertial grade gyroscopes. Even though these sensors are still in a research state, this technology should rapidly progress. Currently, Northrop Grumman, NIST and Princeton University are the main players.

This report on state-of-the-art in atomic gyroscopes is focused on miniature atomic gyroscopes. The first section introduces the parameters that define the gyroscope performance levels and the three gyroscope grades (inertial, tactical and rate). Then, the operating principle and the performances of Nuclear Magnetic Resonance (NMR) gyroscopes are outlined. Co-magnetometer systems, due to their relative complexity and low TRL, are not considered.

## 3.2.2 Performance and applications

### 3.2.2.1 Relevant parameters

Different parameters are considered to define the gyroscope grade: bias stability (i.e. drift), angle random walk, scale factor accuracy, full scale accuracy, maximum shock absorption and bandwidth. We specify here the first three ones:

- Bias stability (in  $^{\circ}/h$ ), also referred as drift, characterizes the output signal drift over time and represents the rotation-free measurement error. This parameter can be affected by the environment (for example: temperature, magnetic field...).
- Angle random walk (ARW) is a noise specification expressed in  $^{\circ}/\sqrt{h}$ , that is directly applicable to angle calculations. ARW describes the noise integrated over one hour<sup>36</sup>. The resolution of a gyroscope is the smallest detectable rotation in  $^{\circ}/s$  and is also used to quantify the noise.

<sup>35</sup> « IMU Market », Yole, 2015

<sup>36</sup> W. Stockwell "Angle Random Walk," <http://www.xbow.com>

- The scale factor is the ratio between a change in the output signal and a change in the input. Scale factor accuracy corresponds therefore to the amount of change in the output rate per unit change of rotation rate.

### 3.2.2.2 Classes and applications of gyroscopes

Based on the previous parameters, gyroscopes are classified into three different grades:

- Inertial grade regroups navigation systems used on board of aircrafts, underwater robots/submarines or satellites. An inertial measurement unit (IMU) uses three gyroscopes in combination with three accelerometers to track the position and orientation of an object.
- Tactical grade corresponds to devices that require lower performance. Areas of applications preferably include missile guidance or control of dynamic systems.
- Rate-grade is used in low-cost and low-performance systems like vehicle stabilization or entertainment.

Requirements for each of these grades is summarized in Table 6 below:

Parameter	Rate grade	Tactical grade	Inertial grade
Angle Random Walk, °/√h	> 0.5	0.5-0.05	< 0.001
Drift, °/h	10-1000	0.1-10	< 0.01
Scale factor accuracy, %	0.1-1	0.01-0.1	< 0.001
Full scale range, °/s	50-1000	> 500	> 400
Max shock in 1 s, g	10 <sup>3</sup>	10 <sup>3</sup> -10 <sup>4</sup>	10 <sup>3</sup>
Bandwidth, Hz	> 70	> 100	> 100

Table 6: Performance requirements for different classes of gyroscopes

A few rare publications also mention a “military or strategic grade” class of gyroscopes<sup>1</sup> requiring higher performances than the “Inertial grade” (drift < 0.001 °/h).

Inertial navigation uses measurements from both gyroscopes and accelerometers to track the position and orientation of an object. The inertial measurement unit (IMU) measures the acceleration and angular velocity of the object using three accelerometers and three gyroscopes.

Several types of gyroscopes exist: Mechanical gyroscopes, Optical gyroscopes (based on Sagnac effect) (FOG, IFOG, RLG), MEMS gyroscopes (based on Coriolis effect) manufactured using traditional silicon microelectronic techniques, low-cost and low-performance sensors, atomic interferometer gyroscopes.

Nowadays, inertial navigation systems are dominated by optical gyroscopes and mechanical gyroscopes as shown in Figure 22. The drift limit of 0.1 °/h is required to maintain inertial navigation error below 1 nautical mile/h inboard of an aircraft. Mechanical gyroscopes and especially

hemispherical resonator gyroscopes (HRG) obtain the best ARW and drift performance with  $10^{-6}$  °/√h and of  $10^{-6}$  °/h, respectively.

Optical gyroscopes, based on the Sagnac effect, have the following properties including some advantages over their mechanical counterparts:

- No moving parts (very high reliability and life time)
- Very high dynamical range (1000 °/s)
- Bias (0.01 °/h)
- Insensitive to accelerations and vibrations
- Negligible warm-up time

Currently, optical gyroscopes are preferred for aircraft navigation.

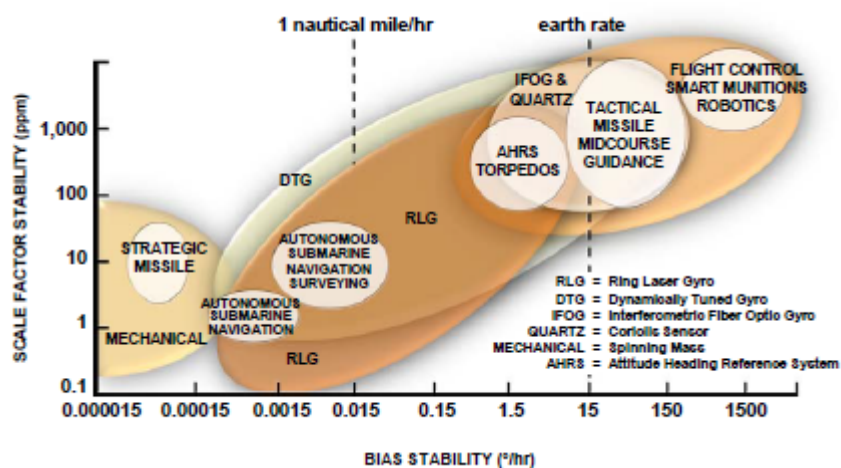


Figure 22: Gyroscopes used for navigation and their performances<sup>37</sup>

### 3.2.3 Nuclear Magnetic Resonance (NMR) Gyroscopes

#### 3.2.3.1 Working principles

Nuclear magnetic resonance (NMR) gyroscopes have been developed since the 60's. The rotation measurement is directly obtained by detecting a shift in the Larmor precession frequency of the

<sup>37</sup> N. Barbour, G. Schmidt, "Inertial sensor technology trends", IEEE Sen J., Vol. 1, N°4, Dec 2001

nuclear spins. In an ambient magnetic field  $\vec{B}_0$ , nuclear spins precess around  $\vec{B}_0$  with a precession rate given by their Larmor frequency that is proportional to  $B_0$ :

$$w_l = \gamma_l B_0 \quad \text{Eq 1}$$

where  $\gamma_l$  is the gyromagnetic ratio representing the ratio of the magnetic moment to the angular momentum. If the cell, containing the nuclear spins, is subject to a rotation around the z-axis of the static field  $\vec{B}_0$ , the precession frequency shift is directly linked to the rotation  $\Omega$ :

$$w_l = \gamma_l B_0 \pm \Omega \quad \text{Eq 2}$$

The sign of the shift depends on the direction of the rotation. Knowing the value of the static magnetic field and the gyromagnetic ratio of the vapor, the rotation frequency can be derived. To decrease the sensor sensitivity to static magnetic field fluctuations, the nuclear gyromagnetic ratio  $\gamma_l$  must be low. The Larmor frequency of an alkali metal is typically 3-4 orders of magnitude larger than that of a noble gas. That is why noble gases are commonly used in NMR atomic gyroscopes (for instance: helium (He), neon (Ne), argon (Ar), krypton (Kr), and xenon (Xe)). The previous relation shows that there are two unknown: the static field and the precession rate. The use of two species with different gyromagnetic ratios (e.g. two isotopes) gives two different Larmor frequencies allowing to solve the equation:

$$w_{l1} = \gamma_1 B_0 \pm \Omega \quad \text{Eq 3}$$

$$w_{l2} = \gamma_2 B_0 \pm \Omega$$

where  $w_{l1}$  and  $w_{l2}$  are the measured frequencies of the two isotopes with gyromagnetic ratios  $\gamma_1$  and  $\gamma_2$ . The rotational shift is the same for both isotopes, while the magnetic-field shift is different for the two isotopes due to the different values of the gyromagnetic ratios. The measurement of the two Larmor frequencies allows to cancel the dependence to  $B_0$ :

$$\Omega = \frac{(\gamma_2/\gamma_1)w_{l1} - w_{l2}}{(1 - \gamma_2/\gamma_1)} \quad \text{Eq 4}$$

### 3.2.3.2 Orders of magnitude

NMRG needs a control system which uses a feedback loop in order to sustain the precession. The feedback loop induces noise<sup>38</sup> that causes a slight phase shift between the observed and the applied observed Larmor precession frequency. The error in phase accumulated during the time can be represented by the Angle Random Walk following the calculations in Ref [39]:

<sup>38</sup> I.A. Geenwood, J.H. simpson, "Fundamental noise limitations in magnetic resonanace gyroscope" , NAECON'77, pp 1249-1250, 1977

<sup>39</sup> E.J Eklund, "Microgyroscope based on Spin-Polarized Nuclei", Ph.D. Thesis, University of California at Irvine, 2008

$$ARW = \frac{1}{T_2 SNR \sqrt{\Delta f}} \tag{Eq 5}$$

where  $SNR$  is the signal-to-noise ratio,  $T_2$  the transversal relaxation time and  $\Delta f$  the bandwidth of the device. Left panel in Figure 23 represents the signal-to-noise ratio and relaxation time required to achieve a given angle random walk.

Inertial class requires an ARW of  $0.001^\circ/\sqrt{h}$ . With a sensitivity of  $0.1\text{pT}/\sqrt{\text{Hz}}$  for a rubidium scalar magnetometer (cell of  $1\text{ mm}^3$ ), the estimate signal-to-noise ratio is  $6.5 \times 10^5 \sqrt{\text{Hz}}$ . Navigation-grade performance can be obtained with a relaxation time of 5s. ARW can be improved by means of an anti-relaxation coating increasing the relaxation time.

The fluctuations of the magnetic field are indistinguishable from the angular rate in a NMR gyroscope. Considering a variation of the magnetic field  $\delta B_z$ , the rotation drift is given by  $w_l = \gamma_l \delta B_z$ . Right panel in Figure 23 Figure 11 shows the stray magnetic field versus the bias drift for four nuclear species with different gyromagnetic ratios.

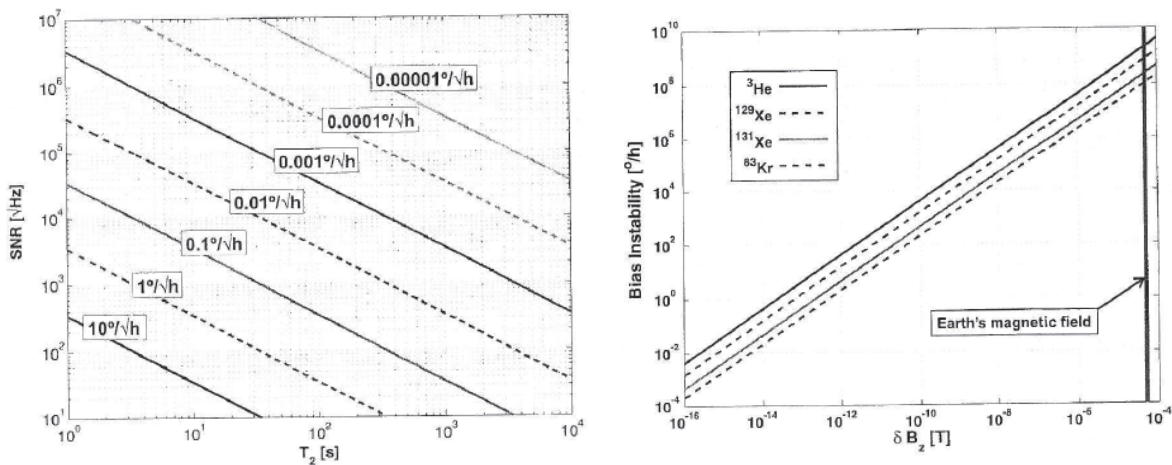


Figure 23 – Left: ARW as a function of signal-noise ratio and relaxation time, Ref [39]. Right: bias instability due to stray magnetic fields for different noble gas nuclei, Ref [39].

A navigation grade gyroscope requires a drift lower than  $0.01^\circ/\text{h}$ . The residual magnetic field has to be in the range of 1 fT to reach it. However, the earth’s magnetic field is about  $50\ \mu\text{T}$ , which is  $10^{10}$  higher. Two methods will make this very low magnetic field stability achievable: the use of a magnetic shield and the steadiness of the two magnetic field measurements combined to compute the rotation angle.

### 3.2.3.3 Technical aspects

The operating principles of a NMR gyroscope are based on the three steps depicted in Figure 24:

- 1) Polarization: to detect the precession, a macroscopic nuclear magnetization vector must be achieved. In thermal equilibrium, atomic sublevels are almost equally populated, therefore, no significant change is induced at resonance. In order to align the individual magnetic moments, an optical pumping is applied. For instance, in the case of alkali and noble-gas atom mixtures, this polarization step is realized by a spin-exchange optical pumping.
- 2) Precession: applying an oscillating field to induce coherence: In a static homogeneous field  $\vec{B}_0$  along the z-axis, the nuclear magnetic moments precess around the direction of  $\vec{B}_0$  but their phases are uncorrelated. The nuclear magnetic moment has no component in the x-y plane. Coherent spin precession is induced by an AC magnetic field perpendicular to  $B_0$  with a frequency equal to the Larmor frequency of the noble gas.
- 3) Detection: several methods can then be used to detect the precessing nuclear magnetization such as a set of coils, or an atomic magnetometer into the NMR cell using the modulation of a probe-beam or the Faraday effect. These key stages are described in details in the following sections.

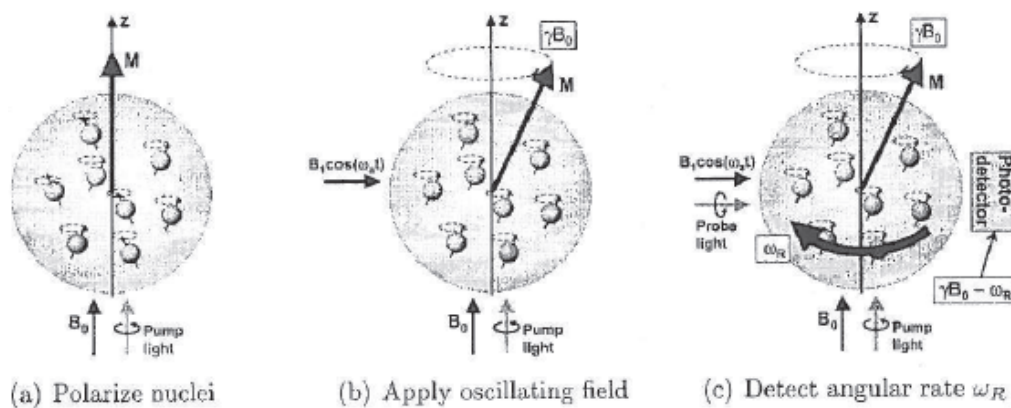


Figure 24 - Principle of operation of an NMR gyroscope, Ref [39]

#### 3.2.3.3.1 Optical pumping

The polarization is defined as the normalized population difference between the hyperfine levels of the ground state of atoms or between sub-Zeeman levels. In thermal equilibrium, the population difference between those levels is very low, leading to a very small spin polarization and a weak NMR signal.

To align the magnetic moments along the same direction and obtain an orientation, several optical pumping techniques can be used<sup>40</sup>. A lamp or a laser tuned to the wavelength of an electronic transition can induce an electronic orientation that is transferred to the nuclei producing a net nuclear magnetization. Depending on the gas species, different optical pumping methods have to be considered<sup>41</sup>:

- Orientation through a strong hyperfine coupling for alkali, similar and 1S0 ground states atoms: during the pumping cycle, nuclear spins do not interact directly with light. Photon absorption only modifies electronic orbital constant. Then thanks to a strong hyperfine coupling in the energy level, nuclear spins are oriented<sup>42</sup>.
- Spin exchange optical pumping (SEOP) for a mixture of alkali and noble gas: noble gases cannot be oriented directly with a laser since their outer shell of valence is full. In SEOP, alkali (such as rubidium) are optically pumped (the single valence electron of the alkali is thus polarized). The alkali atoms further transfer their angular momentum to the noble gas nuclei through magnetic interactions during binary alkali-noble gas collisions.
- Metastability optical pumping (MEOP) for the  $^3\text{He}$  noble gas:  $^3\text{He}$  metastable atoms are created using a radio frequency discharge<sup>43</sup>. Optical pumping for  $^3\text{He}$  metastable atoms ( $\text{He}^*$ ) induces both electronic and nuclear orientation thanks to a strong hyperfine coupling in this energy level (direct electron-nucleus magnetic interaction, within the  $\text{He}^*$  atom). Further transfer of angular momentum from  $\text{He}^*$  atoms to ground state He atoms through metastability exchange (ME) collisions allows an orientation of the nuclear spin (a binary exchange of electronic excitation with no loss of nuclear orientation).

### 3.2.3.3.2 Nuclear coherent spin precession

NMR gyroscopes require a sinusoidal AC magnetic field in addition to the static magnetic field. This field, perpendicular to the main static field and which frequency is close to the Larmor frequency, resonates with the magnetic moments that are precessing coherently.

When two nuclear species are used, two oscillating magnetic fields, which frequencies correspond to the Larmor frequencies, must be used. Usually these fields are locked-in with the detected signal.

### 3.2.3.3.3 Rotation detection

---

<sup>40</sup> W. Happer "Optical Pumping," Rev. Mod. Phys, Vol 44, N 2, pp 169-249, 1972

<sup>41</sup> <http://www.lkb.ens.fr/Optical-pumping-and-detection>

<sup>42</sup> M. Leduc, "Quelques experience d'orientation nucléaire par pompage optique", Ph.D. thesis, université de paris VI, 1972

<sup>43</sup> P.J. Nacher, M. Leduc "Optical pumping in  $^3\text{He}$  with a laser," J. Phys.,46, pp 2057-2073, dec 1985



Different optical detections can be applied to measure the nuclear precession, as described below in the following sub-sections.

#### 3.2.3.3.1 Dehmelt technique

The processes involved in Dehmelt detection are the same as for optical pumping. Absorption depends on the projection of the electronic spins along the axis of propagation of the laser. When spins and light point into the same direction, spins are already oriented therefore absorption is at a minimum<sup>44</sup>. Conversely, if spins point in the opposite direction, absorption is at its maximum level. A combination of two perpendicular beams, one for the pump and the other for the probe enables to create an orientation and to obtain a modulation of the probe beam. Resonance is detected on the modulated probe beam.

#### 3.2.3.3.2 Faraday rotation

A linearly polarized probe beam crossing a magneto-optical system is subjected to a rotation out of the plane of its polarization. This phenomenon, due to the Faraday Effect, is employed to monitor the rotation. Passing through the gas cell, the angle of the plane of polarization of the light beam is modulated at the Larmor frequency. This modulation angle can be converted to an amplitude modulation by a linear analyzer added to the photodiode. The wavelength of the beam is generally detuned from the resonance to limit absorption fluctuations<sup>45</sup>.

#### 3.2.3.3.3 Induction coils

Two detection coils in Helmholtz configuration, positioned on each side of the cell, detect the precession of the spins<sup>46</sup>. The magnetization of the nuclear spins creates an electromotive force into the coils at the Larmor frequency. The induced current in the coils produces a negative feedback field which couples the coil and the magnetization and modifies the Larmor frequency. This shift can be evaluated when designing the coil and the electronic circuit for detection.

#### 3.2.3.3.4 External magnetometer

An alternative to the measurement of the precession frequency of the spins is to use an atomic magnetometer close to the cell containing nuclear species. This was exposed by Dupont-Roc with a rubidium magnetometer and a He3 cell<sup>47</sup>. The relaxation and the precession had been thus monitored.

---

<sup>44</sup> H.G. Dehmelt "Modulation of a Light by Precessing Absorbing Atoms," Phys. Rev., Vol 105, 1924-25, Jan. 1957

<sup>45</sup> D. Budker, W. Gawlik, D.F. Kimbakk, S. Rochester, V.V. Yashchuck and A. Weis, "Resonant nonlinear magneto-optical effects in atoms", Rev. Mod. Phys., Vol. 74, pp 1153-1201, 2002

<sup>46</sup> H. Wang, "Nuclear magnetic resonance gyro" Int. publ. Num. WO 81/00455, Feb 1981

<sup>47</sup> C. Cohen-Tannoudji, J. Dupont-Roc, S. Haroche, F. Laloë, "Detection of the static field produced by oriented nuclei of optically pumped <sup>3</sup>He", Phy. Rev. Lett., Vol 22, 758, 1969





Cryogenic NMR research at Admiralty Research Establishment (ARE) made an experience in a superconducting shield where the precession of He3 was measured by a SQUID<sup>48</sup>.

### 3.2.3.3.4 Magnetic shielding

Typically, magnetic shields are made of several layers of  $\mu$ -metal, a high permeability material, efficient to canalize the magnetic field lines. The shield efficiency depends on its geometry. Although sphere provides an isotropic attenuation of the magnetic field, cylinder geometry is, in practice, preferred for manufacturing reasons. In this configuration, axial and transverse attenuation are distinct. Welds and holes have to be especially carved to limit the intrusion of perturbations inside the enclosure. Although  $\mu$ -metal is efficient, its conductivity induces Johnson noise that can be limiting when noises lower than 10-100 fT/VHz are required. The layer near the sensor can be replaced by a ferrite material. Having a high permeability, ferrite is comparable to  $\mu$ -metal in terms of magnetic shielding performances. However, as a ceramic, ferrite has no eddy current induced noise thanks to its high electrical resistivity<sup>49</sup>.

The magnetic attenuation of the shield defines the ratio of the field measured at the outside of the shield to the one measured inside. Usually, shielding factor is in the range of  $10^7$  for a five layer cylinder shielding of a few tens of centimeters in diameter<sup>50</sup>. NIST reports similar result for shields with volume from 0.01 to 3 cm<sup>3</sup> assembled together.

### 3.2.3.4 Products

#### 3.2.3.4.1 Development before the advent of the optical gyroscopes

Before the large-scale commercialization of fiber optical gyroscopes in the 80's, few options were considered to create an inertial grade instrument. Manufacturers investigated the field of atomic gyroscopes because the solution seemed appealing. Indeed, the NMR technology requires a lower precision in the manufacturing process than the FOG ones, leading to cheaper instruments.

#### Litton System

<sup>48</sup> S.P. potts, J. Preston "A cryogenic nuclear magnetic resonance gyroscope" Jour. of Nav., Vol 34, n°19, 1981

<sup>49</sup> T.W. Kornack, S.J. Smullin, S.K. Lee, M.V. Romalis, "A low-noise ferrite magnetic-shield" Appl. Phys. Lett. 90, 223501, pp 90-93, 2007

<sup>50</sup> E.A. Donley, E. Hodby, L. Holberg, J. Kitching, "Demonstration of high-performance compact magnetic shields for chi-scale atomic devices", Rev. Sci. Instrum. 78, 083102, 2007

Litton<sup>51</sup> develops a gyroscope with one cell filled with two noble gases Kr<sup>83</sup> and Xe<sup>129</sup> and an alkali (Rb<sup>87</sup>). Nuclear polarization is achieved through SEOP. Detection of the nuclear precession is based on the modulation of a probe beam at the Larmor frequencies of the nuclear species. Noble gases create rotating fields that modulate the precessional motions of the rubidium magnetic moment which, in turn, produces corresponding modulations in the transmitted light.

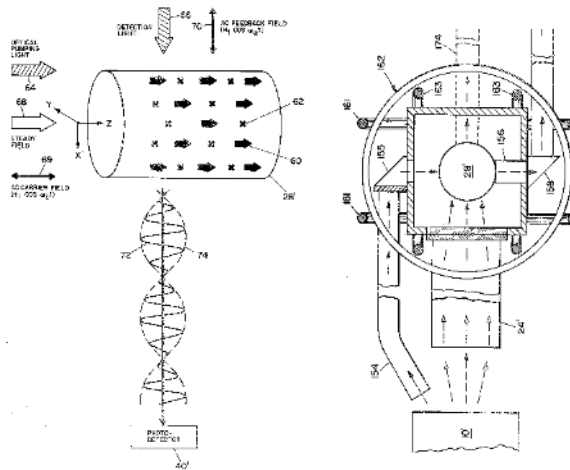


Figure 25 - Scheme of the Litton gyroscope. From Ref [54]

Figure 25 shows the encapsulation of the gas cell into a multiple layer shield. A lamp is used to polarize the rubidium. We can note that an optical fiber is used to move away the lamp and the photodiode from gas cell, improving the optical coupling and reducing the magnetic field perturbation. This also allows the use of a unique source for the pump and the probe beam. The most compact instrument is about 12 cm tall and 10 cm in diameter with performances of 0.1 °/h for the drift and  $0.015^\circ/\sqrt{\text{Hz}}$  for the ARW<sup>52</sup>.

### Singer-Kearfott

Singer-Kearfott<sup>53</sup> built a NMRG based on another technique to eliminate the impact of the variation of the static field. NMRG uses two cells containing two mercury isotopes (mercury Hg<sup>199</sup> and Hg<sup>201</sup>). The cells are situated between two coils, generating fields in opposite directions. This geometry combined with phase detection and a control system allows to reduce the error due to the variation of the

<sup>51</sup> B.C. Grover, A. Kanegsberg, J.G. Mark, R.L. Meyer, "Nuclear magnetic resonance gyro", US pat. 4 157 495, 1979

<sup>53</sup> I.A. Greenwood, "Nuclear gyroscope with unequal field", US pat. 4 147 974, Apr 1979



magnetic static field. The Hg nuclear spins are directly pumped and probed via the Faraday rotation. An ARW value of  $0.015 \text{ }^\circ/\sqrt{\text{h}}$  and a bias of  $0.05^\circ/\text{h}^{54}$  had been reported.

### **Naval Air development center (US)**

This gyroscope designed for the needs of US navy aircraft uses the same isotope as the Singer version. The two isotopes are contained in one cell surrounded by eight coils with adjustable ferrite cores for fine tuning. The adjustment provides the ability to fine tune the field in the area of the cell in order to reduce non-uniformity in the magnetic field. The detection of the Larmor precession is made with Faraday read-out technique. This gyroscope obtains a drift between  $0.1 \text{ }^\circ/\text{h}$  to  $0.25 \text{ }^\circ/\text{h}^{55}$ , performance are still not satisfying enough to fulfil the requirements of the US Navy.

### **Hughes Aircraft Company**

Hughes Aircraft Company proposes a gyroscope using MEOP<sup>56</sup>. Pumping is made in one cell whereas detection is made in another one connected with a tube. This geometry permits to eliminate discharge products and metastable atoms affecting the Larmor frequency of the nuclear precessing spins. Metastable atoms, because of their short life-times, cannot pass in the second cell while long relaxation time polarized ground state atoms can. The detection is made with induction coils tuned at the Larmor frequencies of the two gases.

### **3.2.3.4.2 Resurgence of the atomic gyroscopes in the early 2000's**

As advances made in chip scale atomic clocks (MEMS vapor cells, instrumentation and optronics) can be applied to a gyroscope, recent years have seen a renewed interest for atomic NMR gyroscopes.

### **Northrop Grumman**

Northrop Grumman works actively on the field of micro atomic gyroscopes (US 2009/0033329). They have been working with the financial support of the DARPA for five years and have presented a review of their developments and progresses at the 66th IEEE International Frequency Control Symposium in

---

<sup>54</sup> K.F. Woodman, P.W. Franks and M.D. Richards, "The Nuclear Magnetic Resonance gyroscope : a Review", Jour. of Nav., Vol 40, N°3, pp 366-384, 1987

<sup>55</sup> K.F. Woodman, P.W. Franks and M.D. Richards, "The Nuclear Magnetic Resonance gyroscope : a Review", Jour. of Nav., Vol 40, N°3, pp 366-384, 1987

<sup>56</sup> H. Wang , "Nuclear magnetic resonance gyro" Int. publ. Num. WO 81/00455, Feb 1981

2012<sup>57</sup>. Several patents concerning the architecture and its operating principle including a nonmagnetic heater system have been filed. Their goals in term of performance are to reach an ARW of  $0.01^\circ/\sqrt{h}$  and a bias of  $0.05^\circ/h$ . They obtained it at their third phase of development and they are now in the final phase of conception.



Figure 26 - Gyro internal structure, physics package of the latest version

The device uses an alkali, probably rubidium or cesium, which polarizes two noble-gas isotopes ( $Xe^{131}$  and  $Xe^{129}$ ) by spin exchange optical pumping. The alkali electron state is pumped by a vertical cavity surface-emitting laser (VCSEL). The alkali is also used as a magnetometer to sense the precessions of the xenon isotopes. A second VCSEL in a Faraday rotation system detects the precession of the alkali spin, modulated at the nuclear isotope's Larmor frequencies. The gyromagnetic ratios for the two Xe isotopes have opposite signs: as a result they precess in opposite directions. Expressions of the measured frequencies are:

$$w_{l1} = \gamma_{l1}B_0 + \Omega \quad \text{Eq 6}$$

$$w_{l2} = \gamma_{l2}B_0 - \Omega$$

If the two frequencies are added, the result is independent of the rotation and proportional to the net magnetic field. Sum is held constant by phase locking this signal to an external frequency reference using a feedback on the magnetic field coils which generates the main magnetic field. The case rotation is determined by comparing the measured isotope Xe signal to this external frequency reference.

Figure 26 shows the final physics package of the sensor. It is built to maintain vacuum, allowing the best performances in terms of gas cell control temperature and optical coupling. Previously in 2006, Northrop Grumman presented another architecture (US 7 239 135 B2) for a micro NMRG. They already

<sup>57</sup> M. Larsen, M. Bulatowicz, "Nuclear Magnetic Resonance Gyroscope: For DARPA's micro-technology for positioning, navigation and timing program" 2012 IEEE International Frequency Control Symposium, IFCS 2012, Proceedings, n°6243606, pp. 592-596



wanted to make a compact instrument with low power consumption. Two solutions are described with one for which optics, electronics, sensor and cell and laser are implemented on several stacked wafer.

Four magnets provide a uniform static magnetic field stable from 0.1 to 10 Gauss. It is designed to avoid using electrical power. The magnet design is covered with a patent (US 5 469 256). The projected size is about 16 mm in diameter and 6 mm tall. The cell may contain Xe or Kr as nuclear spin gases and an alkali as pumping gas. There is no known manufactured product or prototype of the patented sensor.

Northrop Grumman also proposes a gyroscope (EP 1 847 846 A1) which main feature is to eliminate shifts in the Larmor frequencies. The patent describes an apparatus with three species to calibrate this shift. The introduced error is described in terms of:

$$w_l = \gamma_l B_0 + b_l c \pm \Omega \quad \text{Eq 7}$$

where  $c$  is a function of the atom density and  $b$  a constant for each species. The different precession frequency measurements give a system of three linear equations with three unknown variables.

Northman Grumman also proposed to improve bias stability by reversing the polarity of the current in the bias field coil, which reverses the polarity of the magnetic field and the polarity of the precession of the nuclear spin (US 2009/0033329). The alternating bias field technique is combined with the use of two nuclear isotopes (see Eq 3). To our knowledge, this patented technical solution has never been realized.

## NIST

The National Institute Standard of Technology also develops its own magnetometer. Also working as a gyroscope<sup>58</sup>, its originality comes from its sensing technique.

The cell is filled with Rb alkali, Xe<sup>131</sup> and Xe<sup>129</sup> which nuclei can be polarized via spin exchange with the alkali atoms. One pair of coils, as shown on Figure 27, produces a static field  $B_0$  setting the axis of the gyroscope. A parallel oscillating field at the Larmor frequency of the alkali is added. This causes the alkali spin to precess.

---

<sup>58</sup> J. Kitching, E.A. Donley, A. Hobdy, A. Shkel, J. Eklund, "Compact Atomic Magnetometer and Gyroscope Based on a diverging Laser Beam" US pat. 7 872 743 B2, Jan 2011

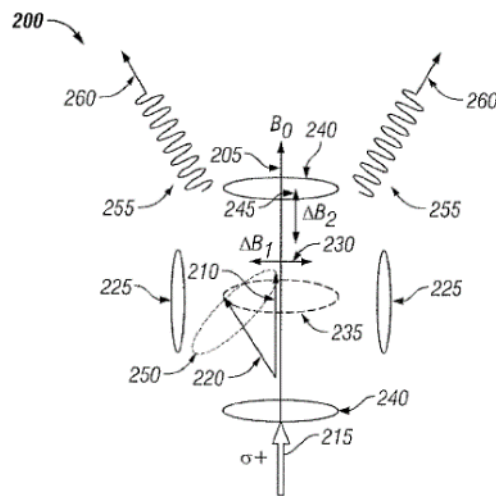


Figure 27 - Schematic of the NIST gyroscope. From Ref [58].

Two alternative fields at Larmor frequencies of xenon isotopes are created. They are transverse to the main axis of the gyroscope and make the nuclear spins precess coherently. The method of detection is based on the modulation of a probe beam. Its originality comes from the use of a diverging beam. The strong central part of the beam is used to optically pump the atoms while the diverging parts act as probes. This technique was first developed for a magnetometer as illustrated on Figure 28.

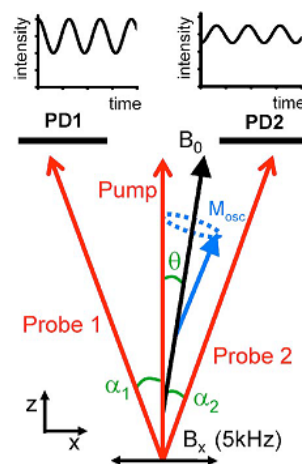


Figure 28 - Schematic diagram of the working principle of the differential magnetometer

The precessing noble spins create a transverse magnetic field, which affects the alkali spins. The precessing alkali spins create a transverse polarization in the atomic vapour, which causes a change in the absorption of the light field that depends on the propagation direction of the light. Thanks to the circularly symmetrical nature of the diverging beam, the transverse polarization generates a

differential absorption on the two photodiodes. By subtracting the signals, the Larmor frequencies of both the alkali and the noble gas can be measured.

### 3.2.3.5 Performance analysis

Table 7 gathers performances of different gyroscopes. Northrop Grumman obtains approximately the same performances as the work done by Litton and Singer previously. The sharp difference between Northrop Grumman and the other manufacturers is the miniaturization. The first has a bulk of a few centimeters while the formers got approximately a dozen centimeters side.

	Northrop Grumman (US 2009/0033329)	Litton	Singer	Northrop Grumman (US 5 469 256)	NIST	Naval Air development center
ARW ( $^{\circ}/\sqrt{h}$ )	0.01	<0,01	0.015	X	X	X
Bias ( $^{\circ}/h$ )	0.05	0.1	<0.05	X	X	0.1~0.25

Table 7 - Summary table of NMRG performances

Litton stopped NMRG developments mainly because of the maturity of fiber optic gyroscopes and the interest of US funding agencies for this technology. Their prototype appears to have a low dynamic range. The hypothesis was that if the system is rotating rapidly around an axis coincident with the central axis of the gas sample, there is no guarantee that the bulk of the gas would rotate when the same cell rotates. Unfortunately, Litton's program was stopped before this point can be explored. Singer also stopped its program and sold its technological rights.

The feasibility of a NMR gyroscope has been demonstrated by NIST<sup>5</sup> but no concrete results have been obtained. The main problem comes from the rubidium magnetometer which is not able to detect a precessing xenon magnetization. Several reasons are discussed, including cell temperature, insufficient optical pumping and mostly magnetic field gradients. Several designs have been envisaged to reduce the gradient but never set up. Another architecture based on a micro spherical cell to minimize the self-magnetization of the atoms is being investigated.

At the time being, Northrop Grumman seems to be the most advanced in the conception. They reached their performance goal and are in their final production stage. They have several recent patents concerning their sensors<sup>59,60,61,62,63</sup> and a review paper<sup>64</sup>.

---

<sup>59</sup> R.E. Stewart, E. Kanesberg, "Self-calibrating nuclear magnetic resonance gyroscope" US pat. N° 2009/0033329

<sup>60</sup> R.E. Stewart, E. Kanesberg, "Gyroscope a resonance magnetique nucleaire à auto-etalonnage" N°2923007, Jul. 2008

<sup>61</sup> M. D. Bulatowicz, M. S. Larsen, "Self-calibrating nuclear magnetic resonance (NMR) gyroscope system", US pat. N° 2016/0202083

<sup>62</sup> R. C. Griffith, "Ratiometric nuclear magnetic resonance (NMR) gyroscope system", US pat. N° 2015/0593827

<sup>63</sup> H. C. Abbink, M. D. Bulatowicz, M. S. Larsen, "Nuclear magnetic resonance probe system", US pat. N° 2013/0907293

<sup>64</sup> T. G. Walker, M. S. Larsen, "Spin-Exchange Pumped NMR Gyros", Advances in Atomic, Molecular and Optical Physics, Vol 65, pp 373-401 (2016)



## 4 Experiments to clarify SoA of technology on integration of clocks and atomic gyroscopes

---

In order to validate the SoA on MACs and MAGs and the integration at process level, experiments have been performed. Initially the experiments were planned using available MEMS cells at CSEM. However considering CSEM progress in MEMS cell fabrication we find that newly fabricated cells will outperform the available ones.

### 4.1 Relation with TRL management plan

In order to prepare and support the ER/IR gate at the end of the project, a TRL roadmap has been developed and TRL milestones have been introduced in the project Gantt chart. These are represented in Figure 29. Since the TRL milestones do not coincide with any of the periodic review milestones, informal TRL review was planned. In particular, the review of TRL2+ level, which is the subject of the present document was scheduled to take place at MS3 (RP2 review scheduled for January 13<sup>th</sup>, 2017). The consortium aims to carry out a number of tests that will support the TRL progress. The list of foreseen tests is presented in the following table. The three first tests are planned for reaching TRL2+ level and report them in present deliverable document D3.1.

ID	Test	Objectives
1	Cell characterization	N <sub>2</sub> and Xe pressure in 8 cells. Hours only for Xe (2 of each)
2	Setup (refurbishing and shielding demagnetization)	
3	$T_2$ spin relaxation time of Rb atoms with FID or Pi/2 vs resonance waveform to estimate res. field	To define res. field and apply demag if needed
4	$T_2$ spin relaxation time of Rb atoms vs cell size and T	To get an estimation for Rb signal bandwidth

5	$T_1$ spin relaxation time of Rb atoms vs cell size and T	To get an estimation for Rb signal bandwidth
6	Observe NMR	NMR could not be observed in AGEN and GYROCELL
7	$T_2$ spin relaxation time of Xe atoms vs cell size and T	To get an estimation for Xe signal bandwidth
8	$T_1$ spin relaxation time of Xe atoms vs cell size and T	To get an estimation for Xe signal bandwidth
9	Cell heating tests	Feedback for laser heating of the cell from Rb absolute amplitude
10	Demonstrate some ways to share hardware with a MAC	Validate approach of NAVISAS

Table 8 – List of tests to support NAVISAS TRL progression

More specifically the target TRL of 2+ at the end of WP3.3 is characterized as follows:

- Target TRL of 2+ at the end of WP3.3. By the end of this point in the project, the consortium expects to have run tests #1-3 of Table 8 and clarified the state of the art on the integration of atomic clocks and gyros. Therefore, the consortium expects to progress from the initial TRL2. However, the amount of testing and result obtained at this stage will not be enough to progress to TRL3. At this level, we expect to compile some results of laboratory tests performed to measure key parameters of interest for the technologies of interest which can validate some of the assumptions of the previous maturity level concerning aspects like performance.

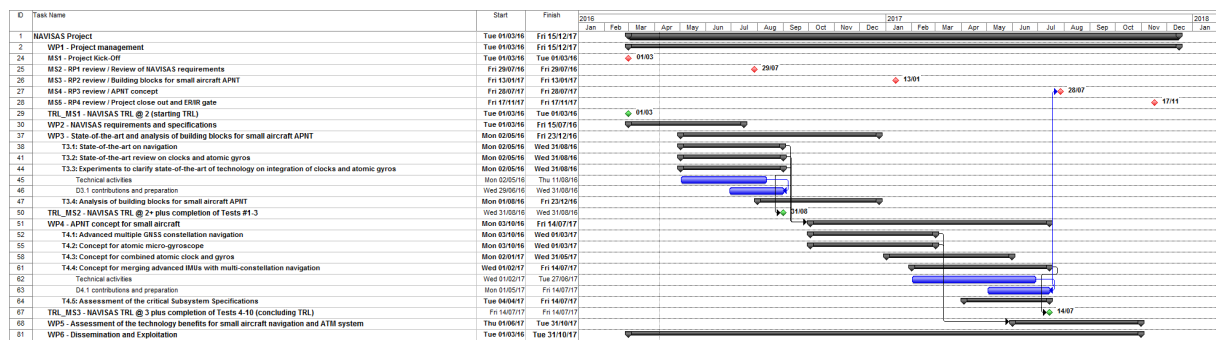


Figure 29 – NAVISAS TRL roadmap

## 4.2 Test 1: MEMS cells fabrication and characterization

### 4.2.1 Fabrication

MEMS cells with thickness 1 mm and with different diameters (1, 2, 3, and 4 mm) have been fabricated at CSEM, see Figure 30. A detail of the fabrication process is given in Figure 31. The gas filling parameters are tuned such that pressures inside the cell at 85°C shall be 200 torr for N<sub>2</sub> and 50 torr for natural Xe.

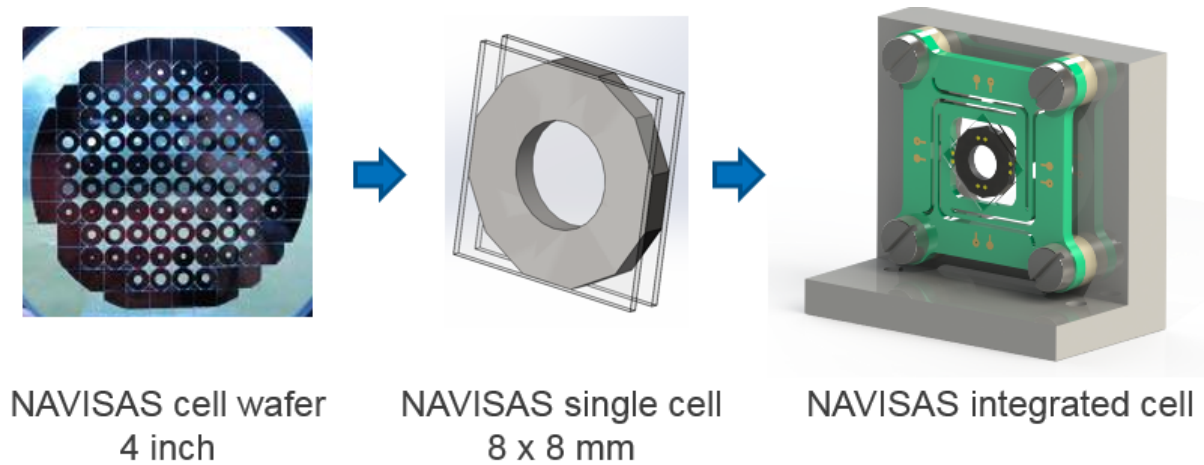


Figure 30 - Description of the MEMS cells. Left: wafer showing cells with different diameters. Middle-Right: Computer simulations of a mounted cell.

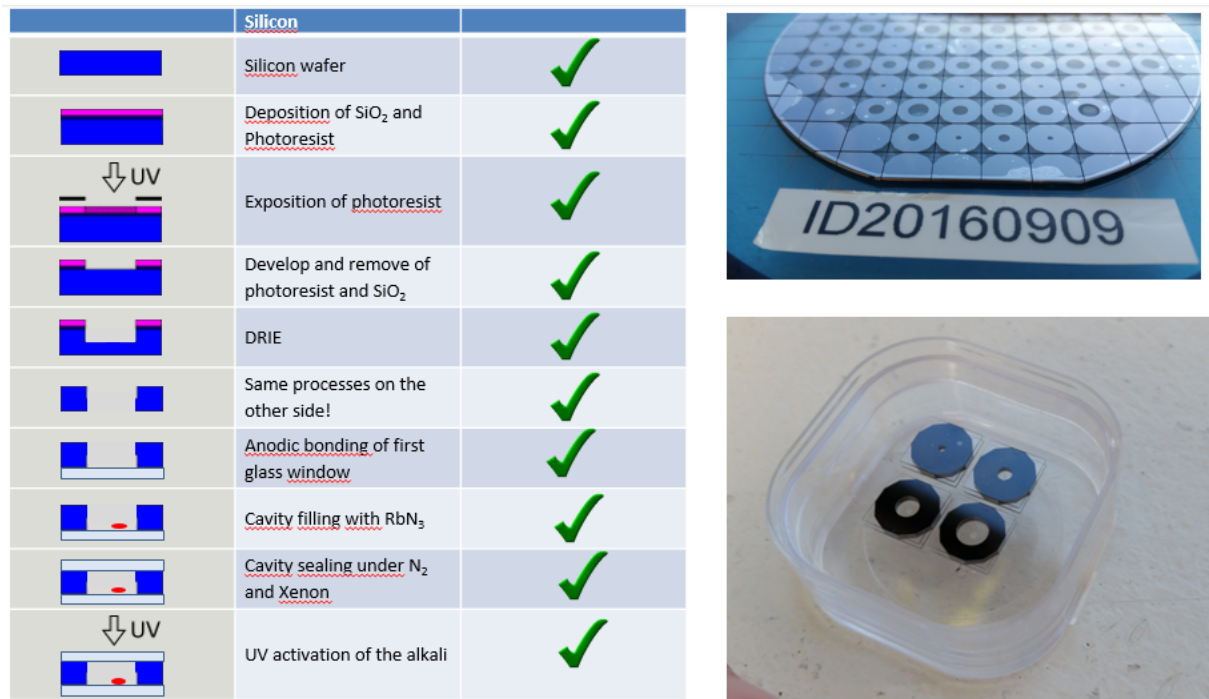


Figure 31 – MEMS cells fabrication process

### 4.2.2 Characterization

The MEMS cell characterization consists in an experimental evidence for the required pressure in the cells (~250 torr total of N<sub>2</sub> and Xe). This pressure can be verified by means of the pressure broadening in the absorption lines. The absorption spectrum  $\alpha(\omega)$  is defined by contributions from the two isotopes (<sup>85</sup>Rb and <sup>87</sup>Rb isotopes), each of which consisting of two hyperfine lines, as indicated in the left panel of Figure 32. The hyperfine splitting provides a scale of 3.0 GHz for <sup>85</sup>Rb and 6.8 GHz for <sup>87</sup>Rb. Due to pressure broadening, the hyperfine lines broaden and strongly overlap, which has a strong impact on the spectral envelope (black curve). Experimentally, we measure the cell transmission  $T$  using a tunable laser and a photodetector with negative trans-impedance amplifier. The expected detector signal for a constant beam intensity and cell temperature of 85°C is shown in the right panel of Figure 32.

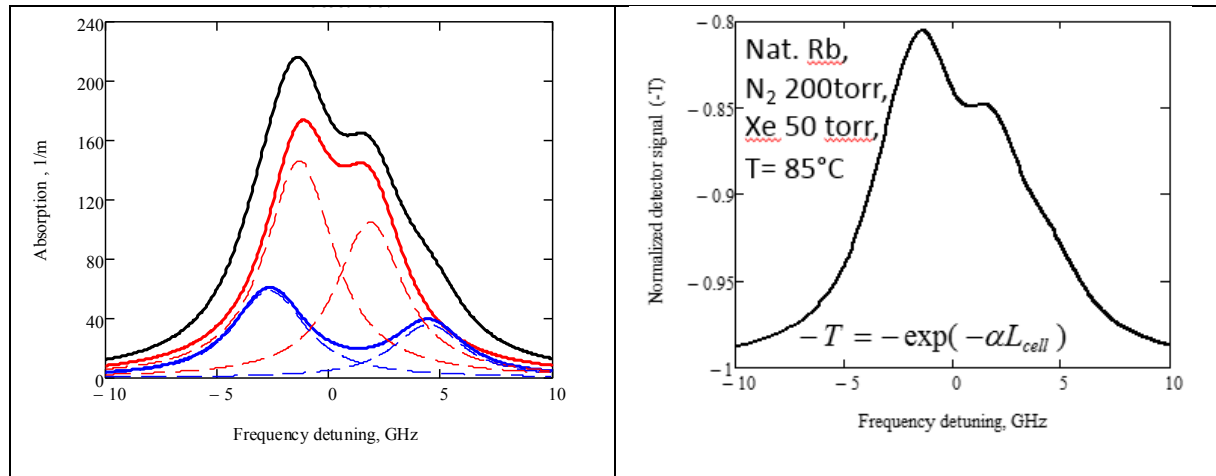


Figure 32 – Simulated absorption spectrum

The left panel in Figure 33 below illustrates the detected cell transmission signal (yellow trace, photodetector with negative trans-impedance amplifier) when the current of the laser is increasing. Its frequency decreases from left to the right. The blue trace indicates transmission of a reference cell with pure <sup>85</sup>Rb isotope (3.0 GHz splitting). The extracted absorption spectrum  $\alpha(\omega)$  is shown in the right panel. It is in good agreement with the expected spectrum shown in Figure 32. The pressure broadening can be assessed from the measured spectral envelope of the cell transmission.

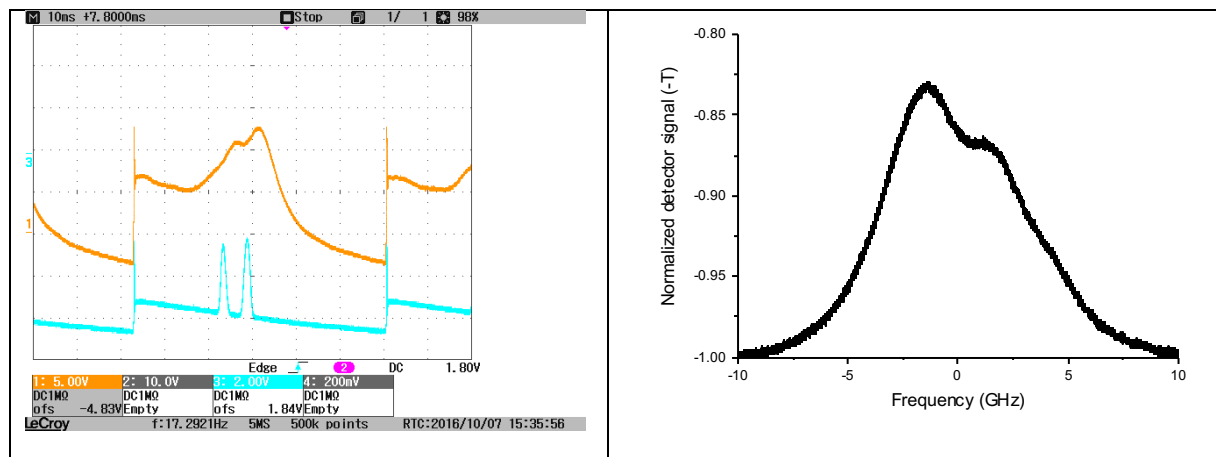


Figure 33 – Absorption measurement

### 4.3 Test 2: Experimental setup

The experimental setup used in NAVISAS is based on a previous setup used for the FP7 project AGEN<sup>65</sup>. A number of modifications and add-ons have been brought up in order to satisfy NAVISAS requirements. A schematic as well as a picture of the complete setup are displayed in Figure 34.

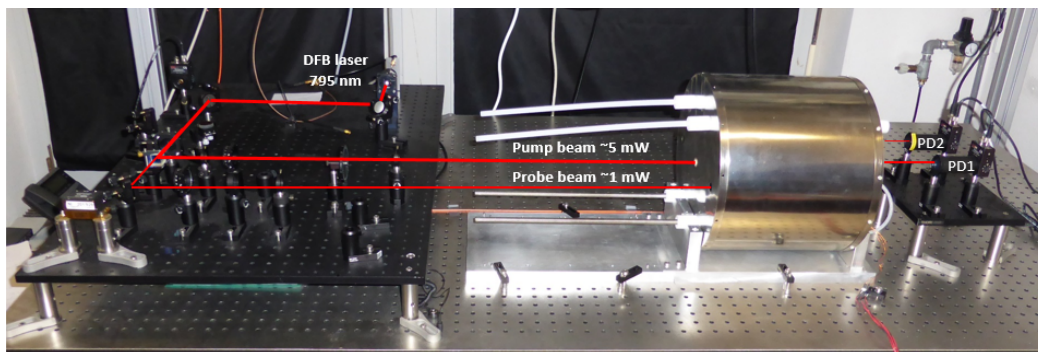
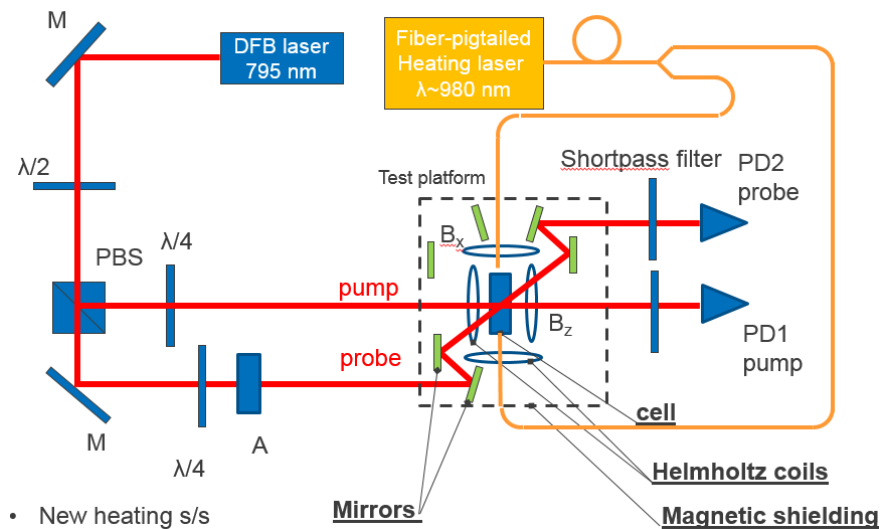


Figure 34 - Schematics and picture of the setup with closed shielding

Here, a DFB laser shining at 795 nm (D1 line Rb) is split at a polarization beam-splitter into pump and probe beams whose intensities can be tuned by means of a  $\lambda/2$  waveplate. The polarization of both beams is then changed from linear to circular by means of  $\lambda/4$  waveplates, before reaching the atomic cell inside the shielding and being detected at photodiodes PD1 (pump) and PD2 (probe). The shielding contains 3 Helmholtz coils for x-y-z magnetic fields (see Figure 35 d)).

<sup>65</sup> <http://agen.tekever.com/>



### 4.3.1 Cell heating

In order to get an appropriate Rb vapour density in the atomic cell, the latter must be heated. For this, a diode laser (BWT) emitting at 980 nm up to 18W into a multimode fiber is used. A picture of the heating laser unit is shown in Figure 35 c). To minimize temperature gradients, the cell is heated from both sides like illustrated in panel a) for the spherical test cell and b) for the MEMS cell. For this, we spliced a 5 meter multimode fiber (Thorlabs MM3L05) at the output fiber of the BWT laser to reach the setup and then a fibered 50/50 beam-splitter (Lightcomm 976 HPMMC 50/50). The two output fibers are terminated with a ferrule (Thorlabs CF126) which is fixed with an epoxy resin (Thorlabs T120) and polished with a right angle. These two extremities are first tested out of the shielding (panels a) and b)).

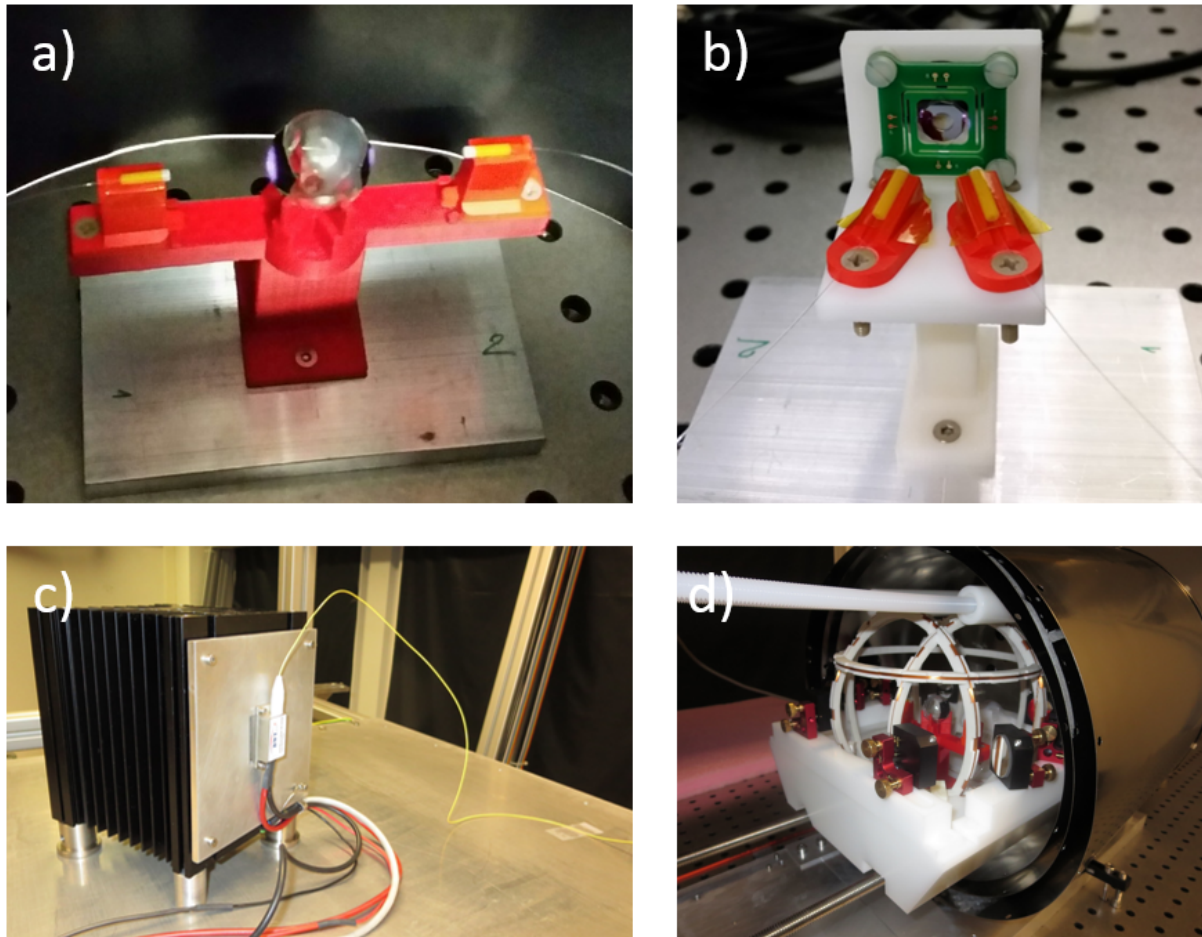


**Figure 35 - a) Test spherical cell with 3D printed ABS + resin cell and ferrules mount. To improve heating efficiency, black aluminium foil tape (Thorlabs AT205-1) is glued on the cell. b) MEMS cell mounted on machined Teflon holder, rotating ferrule holders are 3D printed with a resin. c) 18 W, 980 nm diode laser mounted on a cooling tower. d) Test spherical cell mounted inside the Hemholtz coils and probe-beam mirrors support that is sliding inside the shielding.**

Output light power has been measured at different part of the heating unit for different values of the laser diode current, i.e. directly at the laser output fiber, after the 5 m multimode fiber and at each output. Table 9 summarizes the measured values.

$I_{LD}$ (A)	Out 1 (W)	Out 2 (W)	Total (W)	Laser output (W)	5 meter MM fiber (W)
1.1	0.138	0.135	0.273	0.305	0.291
1.5	0.444	0.450	0.894	0.97	0.96
2	0.830	0.848	1.678	1.903	1.854
2.5	1.22	1.23	2.45	-	
3	1.63	1.65	3.28	-	3.42
4	2.45	2.48	4.93	-	5.24

Table 9 – Output power characterization of the cell heating unit

From these results, we see that both output are well balanced that the losses in the fibers and splices are relatively low (~10%). A summary of the cells heating tests performed with a FLIR camera is given in Figure 36. It can be observed that the heating efficiency is much better for the MEMS cell. Indeed, only 0.37 W in each output is enough to heat the cell at 143 °C, while a lower temperature (106°C) is reached with much more power (4 W) for the spherical cell

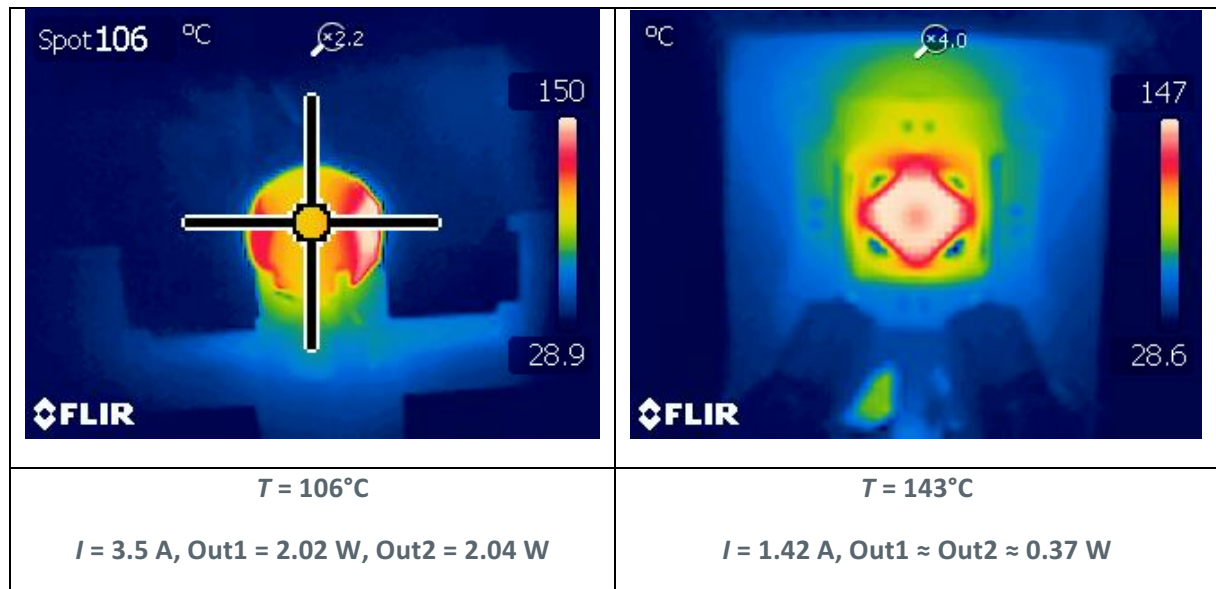


Figure 36 – Left: Spherical test cell, Right: 4 mm  $\varnothing$  MEMS cell



Absorptions measurements on the test spherical cell have been performed with the cell mounted on the setup (Figure 35 d)), for different temperatures. The results are shown in Figure 37.

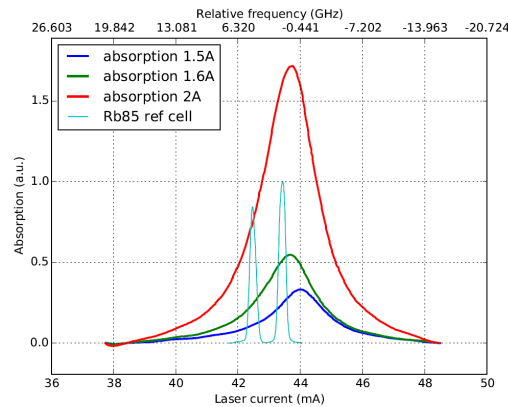


Figure 37 – Test spherical cell absorption spectra

### 4.4 Test 3: Residual fields measurements

An atomic gyroscope is very sensitive to residual magnetic fields in its technical environment. It is important to maintain such fields low or to compensate them for calibration. To characterize this, we need to measure the residual fields inside the shielding. First, we need to define the fields’ axes. A definition is given in Figure 38, together with the field/current coefficients in nT/mA.

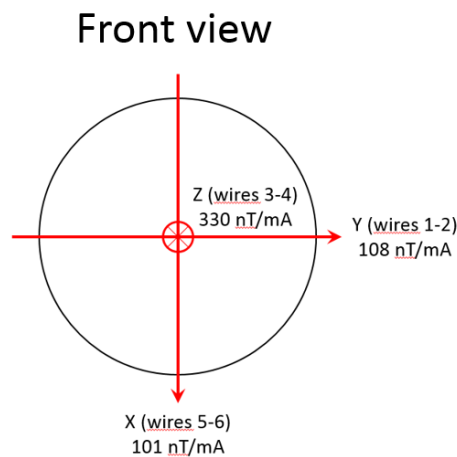
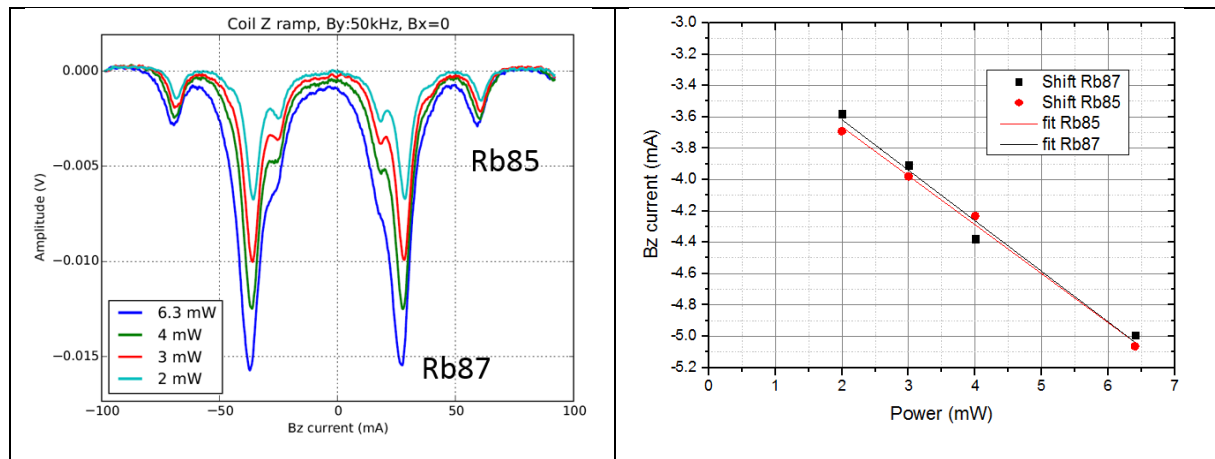


Figure 38 – Magnetic fields axis definition with nT/mA scales

There are different possible ways to measure the residual magnetic fields induced by the shielding cylinder. We choose relatively simple, straight forward methods.

For measuring the residual field along the Z-axis, we switch off the probe beam and we apply a fixed RF frequency on one of the X or Y coil and we slowly (1Hz) sweep the  $B_z$  field typically from  $-30 \mu\text{T}$  to  $30 \mu\text{T}$  ( $-100 \text{ mA}$  to  $100 \text{ mA}$ ), while recording the signal on PD1. For a given power on the pump beam, we obtain a typical signal like the one displayed on the left panel of Figure 39, showing clear dips in transmission corresponding to the Rb85 and Rb87 isotopes resonances<sup>66,67</sup>. By recording the position of these dips for different values of the pump power, we can determine the residual  $B_z$  field at zero optical power (when the light shift effect is removed). This is illustrated in the right panel of Figure 39. We find a residual z-coil current of about  $-3 \text{ mA}$ , corresponding to a residual  $B_z$  field of about  $-0.99 \mu\text{T}$ . The same value is found for a RF field applied on coil X.



**Figure 39 – Left: Signal measured on PD1 for different pump powers (probe beam removed).  $B_z$  is swept at 1 Hz.  $B_x=0$ , 50 kHz RF on coil Y. Right: position of the Rb87 and Rb85 dips as a function of the  $B_z$  field.**

For measuring the residual field along the X (Y) axis, we switch off the probe beam as well as the magnetic fields on coils Z and Y (X) ( $B_z=0$ ,  $B_y=0$ , ( $B_x=0$ )), and we slowly (1 Hz) sweep the magnetic field on coil X around zero. For a given power on the pump beam we obtain a typical signal like the one obtained on the left panel of Figure 40, showing a maximum around zero field<sup>65,66</sup>. By recording the position of these maxima for different values of the pump power, we can determine the residual  $B_x$  ( $B_y$ ) field at zero power. This is illustrated in the right panel of Figure 40. We find a residual x-coil current

<sup>66</sup> C. Cohen-Tannoudji et al., « Diverses résonances de croisement de niveaux sur des atomes pompés optiquement en champ nul », Revue de physique appliquée 5, 95 (1970)

<sup>67</sup> T. Walker and W. Happer, « Spin-exchange optical pumping of noble-gas nuclei », Rev. Mod. Phys. 69, 629 (1997)

of about +66  $\mu\text{A}$ , corresponding to a residual  $B_x$  field of about 6.7 nT. The residual y-coil current is found to about +72  $\mu\text{A}$ , corresponding to a residual  $B_y$  field of about 7.7 nT.

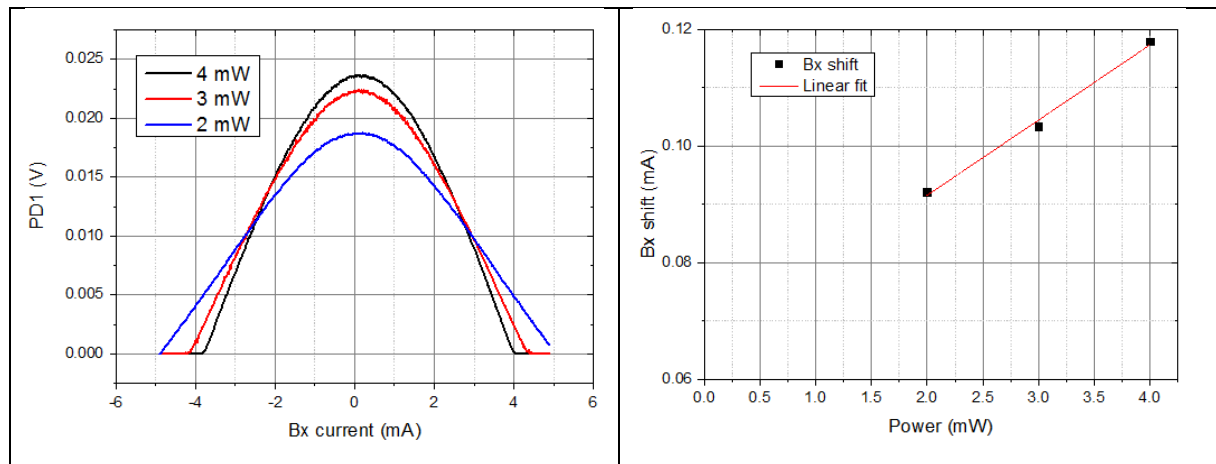


Figure 40 - Left: Signal measured on PD1 for different pump powers (probe beam removed).  $B_x$  is swept at 1 Hz around zero.  $B_z=B_y=0$ . Right: position of the maxima as a function of the  $B_x$  field.

The residual fields along the three axes are summarized in Table 10 below.

Residual $B_x$	Residual $B_y$	Residual $B_z$
$\sim 6.7$ nT	$\sim 7.7$ nT	$\sim -0.99$ $\mu\text{T}$

Table 10 – Residual fields

These results show the shielding is efficient enough and a need for demagnetization is not indicated at this stage.

## 5 Operational Gains of a NAVISAS based A-PNT

The final activity of WP3 was task 3.4 which was foreseen to be dedicated to the creation of a pool of building blocks in line with WP2 requirements that can serve as the subset of the solution workspace for WP4 and the beginning of the definition of the overall system at conceptual level. After internal discussion, the consortium concluded that at the current stage of development of the project (which has fulfilled its foreseen objectives) and given that a block diagram explaining the different blocks of NAVISAS was already proposed in WP2 it would not make sense to carry out these activities as the team would be repeating work from WP2 and unable to progress more on the detailing of the blocks. Alternatively, and based on the conclusions of the analyses of previous Sections, it was agreed that NAVISAS was missing an operational concept for small A/C.

Therefore, the consortium agreed to pursue the development of one or more operational concepts that explain how the consortium envisages the usage of NAVISAS by the small A/C universe. The idea behind this is for the operational concepts to provide a bigger picture on what value NAVISAS can bring to small aircraft and help understand what is achievable and under what conditions. After this analysis is completed it will be possible to progress on the building blocks detailing work that was initially planned for WP3.4.

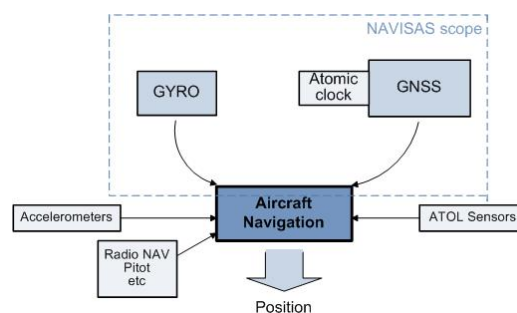


Figure 41: Preliminary NAVISAS functional block diagram (taken from NAVISAS D2.1).

### 5.1 NAVISAS Operational Concepts



From previous sections, it is obvious that the alternate A-PNT technologies studied by SESAR and SESAR2020 do not directly target general aviation neither ultra-lights or UAVs.

Only general aviation aircrafts are considered in the short term A-PNT concept by maintaining a VOR beacon network. If required, GPS-only aircrafts could be managed by ATC through conventional vectoring. It is important to note that in case of GPS loss ADS-B and mode S transponder position would also be unavailable; ATC would rely only on primary radar data.

Except for WAM which does not require airborne modification for general aviation all other short term / mid-term techniques consider airborne navigation equipment not embedded in ultra-light aircrafts or UAV (DME, Loran,..).

Although this may be an acceptable solution at ATM level, additional factors have to be taken into account:

- General aviation or ultra-light pilots usually have less training and experience than commercial pilots. In particular, recurrent training may be non-existent, especially for VFR pilots. The sudden loss of GPS may be felt as very strong reduction in safety margin especially in marginal VFR conditions. Cases where general aviation pilots became totally confused following a GPS failure have been reported.
- VFR navigation is more and more relying on a user friendly 2D-map using GPS position and pilots tend to reduce the search of visual references to confirm their position. In addition, most of the general aviation pilots flying with GPS have not been using VOR or NDB for years and may struggle to revert to conventional aids if needed.
- Ultra-light aircrafts tend to have similar characteristics than general aviation aircraft however may be less equipped in terms of navigation equipment (no VOR or NDB receiver). A GPS loss may have an even worse impact at pilot level.
- Small/medium size UAV are mostly relying on GPS and may not have any additional navigation means, nor always provide a radio link between UAV pilot and ATM. Even in VFR conditions no reversion navigation capability (even visual through cameras) could be available in case of GPS loss.

From the above observations the following operational gains for an A-PNT technique could be proposed in the frame of NAVISAS project targeting general aviation, ultra-light aircraft and UAVs. These are only preliminary proposals and they will be further detailed in the next phases of the project.

- Navigation capability based on GPS + atomic gyroscopes + accelerometers

Mainline aircrafts use hybridization of GPS and inertial position to get the best of both sensors for navigation. Based on low-cost NMR gyros and accelerometers the same solution could be envisioned to consolidate the onboard computed position. Simpler algorithms should be

implemented to cope with lower cost avionics but could provide additional navigation capability in areas where GPS coverage is limited or where constellation geometry is degraded.

- GNSS spoofing / incorrect reacquisition detection

After GNSS outage due to masking, jamming or spoofing there is a risk that one or several satellites are not correctly tracked by the GNSS receiver thus producing erroneous pseudo-range measurements. If only one satellite is false-tracked, the situation will be detected by the regular RAIM process inside the receiver, and there will be no integrity issue. If two or several satellites are false-tracked, the regular RAIM process may not be able to detect the situation. Use of a very stable local clock can provide a way for significantly improving the detection of such situations

- A-PNT in case of GNSS loss

As explained above the loss of GPS in manned aircraft is likely to have a significant Human Factor impact even in VFR. To avoid a sharp transition between a nominal navigation and a total loss of GPS positioning, the use of NMR gyros and accelerometers to provide coasting during a few minutes would bring a significant benefit. While alerting the pilot on a GPS loss it would still provide a position and an associated accuracy, giving pilot time and comfort to revert to other navigation mean and divert to the nearest airport if needed. This would be applicable to VFR and IFR flights (although IFR pilots are trained to revert to VOR / NDB beacons in case of GPS loss).

A similar operational gain would be applicable for UAV where temporary GNSS loss could be even more frequent because of terrain masking due to low level flight. Providing a backup positioning capability could protect the UAV from an unnecessary emergency procedure (landing) every time the GPS is lost or jammed.

- Auto-land

Auto-land capability is currently available only on high end commercial aircraft. Based on radio altimeter, ILS beam tracking and inertial measurement is allows the aircraft to automatically land (including flare).

Auto-land itself does not provide the required integrity to be used in zero visibility conditions with the expected safety requirement.

There are currently two ways to use auto-land:

- CAT II/III landing where autoland is required and where integrity is guaranteed by the system at airborne (system redundancy) and ground (dedicated ILS station) level.
- CAT I approaches where the landing trajectory is monitored by the pilot through visual reference below the decision altitude.

CAT III capability is not implemented on smaller aircraft that are not fitted with the required system and do not fly on large CAT III equipped airports.



Auto-land for CAT I approaches is not implemented in current general aviation avionics and would anyway only target IFR aircraft.

However, an auto-land capability available on smaller aircraft (general aviation, ultra-light, UAV) independent on ILS system would be a major improvement in the existing capability. Although such long term disruptive capability may sound very ambitious (at least for light manned aircraft) it has been decided to refine this concept in the next phase of the project

There is a consensus in the NAVISAS consortium that such capability will require additional sensors and cannot rely only on GPS and inertial positioning. LIDAR or vision based navigation are possible options and should be further investigated.

## 5.2 Method applied to define NAVISAS visions and operational concepts

In order to define the visions and operational concepts for NAVISAS, the following process was applied:

1. Recall of NAVISAS proposed technologies
2. Define the kind of operations we foresee small aircraft performing in the future
3. Answer the question: How can the technologies (or combinations thereof) of bullet 1 contribute to or enable the operations of bullet 2?
4. Identify any assumptions made in previous bullet and possibly assess their impact
5. Based on the results of the previous bullets determine which ambitions, areas and views of SESAR ATM Master Plan NAVISAS aims to contribute to.

We believe this method will enable the reader to have a clearer understanding of the benefits of NAVISAS technologies and how the technologies considered and the block diagram proposed contribute to SESAR solutions in the future.

## 5.3 NAVISAS proposed technologies

This section briefly recalls the technologies and ideas proposed by NAVISAS. These form the baseline for the work of the project and the prime raw materials from which the consortium builds the NAVISAS visions. The base idea of NAVISAS is to combine multi-constellation and/or multi-frequency GNSS capabilities with a set of Spin Nuclear Magnetic Resonance (SNMR) gyroscopes and atomic clock(s) to deliver navigation capabilities to small aircraft.

Any of the concepts presented below may use one or more of these technologies (preferably more) in isolated fashion or combined (preferably combined) to enable some type of operation that is not achievable today or to support an existing type of operation in an improved way (e.g. with lower cost or improved performance).

## 5.4 Foreseen operations

### 5.4.1 RPAS

There is a community wide effort to integrate RPAS into the European Airspace. The visions described below for the RPAS are based on recent developments made by the RPAS community in terms of CONOPS development. Eurocontrol has drafted an ATM CONOPS for RPAS which considers two major groups of operations: IFR or VFR operations conducted in Radio Line of Sight (RLOS) or beyond Radio Line of Sight (BRLOS) following similar rules to manned aviation and Very Low Level (VLL) Operations.

VLL operations take place in the airspace band between ground and 500ft (150m). It is assumed a VLL traffic management system will be put in place capable of providing localisation and information services. Eurocontrol proposes 4 classes of traffic in VLL operations:

- Reserved for buy and fly types of RPAS
- Free flight in Visual Line of Sight (VLOS) and Beyond Visual of sight (BVLOS)
- Free flight or structured commercial routes in BVLOS conditions
- Special operations

Apart from the first traffic class (i.e. the buy and fly types of RPAS), all other VLL traffic types will be expected to require some sort of surveillance equipment. Furthermore, the buy and fly RPAS and RPAS flying free flight will be expected to self-separate in 3D.

For IFR and VFR operations above 500ft, Eurocontrol is proposing two traffic classes, both of which mandate RPAS must meet Communications, Navigation and Surveillance (CNS) airspace requirements. The first class defines IFR or VFR operations outside the networks not flying SIDs (Standard Instrument Departures) and STARs (Standard Terminal Arrivals). The second class corresponds to IFR operations including network, TMA and Airport operations with RPAS capable of SIDs and STARs as designed for manned aviation

Based on this, it is expected that by 2023, VLOS and Extended VLOS (E-VLOS) operations will be fully integrated in day to day operations and IFR will be partially integrated by using approved Detect & Avoid (D&A) solutions. Also, under this timeframe RPAS are expected to be SESAR compatible.

A possible vision for RPAS operations in the timeframe 2020-2030 could be:

Operator 'A' initiates a RPAS based delivery service in low density urban environments. Small RPAS deliver packages to customers by free flying below 500ft BVLOS. Operator 'A's RPAS self-separate from other airspace users, carry onboard surveillance equipment and receive information from an existing VLL traffic management system. In this scenario, a low-cost navigation capability (preferably independent of ground infrastructure, because of the free flight) is required to ensure the success of the operation.

Another possibility consists of regular daily RPAS based maritime and coastline surveillance operations, where Operator 'B' flies its RPAS completely integrated at the airport. The RPAS fly IFR point-to-point missions with possible loitering areas over the coast. Besides the basic requirement of the RPAS being able to deliver the performance necessary to fly procedures designed for manned aviation, it is



expected that some form of robust navigation capable of supporting PBN procedures is available. While the RPAS may rely on alternative positioning techniques similar to those used by manned aviation, economic restrictions will dictate the use of lower cost avionics solutions capable of delivering similar performance for alternative positioning.

## 5.4.2 GA and VLA

It is expected that the use of GA and VLA in the 2020-2030 timeframe will increase. Main uses of GA and VLA will be for:

- Leisure flying
- Aerial work
- Individual transport

According to the SESAR ATM Master Plan (and similar strategic documents such as the FAA PBN NAS Strategy), the vision of GA operations is for these types of aircraft to be fully integrated with other airspace users (which is already true of some situations). This means the aircraft will fly trajectory based operations and therefore be adequately equipped to fly RNAV procedures. This will grant them greater access to airports and airspace in general. As mentioned above, in some situations GA aircraft already follow RNAV routes and have VOR/NDB NAVAIDS backups (although they may not be capable of flying lower RNP). As cost is probably one of the main drivers for GA manufacturers and operators, they will not be equipped with DME/DME equipment and manufacturers will be interested in finding more cost effective alternatives, through relatively cheap equipment capable of supporting the applicable RNAV and RNP procedures.

A possible vision could be:

Mr. Smith (a GA Pilot) leaves his home in Bratislava early in the morning to attend an important meeting in Brussels. Mr. Smith decides to travel to Brussels using his personal GA aircraft. As he leaves for the airport, meteorological conditions over Bratislava deteriorate requiring the flight to be done under IFR.

Mr. Smith is able to fly direct routes to Brussels by applying RNAV procedures and choosing the best possible trajectory.

As he's flying over Germany, his aircraft suddenly loses GNSS signals (due to GNSS outage not because of an A/C system failure) and consequently he has to rely on alternative positioning technology to keep fulfilling the RNAV specifications. His aircraft is equipped with a low cost avionics package that allows him to continue to fly RNAV procedures even after losing GNSS signals without having to rely on ground NAVAID infrastructure.

As he arrives in Brussels, Mr. Smith has used its low cost avionics package to the fullest to perform a precision approach to the airport. Depending on the sensors included in the avionics package (e.g. LIDAR or cameras in addition to gyros and accelerometers) an automatic landing may even be possible.

Happy that he chose to fly his own aircraft, Mr. Smith arrives on time to his meeting in Brussels.

## 5.5 What can NAVISAS contribute

For any of the visions considered above, NAVISAS main contribution will be in terms of potential improvements (performance, cost, functionality or a combination thereof) to NAVAID infrastructures which are a core component of the PBN concept.

### 5.5.1 RPAS

#### 5.5.1.1 VLL Operations

We expect NAVISAS technologies to be able to deliver the main navigation capability to small RPAS operating free flights in VLL.

NAVISAS could offer a single avionics box comprising a multi-constellation, multi-frequency GNSS capability combined with three atomic gyroscopes, atomic clocks and three accelerometers.

RPAs will be able to navigate precisely in urban environments (e.g. to perform parcel deliveries) or mountainous areas (e.g. to perform environmental monitoring or surveillance) using the multi-constellation, multi-frequency GNSS capability with improved satellite visibility in areas with high levels of satellite masking. Whenever the GNSS capability is lost, the NAVISAS gyroscopes and accelerometers provide an alternative positioning and will be used to coast until the GNSS capability can be re-acquired. The multi-constellation capability may be able to provide GNSS based navigation solutions in these environments when one of the available constellation is not visible for example. The multi frequency capability supports the ability to complement same constellation signals by using all the constellation frequencies available. Because operations take place in environments where satellite masking is expected to be intermittent, periods of GNSS loss are expected to be short enabling the coasting capability to be confidently used.

After a GNSS outage due to masking, jamming or spoofing there is a risk that one or several satellites are not correctly tracked by the GNSS receiver thus producing erroneous pseudo-range measurements. The NAVISAS stable local clock can provide a way for significantly improving the detection of such situations and improving the security of the operation.

#### 5.5.1.2 IFR Operations

NAVISAS could deliver a low cost avionics package comprising a multi-frequency GNSS receiver, atomic gyroscopes, atomic clocks, accelerometers and sufficient processing capability to add to the existing navigation equipment aboard the RPAS performing IFR operations described above thereby circumventing the need to include VOR/NDB NAVAIDS on-board. This is of course built on the premise that NAVISAS technologies will be capable of delivering performance capable of complying with the performances demanded from manned aircraft.



Based on low-cost NMR gyros and accelerometers a GNSS + gyros + accelerometers solution could be envisioned to consolidate the on-board computed position. Simpler algorithms should be implemented to cope with lower cost avionics but could provide additional navigation capability in areas where GPS coverage is limited or where constellation geometry is degraded.

The impact of temporary GNSS loss could be minimized by NAVISAS by providing a backup positioning capability which could protect the UAV from an unnecessary emergency procedure (landing) every time the GPS is lost or jammed.

After GNSS outage due to masking, jamming or spoofing there is a risk that one or several satellites are not correctly tracked by the GNSS receiver thus producing erroneous pseudo-range measurements. The NAVISAS stable local clock provides a way for significantly improving the detection of such situations and improving the security of the operation.

The quality of the NAVISAS atomic clock can also be used to synchronize with ground clocks to be able to use pseudolite signals transmitted from ground based equipment with no extra on-board equipment (the pseudolite A-PNT paper provides an example for the use of DME with no extra on-board equipment).

If the RPAs is equipped with additional sensors (currently not considered in NAVISAS) such as a radio altimeter, cameras or LIDAR, NAVISAS components could be used in combination with these to enable automatic landing at the airport or airfield of operations. A caveat must be made here to note that current RPAS regulation is not fully clear on the levels of performance required for auto-land capabilities. EASA has prepared and indeed published Certification Specifications for RPAS (applicable to the certified category of RPAS) tailored from CS-23 and CS-VLA. In particular, in Special Conditions RPAS Flight Control System (SC-RPAS-FCS) which is based on CS-VLA, EASA defines an automatic landing system as one that, once the automatic landing mode has been engaged, the approach, landing and ground roll are fully automatic until the RPA reaches full stop or after a safe taxiing speed is reached and the flight crew changes to a manual taxi mode: RPA flightpath, speed, configuration, engine settings, runway steering and braking after touch down are controlled by the automatic landing system. The performance of such system and more specifically the size of the convergence window and associated tolerances for auto-land and rejecting the landing should be defined with the Certifying Authority based on the tailoring of manned aircraft reference documents such as EASA CS-AWO (All Weather Operations). So as of writing, performance is to be determined in collaboration between the RPAS manufacturer and the certifying authority. Furthermore, if a RPAS from the Specific category is considered then the level of performance of any auto-land function is by default to be discussed and agreed with the certifying authority as the capability to operate in the Specific category is determined by the level of confidence the certifying authority can deposit in the safety assessment made by the RPAS manufacturer for that specific operation.

## 5.5.2 GA and VLA

### 5.5.2.1 Personal transport

Mainline aircrafts use hybridization of GPS and inertial position to get the best of both sensors for navigation. Based on low-cost NMR gyros and accelerometers the same solution could be envisioned to consolidate the on-board computed position. Simpler algorithms should be implemented to cope with lower cost avionics but could provide additional navigation capability in areas where GPS coverage is limited or where constellation geometry is degraded.

After GNSS outage due to masking, jamming or spoofing there is a risk that one or several satellites are not correctly tracked by the GNSS receiver thus producing erroneous pseudo-range measurements. If only one satellite is false-tracked, the situation will be detected by the regular RAIM process inside the receiver, and there will be no integrity issue. If two or several satellites are false-tracked, the regular RAIM process may not be able to detect the situation. Use of a very stable local clock can provide a way for significantly improving the detection of such situations

As explained above the loss of GPS in manned aircraft is likely to have a significant Human Factor impact even in VFR. To avoid a sharp transition between a nominal navigation and a total loss of GPS positioning, the use of NMR gyros and accelerometers to provide coasting during a few minutes would bring a significant benefit. While alerting the pilot on a GPS loss it would still provide a position and an associated accuracy, giving pilot time and comfort to revert to other navigation mean and divert to the nearest airport if needed. This would be applicable to VFR and IFR flights (although IFR pilots are trained to revert to VOR / NDB beacons in case of GPS loss).

An auto-land capacity available on smaller manned aircraft independent on ILS system would be a major improvement in the existing capability. Such capability could be delivered by NAVISAS as long as additional sensors were included in the aircraft. LIDAR or vision based navigation are possible options for this.

## 5.6 NAVISAS relation to the SESAR ATM Master Plan

The SESAR ATM Master Plan (2015 edition) establishes six areas where performance improvement targets have been established and are being pursued:

- Security
- Cost efficiency
- Capacity
- Environment
- Operational efficiency
- Safety

In order to achieve its performance ambitions, SESAR identified the following relevant areas of work:

- Automation support
- Integrated systems
- Integration of all vehicles
- Sharing of information
- Flight- and flow-centric operations



- Virtualisation

Changes to the ATM system are needed and these are grouped in the SESAR ATM Master Plan in four key features:

- Optimised ATM network services
- High-performing airport operations
- Advanced air traffic services
- Enabling aviation infrastructure

The NAVISAS concepts and their underlying technologies will contribute to changes in very specific areas or in very specific features.

NAVISAS impacts solely the Enabling aviation infrastructure key feature and in particular to the rationalization of the Communications, Navigation and Surveillance (CNS) systems and the integration of general aviation (GA) alongside the introduction of remotely piloted aircraft (RPAS) into the ATM environment. NAVISAS can contribute to this by setting the foundations for the supply of alternative positioning technologies which are estimated to be more cost effective.

The integration of all air vehicles into the airspace is an area of work relevant to the performance ambitions of SESAR. In particular, the Master Plan identifies clear standards and low-cost system solutions which support interoperability to allow integration of all airspace users (including airlines but also military, business, general aviation and rotorcraft users, as well as RPAS) in an efficient and non-discriminatory manner while ensuring safety as desired improvements.

NAVISAS contributes to this area of work through its concepts of operations and more specifically through the A-PNT concepts proposed below.

### **SESAR A-PNT short/midterm concept**

The European A-PNT concept is under definition. SESAR2020 project aims at refining this concept based on the technology performance: enhanced DME, Loran C or LDACS are currently studied in the frame of SESAR2020.

Although no final concept is proposed today, currently the following trend seems to emerge.

- The A-PNT objective would be to keep an RNP 1 or RNAV 1 capability within European TMAs in case of GNSS outage.
- One option would be to mandate commercial aircraft to be equipped to meet such a requirement based on current or slightly modified equipment (high grade IRS coasting, enhanced DME/DME localisation). The mandate may change depending on the area (in a widely DME populated area, DME/DME A-PNT would be authorized whereas IRS would be privileged in other regions).

- Alternatively, the mandate could apply to airport operators to provide a RNP/RNAV 1 capability within the TMA. Each TMA may handle it in a different way depending on the surrounding navaid network, the approach published and the traffic type/density. A medium-size airport with limited traffic may decide not to modify its current procedures and use conventional ATM vectoring in case of GNSS outage. On the other hand, a large airport may be willing to add or move some navaid beacons to provide a full RNAV 1 capability based on DME or VOR.
- General aviation flying IFR (representing a low percentile of the total flights) may either revert to conventional VOR/NDB routes or could be vectored by ATC.
- VFR flights are not considered in the SESAR A-PNT concept since visual references would be a natural backup navigation mean and because VFR A/C are not supposed to fly IFR GNSS-based routes.
- RPAS are not currently considered in current SESAR A-PNT solution either. Indeed at the moment RPAS are only flying VFR and in case of GNSS outage they can still be manually flown by the remote pilot. RPAS flying regular IFR routes is not considered in the short/mid term. However, the recent RPAS ATM CONOPS published by Eurocontrol and the U-Space initiative by SESAR may result in short-term changes to this.

It is important to note that not only navigation but also surveillance may be impacted by a GNSS loss at airborne or ground level. Without GPS, the TAWS capability is drastically reduced. At ground level, in the absence of primary radar, secondary radar or ADS-B based surveillance may also be affected depending on the aircraft capability and avionics architecture.

The effect of a GPS loss on existing navigation and surveillance architecture is summarised below:

		Navigation reversion mean		Surveillance reversion mean
		RNP	RNAV	
IFR	Mainline/bizjets	IRS based	IRS based or DME/DME based	ADS-B or Mode-S based on IRS or DME/DME
	Rotorcrafts / regional	NO	VOR/DME based	Primary radar only
	GA	NO	VOR/NDB based	Primary radar only

Table 11 - Effect of a GPS loss on existing navigation and surveillance architecture.

The following two-step A-PNT roadmap is currently foreseen by SESAR2020 (extract from Functional Requirements Document)

- **Short & Medium Term A-PNT (up to 2030)**

*In this timeframe the reversionary navigation solutions will be provided by the current terrestrial nav aids, in an optimized and rationalized network configuration:*

*DME: DME network (including TACAN for civil operations) will provide the main support for reversionary PBN operations in En-route and TMA airspace. It is expected that the DME network will be continuously optimised by decommissioning/relocating facilities in the high DME density areas and by installing new facilities in areas where the DME/DME coverage is poor. Overall the number of the DME facilities in Europe will not change significantly. In this time frame it is expected that the ground and airborne systems will continue to improve their performance, and that the capability of the DME/DME to support RNP reversion will be demonstrated and recognized.*

*VOR: VOR will evolve to a support for a contingency mode enabled by radar vectoring in the case of aircraft not capable of DME/DME navigation or in areas without DME/DME coverage. The overall size of the VOR/DME MON (Minimum Operational Network) required for this purpose was estimated to approx. 300 stations Europe wide.*

*NDB: NDB stations will be progressively decommissioned so that only a residual network will be maintained*

*ILS: ILS is expected to remain the primary enabler of Precision Approach operations although LPV200 and GBAS operations will be gradually implemented as nominal mode which may allow the rationalisation of a limited number of CAT I ILS in some States.*

*MLS: MLS has a limited role in precision approach operations until eventually current facilities (only in one airport) will be replaced by GBAS.*

- **Long Term A-PNT (beyond 2030)**

*Long term A-PNT will be based on a new system/technology that has not yet been defined or standardized by ICAO, which may require major changes of the existing ground and on-board systems. The analysis of the potential future A-PNT solutions was performed by project 15.3.2 in D13 ("A-PNT/ Alternate Technology Options. The main potential new technologies are: Multi-DME solution and RAIM algorithm, Enhanced DME, Mosaic/DME, LDACS-NAV, Enhanced LORAN – eLORAN, Wide Area Multi-lateration (WAM), Pseudolite network and Mode N.*

As explained above, VFR flights and RPAS are not included in this SESAR high level roadmap. The following table summarizes the impact on already deployed avionics of a total GPS loss.

	Navigation reversion mean			Surveillance reversion mean
	Visual references	Nav aids (VOR, NDB)	ATM vectoring	
Rotorcrafts	YES	If available	If available	Primary radar only
GA	YES	If available	If available	Primary radar only
Ultralights	YES	NO	If available	Primary radar only
Small RPAS	If available	NO	NO	NO

Table 12 - Impact of total GPS loss on already deployed avionics.

Based on current NAVISAS work and state-of-the-art alternative technologies a similar A-PNT roadmap for VFR general aviation, ultralights and RPAS is proposed below. It is important to mention that at the moment of writing and given the current technology maturity levels it is risky (and maybe even counterproductive) to estimate cost for a complete NAVISAS sensor suite except than to note that providing navigation capabilities based cameras and image processing techniques is currently cheaper than a high grade inertial reference unit. So, one can expect that, if these techniques are combined with NAVISAS technologies such as the atomic gyros and clocks they will still bear a lower price than high grade inertial units.

- VFR flights

As stated above, VFR flights have to rely on visual reference. It is very unlikely that any A-PNT technology may be mandated for this type of operations, even to improve surveillance since most ultralights and GA are not fitted with a mode-S squawk or ADS-B today.

However, if GPS outages become more and more frequent, alternative technology may be proposed by avionics manufacturers to cope with temporary GPS losses and improve navigation continuity.

- RPAS

Currently, RPAS operations rely massively on GPS based navigation.

However RPAS manufacturers start to provide newer methods for navigation based on autonomous image processing or LIDAR.





It is more than likely that such technology will gain full maturity within the next years providing A-PNT for the RPAS under VMC conditions. Based on the RPAS type of operation such capability may be accepted as a safe means of navigation or may even be required by regulators.

While these technologies have limitations (e.g. flight height, meteorological conditions,..) they may be complemented by multi constellation GNSS hybridized with atomic gyros (when available), providing A-PNT capability in all weather and flight conditions.

RPAS surveillance is still under discussion. It is likely that RPAS flying in civil airspace may be required to have ADS-B. In this case, initiatives like UTM in the US and the SESAR led U-Space may bring new data and variables onto the table. The above alternative technologies could complement ADS-B by adding another position source to the ADS-B system inputs.

Based on the above elements, a high-level diagram of the foreseen A-PNT roadmap (including SESAR IFR current vision) is depicted below:

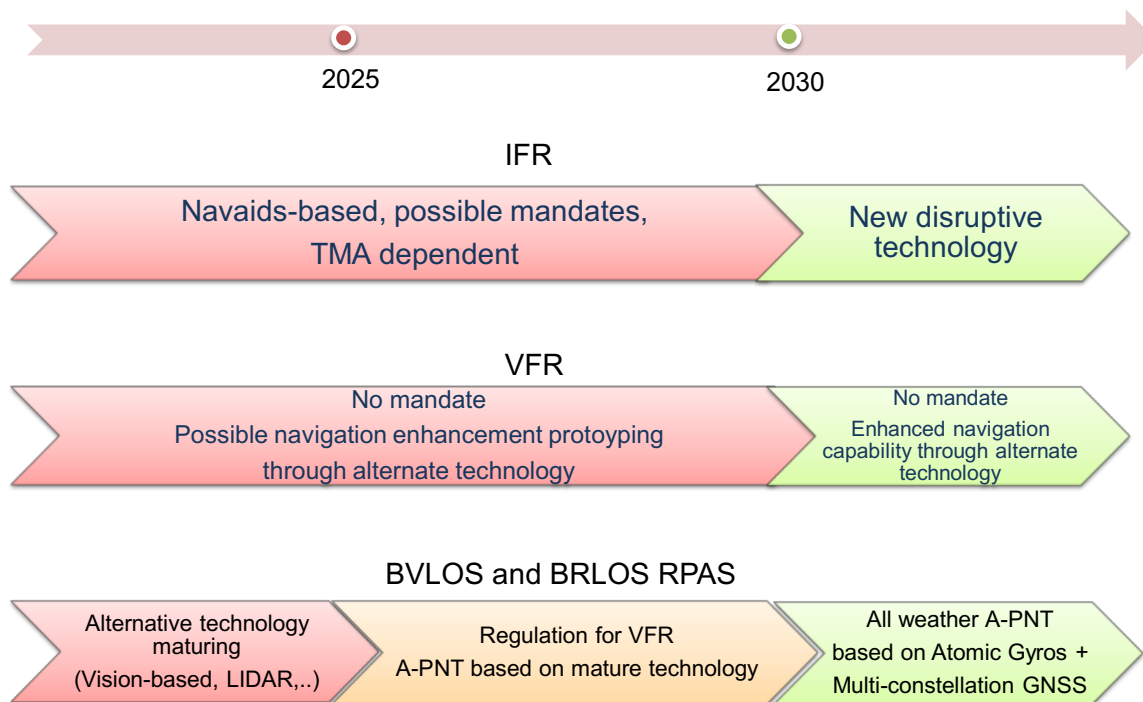


Figure 42 – Proposed A-PNT roadmap.



## 6 Conclusion

---

Concerning the state of the art in navigation, the consortium concluded the majority of small aircraft (GA, VLA, UL and UAVs as defined by the project) rely on GNSS and the combination of GNSS with INS for navigation. Manned small aircraft tend to rely on GNSS receivers and make use of beacon based navigation mostly for instructional purposes. The vast majority of unmanned aircraft rely purely on GNSS or on the combination of GNSS with INS or other sensors (such as radio altimeters or imagery) to navigate and perform automatic approaches and landings. The combination of GNSS with imagery is being exploited mostly by very small UAVs flying indoors (outdoor flight tends to use the more versatile GNSS). Some small A/C also make use of SBAS but to a much smaller extent.

GBAS is almost solely used by commercial aircraft while SoOP techniques are not mature enough at the moment for regular use in aerial navigation.

Performances and levels of equipage vary greatly between techniques. Accuracies range between hundreds and a few meters with some techniques supporting up to RNP1, APV-II and CAT I operations. Techniques and systems such as GBAS and beacons rely heavily on ground infrastructure while INS requires solely on-board equipage on the aircraft which means the spectrum of possible solutions for navigation is wide.

Due to the fact that WP2 had identified the landing phase as one of the phases with highest potential for applicability of NAVISAS technology, the consortium analysed also the use of LIDAR technology for navigation. Its performance is not completely clear at the moment and it is mostly used for obstacle detection and clearance.

Concerning the applicability of current SESAR work on APNT to small aircraft it was concluded that only the WAM technique may be applied (and it will require equipping transponders). Therefore, there is a clear gap for small aircraft.

With respect to the atomic clocks, the consortium explained the principles of operation behind their operation and the most relevant performance (e.g. frequency stability) and design parameters (form factor, power consumption and production cost). The importance of the physics package was stressed and survey of existing MAC realizations was provided.

For the gyros, the consortium discussed the relevant parameters, classes of gyros and their working principles as well as technical aspects. Performances for different atomic gyros were compared and the consortium concluded that Northrop Grumman's obtains approximately the same performances as the work done by Litton and Singer previously. The sharp difference between Northrop Grumman and the other manufacturers was the miniaturization. At the time being, Northrop Grumman seems

to be the most advanced in the conception. They reached their performance goal and are in their final production stage.

The consortium carried out tests to verify the TRL of the NAVISAS gyro concept. The experimental setup and actual tests carried out as well as their results are presented. Some results of laboratory tests performed to measure key parameters of interest for the technologies of interest were obtained and the partners believe these can validate some of the assumptions of the previous maturity level concerning aspects like performance.

Finally, having identified the need for developing an operational concept that can guide the development of NAVISAS and the gap that exists concerning the application of APNT techniques to small aircraft, the consortium has presented the initial stages of an operational concept that will drive the next stages of the project and allow the consortium to progress on the NAVISAS design concept as well as hopefully provide clarity on the big picture of how the proposed technologies of this project can be used in the future.